Stony Brook University

The Role of Laminin α2 in Oligodendrocyte Development and CNS Myelination

A Dissertation Presented

by

Jenne Liza Villaranda Relucio

to

The Graduate School

In Partial Fulfillment of the

Requirements

for the Degree of

Doctor of Philosophy

In

Molecular and Cellular Biology

(Cellular and Developmental Biology)

Stony Brook University

May 2011

Stony Brook University

The Graduate School

Jenne Liza Villaranda Relucio

We, the dissertation committee for the above candidate for the

Doctor of Philosophy degree, hereby recommend

acceptance of this dissertation.

Holly A. Colognato, Ph.D. – Dissertation Advisor
Assistant Professor, Department of Pharmacological Sciences
Stony Brook University

Joel M. Levine, Ph.D. – Chairperson of Defense
Professor, Department of Neurobiology and Behavior
Stony Brook University

Styliani-Anna E. Tsirka, Ph.D.
Professor, Department of Pharmacological Sciences
Stony Brook University

Gary G. Matthews, Ph.D.
Professor, Department of Neurobiology and Behavior
Stony Brook University

William J. Brunken, Ph.D.
Professor, Director of Ophthalmic Research
Department of Cell Biology
SUNY Downstate Medical Center

This dissertation is accepted by the Graduate School.

Lawrence Martin
Dean of the Graduate School

Abstract of the Dissertation

The Role of Laminin α2 in Oligodendrocyte Development and CNS Myelination

by

Jenne Liza Villaranda Relucio

Doctor of Philosophy

in

Molecular and Cellular Biology

(Cellular and Developmental Biology)

Stony Brook University

2011

The myelin-producing oligodendrocytes of the central nervous system are critical to normal brain function and physiology. The molecular mechanisms that influence oligodendrocyte development and CNS myelination, however, remain poorly understood. One potential factor that may regulate these processes is the extracellular matrix (ECM) molecule laminin. Children with mutations in one type of laminin – the alpha 2 subunit (LAMA2) – have defects in the size and shape of the forebrain and cerebellum, along with white matter abnormalities. However, it is not clear whether laminin α2 modulates oligodendrocytes *in vivo*, and if so, through which cellular signaling pathways. In this dissertation, I used LAMA2-deficient (*dy/dy*) and LAMA2-knockout (dy^{3k}/dy^{3k}) mice to investigate the influence of

laminin α2 on oligodendrogenesis, oligodendrocyte maturation, and CNS myelination. We found that laminin α2 regulates the organization and cellular composition of the postnatal subventricular zone (SVZ), a major gliogenic niche. Loss of LAMA2 resulted in abnormal oligodendrogenesis, such that initially LAMA2-knockout mice had fewer oligodendrocyte progenitor cells (OPCs) compared to their wildtype littermates. During the active myelination period, LAMA2-deficient brains were also found to have a developmental delay in oligodendrocyte maturation. These defects in OPC genesis and maturation correlated with axonal dysmyelination in various CNS white matter regions. We also identified several signaling abnormalities that may be contributing to these oligodendrocyte defects. LAMA2-deficient brains showed dysregulated Fyn (a Src Family Kinase known to regulate myelination) and elevated levels of C-terminal Src kinase (Csk) and Csk-binding-protein (Cbp), proteins that suppress Fyn activity. Laminin substrates were furthermore found to modulate Fyn regulation and to promote the transition of cultured oligodendrocyte progenitors to newly-formed oligodendrocytes in a Fyn-dependent manner. These findings indicate that the dysregulation of signaling pathways required for normal oligodendrocyte development may contribute to CNS abnormalities observed in congenital muscular dystrophy type 1A (MDC1A), and identify novel mechanisms by which laminins regulate oligodendrogenesis, oligodendrocyte lineage progression, and CNS myelination in the developing brain.

For those whose encouragement, understanding, and love

helped me make molehills out of mountains

and kept me going against insurmountable odds

My father Mel

My mother Grace

My husband Tom

Table of Contents

List of Tables

List of Figures

List of Abbreviations

AP	apical progenitor
APC	adenomatous polyposis coli
AraC	Arabinose C
BBB	blood-brain barrier
BL	basal lamina
BME	beta-mercaptoethanol
BP	basal progenitor
bs	brain stem
BSA	bovine serum albumin
Calb	calbindin
CB	cerebellum
Cbp	C-terminal Src kinase binding protein
CD140a	PDGFRα, platelet-derived growth factor receptor alpha polypeptide
CNPase	2',3'-cyclic nucleotide 3' phosphodiesterase
CNS	central nervous system

CO2	carbon dioxide
Csk	C-terminal Src kinase
CTX	cerebral cortex
CY3	cyanine3
DAPI	4',6-diamidino-2-phenylindole
DGC	dystrophin-associated glycoprotein complex
DMEM	Dulbecco's modified Eagle's medium
DMSO	dimethyl sulfoxide
DRG	dorsal root ganglia
DS	donkey serum
dy/dy	dystrophia muscularis; laminin α2–deficient mouse
dy^{3k}/dy^{3k}	laminin alpha2 chain-null mutant mouse
ECM	extracellular matrix
EGF	epidermal growth factor
EGL	external granule layer of the cerebellum
EM	electron microscopy
FAK	focal adhesion kinase

FITC	fluorescein isothiocyanate
GC	granule cells
GFAP	glial fibrillary acidic protein
IgG	immunoglobulin G
IGL	internal granule layer of the cerebellum
ILK	integrin-linked kinase
INM	interkinetic nuclear migration
iPC	intermediate progenitor cell
kDa	kilodalton
L4	laminin internal domain
LAMA2	laminin alpha 2 subunit
LAMA2KO	laminin alpha 2 subunit-knockout mouse
LE	laminin tandem EGF repeats
LG	laminin globular domain
Lm	laminin
LmA2	laminin alpha 2 subunit
LmC1	laminin gamma 1 subunit

LmC3	laminin gamma 3 subunit
LN	laminin N-terminus domain
LSB	Laemmli solubilizing buffer
Lu/B-CAM	Lutheran blood group glycoprotein/basal cell adhesion molecule
MAPK	mitogen activated kinase-like protein
MBP	myelin basic protein
MDC1A	congenital muscular dystrophy type 1A
MEB	Muscle-Eye-Brain disease
MRI	magnetic resonance imaging
mRNA	messenger ribonucleic acid
NA	numerical apperture
NEP	neuroepithelium
NF	neurofilament
NG2	nerve/glial antigen 2
NIH	National Institute of Health
NS	not significant
NSC	neural stem cell

OCT	Optimum Cutting Temperature
Olig2	oligodendrocyte lineage transcription factor 2
OPC	oligodendrocyte progenitor cell
p27	cyclin-dependent kinase inhibitor 1B; Kip1
p57	cyclin-dependent kinase inhibitor 1C; Kip2
PBS	phosphate buffered saline
PBS-T	phosphate buffered saline with Triton
PCNA	proliferating cell nuclear antigen
PDGF	platelet-derived growth factor
PDGFRα	platelet-derived growth factor receptor alpha polypeptide
PDL	poly-D-lysine
PFA	paraformaldehyde
PI3K	phosphoinositide-3-kinase
PNS	peripheral nervous system
POMT1	protein-O-mannosyltransferase 1
POMGnT1	protein O-linked mannose beta1,2-N-acetylglucosaminyltransferase
PP2	(4-amino-5-(4-chlorophenyl)-7-(dimethylethyl)pyrazolo[3,4-d]pyrimidine
QKI	quaking homolog, KH domain RNA binding protein

RMS	rostral migratory stream
RNA	ribonucleic acid
R-Ras	related Ras viral oncogene homolog
SDS-PAGE	sodium dodecyl sulfate-polyacrylamide gel electrophoresis
SEM	standard error of the mean
SFK	Src family kinase
SGZ	subgranular zone
Shh	Sonic hedgehog
Sox2	sex determining region Y-box 2
str	striatum
SVZ	subventricular zone
TBS-T	Tris buffered saline with Triton
TUNEL	terminal deoxynucleotidyl transferase 2´-deoxyuridine, 5´-triphosphate nick end labeling
VS	ventricular surface
VZ	ventricular zone
WM	white matter
WT	wildtype

WWS	Walker-Warburg Syndrome

Acknowledgements

The explorer Christopher Columbus has been credited in saying “You can never cross the ocean unless you have the courage to lose sight of the shore.” Almost six years after taking the biggest gamble in my life and leaving one island for another, I remain grateful to the many people who made me the person I am today, and continue to inspire me to become the best version of myself.

I begin by acknowledging my advisor, Dr. Holly Colognato for her mentorship throughout my PhD studies. Joining her lab is arguably one of the best decisions I made in graduate school. I thank Holly for all the trust, encouragement, and guidance that she has given me as a student, a colleague, and a friend. I would also like to thank the members of my Dissertation Committee, Drs. Joel Levine, Gary Matthews, Stella Tsirka, and Bill Brunken, for all their advice, support, and enormous amounts of patience as they guided me from proposal to defense. All of you have made me a better student of science.

I am deeply grateful to the past and present students and members (both *de facto* and honorary) of the Colognato lab: Dr. Jason Galvin, Dr. Iva Tzvetanova and Christos Nardis, Christopher Eyermann, Freyja McClenahan, Cindy Leiton, Amy DeMarco, Soyoung Rhee, Michael Menezes, Emory Kuo, Wei Ao, Brian Cho, and Dan Park. You all made graduate school a wonderful experience, and you are truly friends that I will never forget.

I also thank our many research collaborators and colleagues who helped us with the laminin α2 knockout and *dy/dy* projects: Drs. Emily Chen and Toni Koller, Sara Nik, Dr. Kyungmin Ji, Sue Van Horn, and Laurie Levine from Stony Brook University; Dr. Shinichi

Takeda from Osaka University; Dr. Bruce Patton and Caitlin Letts from the Oregon Health Sciences University; Drs.Jon and Sabine Lindquist from the Otto-von-Guericke University in Germany; and Drs. Karine Loulier and Taryk Haydar from the Center for Neuroscience Research.

I thank the ever-important (yet often under-appreciated) members of the administrative staff: Carol Juliano and Beverly Piazza of the MCB Graduate Program; and Lynda Perdomo-Ayala, Janice Kito, June Moriarty, Beverly Campbell, and Melissa Daley of the Department of Pharmacology. You kept our lab and my stay at Stony Brook running smoothly.

I thank the friends I made here and the ones who remain back home, especially Gelo dela Cruz, Jopet Abaya, Russell Jayme, Dr. Victor de Luna, Dr. Dumaine Williams, Boris San Luis, Bernadette and Terrence Henares, Bonnie Calizo, Francis Paraan, Marvin Altamia, and Eloise Prieto.

For their unconditional support and astounding amount of confidence in me, I remain very grateful to my family: my dad Mel, mom Grace, sisters Cielo and Sheryl, aunts Joy and Pam, grandmother Carol, grandfather Fernando, and my husband Tom.

The text of this dissertation in part is reprinted, with permission, as it appears in the Journal of Neuroscience.

Vita, Publications, and Field of Study

Personal Data
Jenne Liza Villaranda Relucio, BS, PhD
Date of Birth: June 29, 1982
Place of Birth: Quezon City, Philippines
Country of Citizenship: Philippines

Education

1998–2002	UNIVERSITY OF THE PHILIPPINES, Quezon City, Philippines BS in Molecular Biology and Biotechnology Thesis entitled "Genetic Variation in Hatchery-Bred *Chanos chanos* Forsskal: Detection and Assessment Using RAPD Markers"
2005-2011	STONY BROOK UNIVERSITY, Stony Brook, NY, USA PhD in Molecular and Cellular Biology Dissertation entitled "The Role of Laminin α2 in Oligodendrocyte Development and CNS Myelination"

Training and Employment

2001	UNITED LABORATORIES, INC., Mandaluyong City, Philippines Intern, Medical Affairs Division. Worked on various aspects of drug discovery and development, including clinical studies, high-throughput assays, and QC/QA at a leading pharmaceutical company in Southeast Asia.
2002-2005	UNIVERSITY OF THE PHILIPPINES, Quezon City, Philippines University Research Associate, National Institute of Molecular Biology and Biotechnology (NIMBB). Worked on projects entitled "Determination of antigenicity in humans and/or immunogenicity in mice of known and putative epitopes of dengue virus," and "Development of DNA vaccines against dengue virus," both in collaboration with the Research Institute for Tropical Medicine.
2005-2006	STONY BROOK UNIVERSITY, Stony Brook, NY Teaching Assistant, Department of Biochemistry. Supported teaching and preparation for junior-level lecture course with 150 students. Taught biochemistry lab course to 15 undergraduates in formal classroom setting 4 hours a week during the Fall semester.

2006-2011 STONY BROOK UNIVERSITY, Stony Brook, NY
Research Assistant, Department of Pharmacology. Conducted independent research used in 2 successful scientific grants amounting to $215,000. Collaborate with in-house research groups to generate patentable technology for proteomics analysis. Provide junior research group members with training and technical support.

Publications

Ramos, E. A., **J.L. Relucio**, and C.A. Torres-Villanueva CA. 2005. Gene expression in tilapia following oral delivery of chitosan-encapsulated plasmid DNA incorporated into fish feeds. *Mar Biotechnol (NY)*. 7(2):89-94.

Relucio, J., M. Dacanay, A. Maligalig, R. Osorio, E. Ramos, A. Santos, C. Torres-Villanueva, and C. Deocaris. 2005. Complementing nuclear techniques with DNA vaccine technologies for improving animal health. *In* H Makkar and G. J. Viljoen (eds.) Applications of Gene-Based Technologies for Improving Animal Production and Health in Developing Countries. Kluwer Academic/Plenum Publishers, NY. pp. 701-708.

Colognato, H., J. Galvin, Z. Wang, **J. Relucio**, T. Nguyen, D. Harrison, P.D. Yurchenco, and C. Ffrench-Constant. 2007. Identification of dystroglycan as a second laminin receptor in oligodendrocytes, with a role in myelination. *Development*. 134(9):1723-1736.

Loulier, K., J.D. Lathia, V. Marthiens, **J. Relucio**, M.R. Mughal, S.C. Tang, T. Coksaygan, P.E. Hall, S. Chigurupati, B. Patton, H. Colognato, M.S. Rao, M.P. Mattson, T.F. Haydar, and C. Ffrench-Constant. 2009. β1 integrin maintains integrity of the embryonic neocortical stem cell niche. *PLoS Biol*. 7(8): e1000176.

Relucio, J., I.D. Tzvetanova, W. Ao, S. Lindquist, and H. Colognato. 2009. Laminin alters fyn regulatory mechanisms and promotes oligodendrocyte development. *J Neurosci*. 29(38):11794-11806.

Relucio, J. 2011. The role of laminin α2 in oligodendrocyte development and CNS myelination. PhD Dissertation. Stony Brook University, NY.

CHAPTER I: GENERAL INTRODUCTION

Myelin is crucial for normal axonal physiology and function in the vertebrate nervous system. For CNS myelination to occur effectively, the production and development of myelin-producing oligodendrocytes needs to be regulated spatially and temporally. The appropriate organization and specification of progenitors in germinal niches are needed to confer oligodendroglial identity and, in turn, to allow precursors to populate their target white matter tracts and differentiate into mature myelinating oligodendrocytes. While many cell-intrinsic factors are known to regulate these processes, extrinsic cues provided by the extracellular matrix (ECM) could potentially also influence the development of these specialized glial cells. Model organisms with mutations in genes encoding matrix molecules provide evidence for the ECM-mediated regulation of virtually all cellular processes, such as adhesion, survival, proliferation, migration, and differentiation. The ECM's roles in regulating cell behavior are primarily due to its ability to engage morphogens and cell-surface receptors, thus modulating respective downstream intracellular signals (Streuli, 1999). However, while several studies have provided insight as to how the ECM-containing pial basal lamina, blood vessels, and embryonic stem cell niches of the brain regulate neurogenesis, the role of ECM molecules during oligodendrogenesis, oligodendrocyte maturation, and axonal myelination remain poorly understood. In this dissertation, I studied the influence of an ECM molecule, laminin α2, on oligodendrocyte development and myelination in the white matter regions of the CNS, as well as in the production of oligodendrocyte-lineage committed progenitors from the germinal niches of the developing postnatal brain.

The extracellular matrix.

The extracellular matrix (ECM) is a three-dimensional macromolecular structure that surrounds various cell types in vertebrate tissues. Far from simply providing static structural support, the ECM has dynamic roles in many cellular functions, including cell adhesion, survival, proliferation, migration, and differentiation. The ECM is able to mediate these effects through two primary mechanisms: (1) through regulation of growth factor availability (Edwards et al., 1998; Farrelly et al., 1999; Lee and Streuli, 1999), and (2) through engagement of cell-surface receptors (Howe et al., 1998; Schwartz and Baron, 1999). The four general types of proteins found in the ECM (i.e., collagens, glycoproteins, proteoglycans, and elastins) assemble to generate varying mechanical properties among different types of matrices, such as basement membranes and connective tissue. In addition to this structural role, each ECM component may be able to locally induce different signaling cascades to elicit the necessary cellular responses during development (Streuli, 1999; Tsang et al., 2010).

Results from multiple *in vivo* studies on animal models with genetic alterations in specific matrix molecules indicate ECM involvement in tissue morphogenesis and organogenesis. In most tissues, the ECM localizes mostly to the basement membrane, a specialized structure that gives structural integrity, provides a selective barrier, and regulates signaling cues for adjacent cells (Miner and Yurchenco, 2004). In contrast, the organization of the ECM in the CNS remains poorly understood. ECM-rich structures in the brain, for example, are largely confined to the endothelial cells of the vasculature and the pial basal lamina surrounding the meningeal cell layer (Colognato et al., 2005). This is hypothesized to be due to the brain's highly organized ultrastructure which leaves little room for significant amounts of

ECM, a theory which remains controversial to this date (Bonneh-Barkay and Wiley, 2009; Yamaguchi, 2000). However, non-basement membrane ECM described in the developing brain (Hunter et al., 1992a; Lathia et al., 2007; Sharif et al., 2004) has been shown to play crucial roles in proliferation, migration and differentiation of neural cells. In mature animals, where the ECM has been reported to persist in brain regions such as the hippocampus and adult subventricular zone, the ECM has been shown to support multiple processes, including neural stem cell (NSC) maintenance, neuronal survival, and synaptic organization and development (Anderson et al., 2005; Campos, 2005; Chen et al., 2003; Dityatev and Fellin, 2008; Dityatev et al., 2010; Egles et al., 2007; Emsley and Hagg, 2003; Indyk et al., 2003; Kerever et al., 2007; Libby et al., 2000). One particular type of matrix component that has been consistently implicated in stem cell maintenance, cell survival, and synaptic function is the laminin family of glycoproteins.

Laminins.

The laminin glycoproteins are major components of basement membranes. In vertebrates, these large cross-, T-, or rod-shaped molecules are assembled from three different gene products; an alpha (α), a beta (β), and a gamma (γ) subunit. Laminin nomenclature is based on the combination of α, β, and γ subunits in the trimer. Currently, there have been fifteen types of laminins identified *in vivo*, along with another three proposed heterotrimers that have yet to be confirmed. These molecules are composed of different combinations of five alpha, three beta, and three gamma subunits (Fig. I-1A, modified from Durbeej, 2010). The subunits are targeted to the endoplasmic reticulum where they form heterotrimers before eventually being secreted into the extracellular environment (Durbeej, 2010; Miner, 2008). This differential composition of

various subunits is believed to confer tissue- and site-specific properties to the assembled trimers.

Laminin chains share a general structure with a number of globular, coiled-coil, and rod-like domains (Fig. I-1B, modified from Durbeej, 2010). Covalent disulfide bonds between all three subunits give laminin molecules a triple α helical coiled-coil domain. The long arm C-terminus contains several α chain globular (LG) domains responsible for engaging target cell receptors and other ECM molecules (Aumailley et al., 2005; Schéele et al., 2007; Timpl et al., 2000; Tzu and Marinkovich, 2008). The α, β, and γ short arms also have their own globular domains, the N-terminal (LN) and the internal (L4) domains, separated by tandem EGF repeats (LE). These domains confer key biological capabilities, enabling laminin molecules to influence tissue morphogenesis (Miner and Yurchenco, 2004; Yurchenco et al., 1992). The N-terminus LN domains, for example, are essential for the self-assembly of laminin molecules and their consequent incorporation into basement membranes. This laminin polymerization preferentially occurs also when the C-terminal LG domains of the α subunit engage and cluster their target cell-surface receptors. This, in turn, induces cytoskeletal organization and triggers signaling cascades that affect various cellular processes (Colognato et al., 1999; Smirnov et al., 2002). And while most functions of the LE domain remain uncharacterized, studies have shown that certain LE domains in the laminin γ1 and γ3 chains interact with another ECM molecule, nidogen (Ho et al., 2008; Sasaki et al., 2004; Willem et al., 2002). Nidogen serves as a crosslink between the laminin and type IV collagen networks of the ECM and thus provides structural integrity for the basement membranes of various organs, such as the brain, kidney, lungs, and heart (Chung et al., 1993; Erickson and Couchman, 2000; Halfter et al., 2002; LeBleu et al., 2007; Timpl et al., 1990; Willem et al., 2002).

Contextual specificity for laminin function is also conferred by the cell-surface receptors that link the ECM molecules to intracellular signaling pathways (Durbeej, 2010). Historically, the integrins have been classified as major laminin receptors. As many as 8 members of this class of heterodimeric adhesion molecules have been shown to bind to the LG and LN domains of the laminin α chain, as well as to the C-terminus of most laminin β and γ subunits (Ido et al., 2008; Miner, 2008; Nishiuchi et al., 2006; Schéele et al., 2007; Suzuki et al., 2005; Taniguchi et al., 2009). Additionally, non-integrin laminin receptors have also been identified. Dystroglycan, a component of the dystrophin-glycoprotein complex (DGC), binds with high affinity to the laminin α1 and α2 chains to induce changes in the cytoskeleton and downstream signaling cascades (Barresi and Campbell, 2006; Bozzi et al., 2009; Colognato et al., 2007; Galvin et al., 2010; Henry and Campbell, 1996; Waite et al., 2009). Four types of cell-surface syndecans have also been demonstrated to bind laminins or laminin-derived peptides containing the LG4 domain (Bachy et al., 2008; Kazanis et al., 2010; Ogawa et al., 2007; Salmivirta et al., 1994; Suzuki et al., 2003; Utani et al., 2001). Finally, the Lutheran blood group glycoprotein/basal cell adhesion molecule (Lu/B-CAM), a transmembrane protein found on erythrocyte, muscle, and epithelial cells, has been classified as a novel receptor for the α5 subunit of laminin (El Nemer et al., 1998; Kikkawa et al., 2007; Parsons et al., 2001; Rahuel et al., 2008; Udani et al., 1998). Because of their multidomain structure and affinity for various receptors, laminins are thus able to dynamically regulate cellular functions within multiple contexts.

Functional roles for laminins in central nervous system development.

Laminins have been notoriously difficult to detect outside of traditional basal lamina, at least in part due to their sensitivity to fixation. In spite of the difficulty in detecting ECM

molecules in the brain, considerable efforts have now gone into determining the functional role of laminins in CNS development. Earlier *in vitro* studies suggest that laminin substrates enhance neurite outgrowth (Gundersen, 1987; Rogers et al., 1983), guide axonal migration (Liesi, 1985; Riggott and Moody, 1987), and promote the survival and differentiation of certain subsets of the neuronal population (Baron-Van Evercooren et al., 1982; Edgar et al., 1984; Ernsberger et al., 1989; Hunter et al., 1992a; Hunter and Brunken, 1997). Some of these proposed functions remain controversial and some have attributed these effects to other axon guidance molecules that are homologous to laminins (Dickson, 2002; Miner and Yurchenco, 2004).

More recent ECM expression studies indicate that laminins can be found in the basement membrane, as well as in non-basement membrane structures of both the developing and the adult CNS (Colognato et al., 2002; Halfter et al., 2002; Hunter et al., 1992a; Hunter et al., 1992b; Lathia et al., 2007; Mercier et al., 2002; Yin et al., 2003). This pattern of spatial distribution suggests that laminins may be able to influence various cell types throughout CNS development. At the early stages of retinal neurogenesis, for example, the initial expression of the molecule laminin β2 (formerly known as s-laminin) can be detected in association with the progenitor cells of the subretinal space (Hunter et al., 1992b; Libby et al., 1996; Libby et al., 1997). As retinal development proceeds, levels of laminin β2 become increased in the matrix surrounding the photoreceptor cells (i.e., specialized neurons capable of phototransduction), suggesting that laminin β2 is expressed at the appropriate time and location to influence photoreceptor development (Hunter et al., 1992b; Libby et al., 1999). In addition, valuable insights into the role of laminins in the brain have come from human diseases resulting from mutations in genes encoding for laminins. For example, laminin-deficient children exhibit abnormalities in the expansion and gyration (folding) of the cerebral cortex, the cerebellar vermis, and the pons,

indicating possible roles for laminins in CNS morphogenesis (Hunter et al., 1992b; Miyagoe-Suzuki et al., 2000; Philpot et al., 1999; Sunada et al., 1995; van der Knaap et al., 1997). Additionally, these children also display characteristic white matter abnormalities, delays in motor and cognitive development, and occasional epileptic manifestations (Caro et al., 1999; Collins and Bönnemann, 2010; Leite et al., 2005a). Along with the generation of laminin chain- and laminin receptor-deficient animal models, the analysis of the CNS phenotypes in mutant animals and human patients reveal important functions for this family of ECM molecules during neural development.

Laminins and neuroepithelial (NEP) cells.

Due to their therapeutic significance for neurodegenerative disease, neural stem cells (NSCs) have been the subject of substantial amounts of research in recent years. Specifically, scientists are racing to understand how extrinsic and intrinsic factors regulate NSC maintenance, proliferation, and eventual specification into lineage committed progenitors. Since laminins have been shown to function as critical regulators of stem cells *outside* the CNS (Li et al., 2010; Lin et al., 2010; Sawitza et al., 2009), the roles of laminins in the brain's embryonic and adult NSC niches are also being explored.

Early in the embryonic rodent brain, NSCs are called neuroepithelial (NEP) cells, and they form a single layer of cells lining the germinative ventricular zone (VZ) of the lateral ventricles. As these NEPs proceed through the cell cycle and divide symmetrically, their nuclei translocate along an apical-basal axis in a process called interkinetic nuclear migration (INM). This INM causes the VZ to appear pseudostratified, such that M-phase nuclei are found at the ventricle surface, while nuclei in S-phase are found at basal positions (Gotz and Huttner, 2005;

Kazanis et al., 2008). While little is known about the functions of INM, this process has been studied in the retinal neuroepithelium and is thought to be important in producing and maintaining the pool of NSCs for neurogenesis (Baye and Link, 2007; Del Bene et al., 2008).

Although an earlier *in vitro* study showed that NEP cell proliferation and differentiation were increased upon adhesion to laminin substrates (Drago et al., 1991), *in vivo* roles for laminins at this stage of cortical development are largely uncharacterized. Expression studies show laminin proteins in the periventricular (i.e., apical) regions of the E8-10 rat cerebral cortex (Colognato et al., 2005; Liesi, 1985). In the neural retina, laminins found in association with the ventricular compartment and the cells of the retinal pigmented epithelium are able to influence photoreceptor cell fate choice and differentiation (Halfter et al., 2000; Hunter et al., 1992b; Libby et al., 1996; Libby et al., 2000; Libby et al., 1999). Levels of the integrin α6 receptor in *Drosophila* NEPs were also found to be enriched at the basal end that makes contact with basement membrane (Wodarz and Huttner, 2003), suggesting putative cell-laminin interactions within this context. In medaka fish (*Oryzias latipes)* expressing a truncated form of the laminin γ1 gene, the loss of basement membrane integrity correlated with INM defects in NEPs, such that M-phase cells became displaced from their normal apical positioning on the neural tube (Tsuda et al., 2010). Together, these studies suggest functions for laminins during neuroepithelial development.

Laminins and neurogenesis in the embryonic ventricular zone.

Around E8.5 in mice, NSCs specialize and become known as radial glial cells. Spanning the width of the embryonic cortex, these bipolar radial glial cells have processes that associate with both the apical and basal (i.e., the ECM-rich pial basal lamina) sides of the developing

tissue. Radial glia have two principal characteristics: (1) as stem cells, they undergo asymmetric divisions to self-renew and generate either a daughter neuron or a more lineage-restricted intermediate progenitor cell (iPC) that populates the subventricular zone (SVZ), and (2) as structural scaffolds, they provide discreet radial migratory pathways for newborn neurons from the VZ to the cortical mantle (Campbell and Götz, 2002; Kriegstein and Alvarez-Buylla, 2009; Pinto and Götz, 2007). The iPCs that would give rise to neurons and glia also associate with and migrate along the length of the radial glia, eventually populating the cortex in an inside-out fashion (i.e., earlier born cells populate the deeper parts of the cortex, while younger cells eventually reside in more superficial layers) to generate the cortical plate by E14.5 (Colognato et al., 2005; Kazanis et al., 2008; Kriegstein and Alvarez-Buylla, 2009). During neurogenesis, radial glial cells receive signals from various microenvironments: (1) the VZ, where radial glial soma reside and are anchored via apical processes; (2) the SVZ, now an expanding germinal niche composed of iPCs, neurons, and glia; (3) the cortical mantle, a region whose complexity increases as neurogenesis and brain vasculogenesis proceeds; and (4) the laminin-rich pial basement membrane, the site of contact for radial glial endfeet (Brazel et al., 2003; Colognato et al., 2005; Kazanis et al., 2008; Tramontin et al., 2003).

Laminins are expressed in the embryonic VZ (Campos et al., 2004; Hunter et al., 1992a; Lathia et al., 2007) and have been proposed to provide signals that influence NSC differentiation and proliferation. *In vitro* studies indicate that laminins may be able to regulate distinct aspects of NSC behavior in a context-dependent manner. When presented to human neural precursor cells in substrate form, laminin matrices enhanced migration, expansion, and differentiation into neurons and glia (Flanagan et al., 2006). Laminins have also been found to influence cell fate choices *in vitro*: retinal progenitors cultured on laminin β2-rich matrices differentiate

preferentially into photoreceptors, while progenitors grown on laminin β2-depleted substrates give rise to other cell types at the expense of the photoreceptor population (Hunter and Brunken, 1997). In another study, however, addition of exogenous laminin to NSC culture media instead promoted NSC proliferation and survival (Hall et al., 2008).

β1 integrins, on the other hand, are also expressed in the embryonic VZ and have been implicated as possible NSC receptors for these laminin-mediated effects (Campos et al., 2004; Lathia et al., 2007; Loulier et al., 2009). The genetic ablation of β1 integrins resulted in reduced migratory capacity, proliferation, and survival of cultured neurospheres (Campos et al., 2004; Leone et al., 2005). A recent *in vivo* study also shows that blocking β1 integrin function transiently at the VZ apical surface of embryonic brains perturbs radial glial attachments, disrupts NSC proliferation, and causes cortical lamination defects. Similarly, embryonic brains in which laminin α2 expression has been knocked out also show altered NSC proliferation and radial glia apical attachments in the VZ (Loulier et al., 2009). Together these findings suggest that cell-ECM, and potentially cell-laminin, interactions provide the appropriate developmental cues that affect NSCs within the brain's germinal niches.

Since radial glial cells also make contact with the basal lamina in the embryonic brain, disruption of appropriate contacts between the laminin-rich pial basement membrane and the radial glia basal process often results in abnormal neuronal precursor migration and cortical lamination. These phenotypes are evident in mice that have deficiencies in pial basal lamina components. Genetic deletion of the nidogen-binding site of the laminin γ1 chain caused basement membrane disruption, leading to radial glial endfeet retraction and ectopic positioning of Cajal-Retzius cells and other radially migrating neurons (Halfter et al., 2002). Similarly, mutations in the genes coding for α6 integrin, β1 integrin, the non-integrin receptor dystroglycan,

or the POMT1 and POMGnT1 glycosyltransferases that posttranslationally modify dystroglycan (Cohn and Campbell, 2000) result in several common defects. Two independent studies on α6 integrin-null embryos report basal lamina disruption and glial endfeet detachment in the cortices, but arrived upon contradictory conclusions for the role of this integrin subunit in neuronal migration (Georges-Labouesse et al., 1998; Haubst et al., 2006). Mice lacking all β1 integrin expression in neurons and glia exhibit defective basal lamina formation, resulting in abnormal "wave-like" cortical lamination, glial endfeet irregularities, and ectopic clusters of Cajal-Retzius cells (Graus-Porta et al., 2001). Likewise, brain-specific deletion of the non-integrin receptor dystroglycan disrupted both radial glial endfeet and the glia limitans at the embryonic stage (Satz et al., 2010). Mutations in the human genes coding for POMT1 and POMGnT1 also result in the diseases Walker-Warburg Syndrome (WWS) and muscle-eye-brain disease (MEB), both displaying cobblestone lissencephaly and cortical lamination abnormalities resulting from severe neuronal migration defects (Beltrán-Valero de Bernabé et al., 2002; Olson and Walsh, 2002; Yoshida et al., 2001). These similarities in observed cortical defects between human patients and animal models of laminin/laminin receptor loss-of-function indicate a crucial role for pial basement membrane laminins in regulating radial glial cell adhesion and neuronal migration.

Laminins and neurogenesis in adult neural stem cell niches.

Within the last decade, interest in the ECM-mediated regulation of adult NSC niches has grown. Adult NSCs are maintained in the SVZ of the lateral ventricles and in the subgranular zone (SGZ) of the hippocampus. Laminins have been implicated mostly in mediating NSC migration to the olfactory bulb via the rostral migratory stream (RMS) (Belvindrah et al., 2007; Emsley and Hagg, 2003). Recently, SVZ precursors have been found to associate with structures

called fractones, laminin- and collagen-rich basal lamina projections that may serve to modulate growth factor availability (Kerever et al., 2007; Mercier et al., 2002; Mercier et al., 2003).

Three seminal studies (Mirzadeh et al., 2008; Shen et al., 2008; Tavazoie et al., 2008) provide compelling rationale for laminin-mediated regulation of neurogenesis in the adult brain. The existence of an extensive, laminin-rich vascular complex has been observed beneath the ependymal layer underlying the adult SVZ. Interestingly, proliferating adult NSCs and their progeny associate closely with these laminin-rich blood vessels (Shen et al., 2008). This association was shown to be dependent on the laminin receptor α6β1 integrin and is critical for adult neurogenesis. The administration of integrin blocking antibodies inhibited NSC adhesion to the endothelial cells of the vasculature, altering NSC position, proliferation, and ultimately adult neurogenesis *in vivo*. This network of blood vessels appears to create a specialized vascular niche for adult NSCs (Tavazoie et al., 2008). Closer analysis of the sites where NSCs associate with SVZ blood vessels reveals that pericytes and astrocytic endfeet are absent at these points of contact, indicating that blood-brain barrier (BBB) permeability at these sites may be modified. This altered BBB permeability may be specific to the SVZ vascular niche. While NSCs in the SGZ also associate closely with blood vessels, there was no evidence for "leakiness" in the vasculature of this hippocampal stem cell niche. This increased BBB permeability may allow entry of blood-borne molecules into the SVZ where they may influence the niche's resident NSCs. Additionally, the vasculature may also play a supporting role in regeneration. Type B1 stem cell astrocytes, which normally have long basal processes that contact blood vessels directly (Mirzadeh et al., 2008), were observed to divide in close apposition to these blood vessels 12 hours after cessation of AraC treatment (an anti-mitotic drug which kills transit amplifying cells

and neuroblasts). Uncovering the regenerative ability of the SVZ stem cell niche provides a critical step in understanding the brain's endogenous repair mechanisms.

Laminins and oligodendrocytes: from oligodendrogenesis to myelination.

Oligodendrocytes are the specialized glial cells responsible for myelinating axons in the central nervous system. The importance of CNS myelination becomes apparent in diseases such as multiple sclerosis, where the loss of myelin leaves the axons exposed, resulting in progressive neuronal degeneration and irreversible disability (Dutta and Trapp, 2007). Although normal CNS functions are clearly reliant on proper oligodendrocyte production, development, and myelination, the molecular mechanisms that underlie these processes remain poorly understood. One potential factor that may regulate the myelination process is the laminin family of ECM molecules. Mutations in one type of laminin – the alpha 2 (α2) subunit – cause a form of human congenital muscular dystrophy called MDC1A (congenital muscular dystrophy type-1A). This dystrophy is characterized by muscular deficits accompanied by abnormal white matter in the brain, indicating that CNS myelination may become disrupted when laminin is mutated or absent. (Allamand and Guicheney, 2002; Buteică et al., 2008; Helbling-Leclerc et al., 1995; Leite et al., 2005b; Miyagoe-Suzuki et al., 2000; Philpot et al., 1999; Sunada et al., 1995). Laminin α2-deficient animal models have also been described as exhibiting myelin deficits in the brain (Chun et al., 2003). Furthermore, *in vitro* studies have shown that laminin-mediated signaling in oligodendrocytes can modulate survival and differentiation in response to known trophic factors (Baron et al., 2003; Buttery and ffrench-Constant, 1999; Colognato et al., 2002; Frost et al., 1999).

As described above, a recent study has also shown roles for laminin-α2 in regulating NSC proliferation and adhesion to the neocortical niche during embryonic corticogenesis (Loulier et al., 2009). Early in development, laminin-α2 is expressed in the VZ while laminin receptors (such as integrins) are found on the surface of neural stem cells (Lathia et al., 2007). These laminin ligands/integrin receptor interactions in NSC regulation could also potentially regulate postnatal oligodendrogenesis.

Laminin α2 and oligodendrogenesis: insights from the neocortical niche.

Neuronal and glial cells are generated in the cortex in a sequential, yet overlapping fashion. As neurogenesis in the embryonic brain begins to reach its peak by E14, the VZ begins to decline and a second pool of progenitors expands to form the SVZ. By E19, the SVZ becomes the major germinal zone in the cerebral cortex. Generally, cells originating from the rodent SVZ from E17 until the second postnatal week are glial progenitors, with most astrocytic lineage cells generated within the first two days of postnatal life, and the peak of oligodendroglial cell production occurring after P14 (Bayer and Altman, 1991; Levison et al., 1993; Lewis and Lai, 1974; Marshall et al., 2005; Miller and Gauthier, 2007; Sauvageot and Stiles, 2002; Zerlin et al., 1995).

Oligodendrocyte precursor specification from NSCs depends on the expression of intrinsic lineage-specific transcription factors (e.g., Olig1, Olig2, Sox10, Nkx2.2) and various local extrinsic signals, including Sonic Hedgehog (Shh), Notch, and growth factors (e.g., PDGF) (Bongarzone, 2002). After oligodendroglial fate is determined, these precursors migrate from their initial locations in the VZ over large distances to populate their target CNS white matter (Sypecka et al., 2009). In the rostral CNS, oligodendrocyte precursor cells (OPCs) first appear in

restricted domains of the VZ and SVZ (Ono et al., 1997). During oligodendrocyte lineage specification, the behavior of NSCs may be influenced by the microenvironment of the SVZ niche. However, while much insight has been gained on how ECM molecules regulate neurogenesis in embryonic and adult germinative zones, the extrinsic factors that shape postnatal SVZ oligogliogenesis remain largely unknown. As components of the SVZ germinal niche, laminins could potentially have functional roles during oligodendroglial specification. Findings from our group's collaboration with Drs. K. Loulier and T. Haydar (Children's Medical Center, Washington, DC) indicate possible roles of laminin-α2 in regulating the NSC niche during cerebral corticogenesis. The loss of laminin-α2 disrupted embryonic NSC development, such that NSC proliferation became dysregulated and radial glia apical attachment to the VZ niche became disrupted (Loulier et al., 2009). This study also provided evidence for a requirement of β1 integrin signaling at the VZ apical surface of embryonic brains for proper radial glial adhesion, NSC proliferation, cortical lamination. This, along with our findings that laminin α2 is expressed in the SVZ during early postnatal development (see Chapter III), suggest a potential requirement for laminin-α2 in postnatal oligodendrogenesis.

Oligodendrocyte development in vivo.

In the CNS, oligodendroglial specification, maturation, and myelination occur through a series of regulated developmental steps that can be identified through cell morphology and the expression of stage-specific markers (Colognato et al., 2005; Nishiyama, 2007) (Fig.I-2, modified from Colognato et al., 2005 and Nishiyama, 2007). At the embryonic stage, subsets of Sox2-positive intermediate progenitor cells arise from the germinal SVZ niche and generate progenitor cells (OPCs) that express the transcription factor Olig2, the early progenitor marker

PDGFRα, and/or the cell-surface proteoglycan NG2. Under the influence of chemoattractant/repellent cues, these OPCs migrate towards their target axons. Concurrently, mitogenic factors such as platelet-derived growth factor (PDGFα) stimulate proliferation and lead to the expansion of the OPC population. Eventually, OPCs exit from the cell cycle to differentiate into newly-formed oligodendrocytes. At this stage, oligodendrocytes begin expressing differentiated stage specific markers, including 2',3'-cyclic nucleotide 3'-phosphodiesterase (CNPase), and undergo extensive morphological changes (e.g., process extension and branching) that allow them to establish contact with axons, a particularly crucial step since cells that fail to associate with axons have been observed to undergo apoptotic cell death more readily (Trapp et al., 1997). Upon successful association with axons, mature oligodendrocytes acquire immunoreactivity to the protein APC (clone CC1), begin to synthesize myelin components such as myelin basic protein (MBP), and proceed with the myelin ensheathment of axons (Baron et al., 2005; Colognato et al., 2005).

Laminin α2 and myelination: insights from the peripheral nervous system.

Possible functions for laminin α2 in CNS myelination may be revealed by known roles of laminins in the peripheral nervous system (PNS). In the PNS, axon myelination is carried out by Schwann cells. These myelinating cells are surrounded by basal lamina (BL) and express laminins throughout development (Wallquist et al., 2002). Schwann cells also differentially express a whole repertoire of laminin receptors as they mature, suggesting distinct roles and requirements for different laminin ligands during PNS development and myelination (Previtali et al., 2003). Defects arising from the genetic loss of either BL components or their corresponding receptors led to varying defects in the Schwann cell development program or in PNS

myelination. Loss of laminin α2 or β1 integrin, for example, prevented Schwann cells from properly myelinating their target axons (Chen and Strickland, 2003; Feltri et al., 2002), resulting in amyelination (naked axon bundles) or improper axon defasciculation (Occhi et al., 2005; Yang et al., 2005). The Schwann cell-specific deletion of laminin γ1, on the other hand, resulted in decreased proliferation and increased apoptosis in these myelinating cells (Yu et al., 2005).

Unlike Schwann cells, oligodendrocytes do not have an associated basal lamina. In some developing white matter tracts in the CNS, the laminin α2-subunit expression can be found in association with axons prior to the onset of myelination (Colognato et al., 2002). Evidence supporting the role of laminin in CNS myelination, however, has been provided by studies on cultured oligodendrocytes and laminin-deficient animals. When provided as a substrate *in vitro*, α2 subunit-containing laminins have been shown to enhance both survival and myelin membrane formation in oligodendrocytes (Buttery and ffrench-Constant, 1999; Colognato et al., 2002; Howe, 2006). Synthetic microfibers coated with laminin-rich Matrigel have been shown to induce oligodendrocytes to extrude thick myelin membrane sheaths that wrap the fibers in a manner similar to nascent myelination *in vivo* (Howe, 2006). This pro-differentiation effect seems to be laminin-specific, as other ECM molecules such as fibronectins do not produce this similar magnitude of myelin membrane spreading and morphological complexity (Olsen and Ffrench-Constant, 2005).

The enhancement of morphological differentiation leading to myelin sheet formation by oligodendrocytes on laminin-2 is α6β1 integrin-dependent. Both modalities of integrin signaling (i.e., outside-in and inside-out) have both been shown to be critical for integrin function within the context of laminin-driven oligodendrocyte differentiation (Olsen and Ffrench-Constant, 2005). Disruption of outside-in signaling via addition of a β1 integrin-blocking antibody results

in decreased areas of myelin membrane formation in oligodendrocytes grown on laminin, compared to cells grown on the non-physiological substrate poly-D-lysine (PDL). Inside-out signaling via integrins is also critical. Oligodendrocytes infected with a constitutively active form of R-Ras, a known positive regulator of integrin inside-out signaling, exhibit an even bigger increase in myelin membrane sheet formation when cultured on a laminin substrate. Conversely, oligodendrocytes infected with a lentiviral-vector coding for the dominant negative form of R-Ras formed smaller myelin sheets on laminin, compared to wildtype R-Ras-infected cells (Olsen and Ffrench-Constant, 2005).

An *in vivo* study of the CNS myelin found in the laminin α2-deficient *dy/dy* (dystrophia muscularis) mouse showed that this animal model displays white matter abnormalites. Electron microscopy further revealed that *dy/dy* mice exhibited regional hypomyelination and dysmyelination of the CNS axons (Chun et al., 2003), suggesting that distinct phases of oligodendrocyte development may be perturbed by deficiencies in laminin-α2 expression.

Another role for laminin α2 is the enhancement of target-dependent survival of newly-formed oligodendrocytes in response to trophic factors, such as PDGF or neuregulin (Colognato et al., 2002; Frost et al., 1999). This hypothesis is substantiated by reduced oligodendrocyte survival observed when the oligodendrocyte α6β1 integrin is blocked from binding to laminin-2 expressed on dorsal root ganglia (DRG) neurons in culture (Frost et al., 1999). In addition, cell-specific deletion of the β1 integrin laminin-2 receptor promotes apoptosis of cells in the white matter of the developing cerebellum (Benninger et al., 2006). Thus, non-BL laminins in target axon tracts could regulate both oligodendrocyte survival and the active phase of myelin ensheathment, in contrast to Schwann cells, in which the BL appears to provide the necessary laminin signals.

A working model: laminin α2 in oligodendrogenesis, development, and CNS myelination.

The results presented in this dissertation reveal that α2-containing laminins are able to regulate postnatal oligogliogenesis and oligodendrocyte progenitor differentiation and do so, at least in part, by modulating downstream signaling molecules. These findings indicate that the dysregulation of signaling pathways required for normal oligodendrocyte development may contribute to CNS abnormalities observed in MDC1A, and identify novel mechanisms by which laminins regulate oligodendrogenesis, oligodendrocyte lineage progression, and myelination in the developing brain (Fig. I-3).

Figure I-1. Laminin heterotrimers are assembled from three different laminin subunits, and feature globular, coiled-coil, and rod-like domains in their general structure.

(A) All laminin molecules that have been identified *in vivo* are composed of three different gene products, one alpha (α), one beta (β), and one gamma (γ) subunit. These laminin subunits have a number of globular (represented by circles) domains and rod-like spacers (horizontal rectangles) containing epidermal-growth-factor-like repeats (short vertical lines in the rectangular spacer domains). (B) Laminin molecules have a coiled-coil domain formed via disulfide bonds between all the three different laminin chains (α chain in red, β chain in green, and γ chain in blue). At the C-terminus, several α globular (LG, numbered 1-5) domains provide discrete binding sites to allow laminin engagement with receptors (such as integrins and dystroglycan). The N-terminal (LN) globular domains at the short arms of the α, β, and γ chains allow laminin molecules to self-assemble and form part of the basement membrane. The internal domains (L4) are separated by tandem EGF repeats (LE). The nidogen-binding domain is shown in black on the blue γ chain. Figure modified from Durbeej, 2010.

A

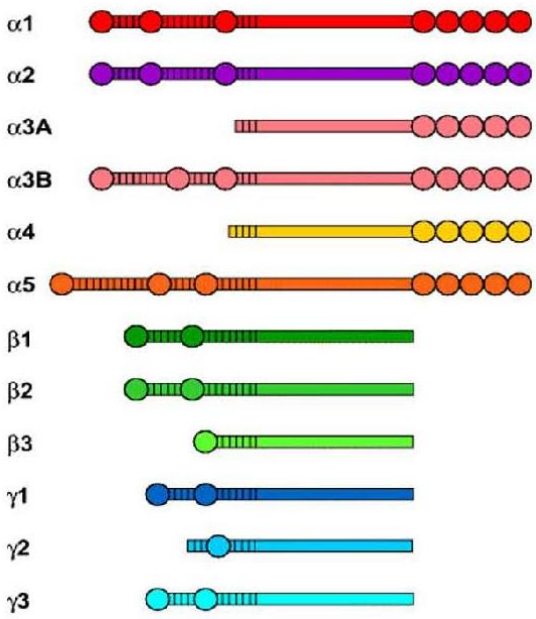
α1
α2
α3A
α3B
α4
α5
β1
β2
β3
γ1
γ2
γ3

B

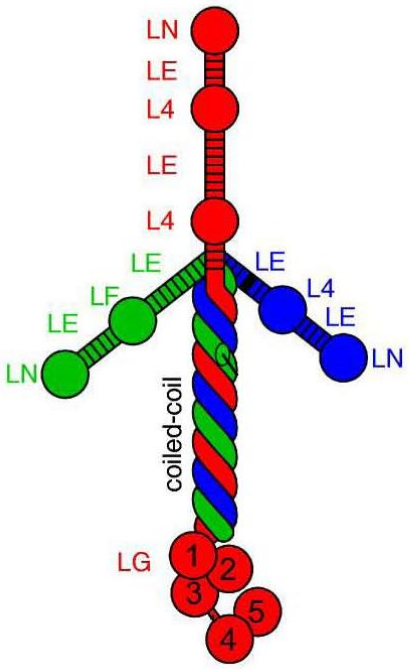
LN
LE
L4
LE
L4
LE
LE
LF
LE
LN
L4
LE
LN
coiled-coil
LG
1
2
3
4
5

Figure I- 2. Oligodendrocyte formation, maturation, and myelination *in vivo* can be identified through the expression of stage-specific markers.

From the germinal SVZ niche, a population of Sox2-positive intermediate progenitor cells (iPCs, colored pink) gives rise to oligodendrocyte precursor cells (OPCs). These OPCs express the transcription factor Olig2, early marker PDGFRα, and/or the cell surface proteoglycan NG2. As OPCs migrate towards future white matter tracts, these OPCs continue to proliferate, due in part to mitogenic factors (e.g., PDGFα). Oligodendrocyte progenitors eventually differentiate into newly-formed oligodendrocytes, which express maturation markers, such as CNPase. These newly differentiated oligodendrocytes also extend their processes to establish contact with axons, a step observed to promote target-dependent survival in oligodendrocytes. Upon associating with axons and receiving other differentiation signals, mature oligodendrocytes begin to synthesize myelin components (e.g., MBP), express other later-stage maturation markers (e.g., CC1), and proceed with myelin ensheathment of axons. Figure modified from Colognato et al., 2005 and Nishiyama, 2007.

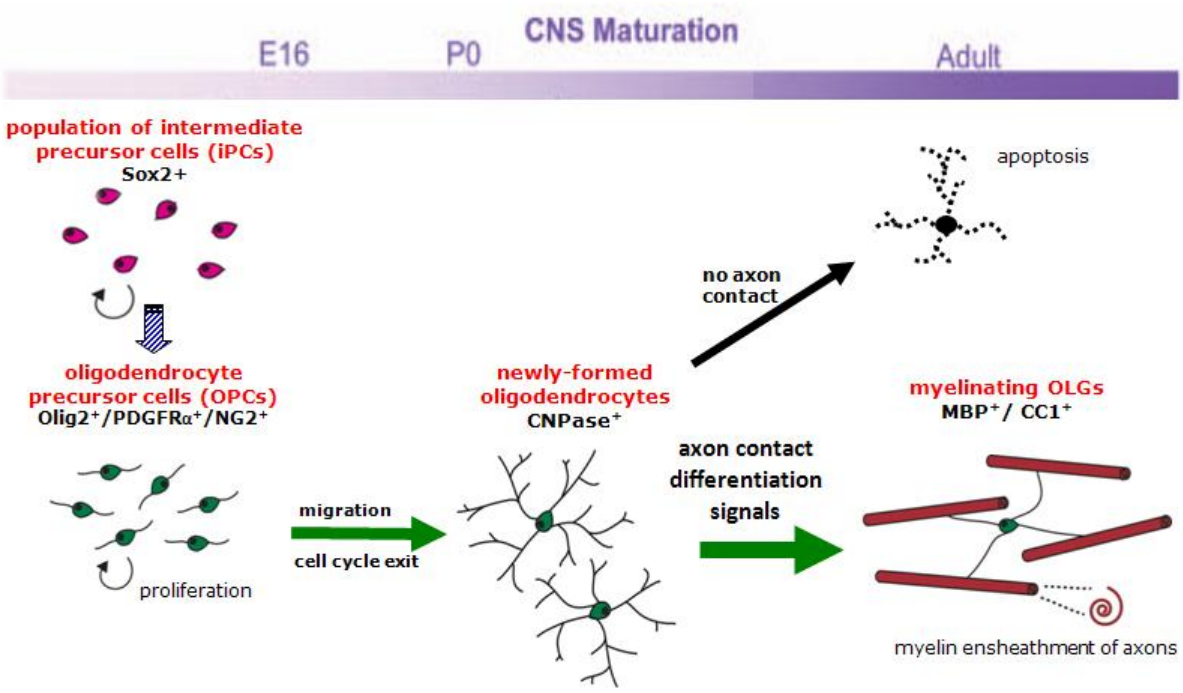
CNS Maturation
E16
P0
Adult
population of intermediate precursor cells (iPCs)
Sox2+
apoptosis
no axon contact
oligodendrocyte precursor cells (OPCs)
Olig2+/PDGFRα+/NG2+
newly-formed oligodendrocytes
CNPase+
myelinating OLGs
MBP+/ CC1+
axon contact differentiation signals
migration
cell cycle exit
proliferation
myelin ensheathment of axons

Figure I- 3. A working model: roles for laminin α2 in oligodendrogenesis, development, and CNS myelination.

Laminins (particularly α2-chain containing heterotrimers; Lm) have critical roles during postnatal oligodendrogenesis and oligodendrocyte progenitor differentiation. (1) Laminin promotes both OPC survival in the SVZ niche and OPC differentiation in the white matter tract. Laminin loss-of-function (red arrows) caused OPCs to die more readily early in postnatal development, and for fewer OPCs to be found in the white matter tract. (2) Laminin also promotes oligodendrocyte maturation by altering regulatory molecules in signaling pathways that normally promote myelination. Laminin deficiencies correlate with increased levels of Src family kinase inhibitors (Csk/Cbp) and the inappropriate inhibition of a positive regulator of myelination, Fyn. This work thus identifies novel mechanisms by which laminins regulate oligodendrocyte development and CNS myelination.

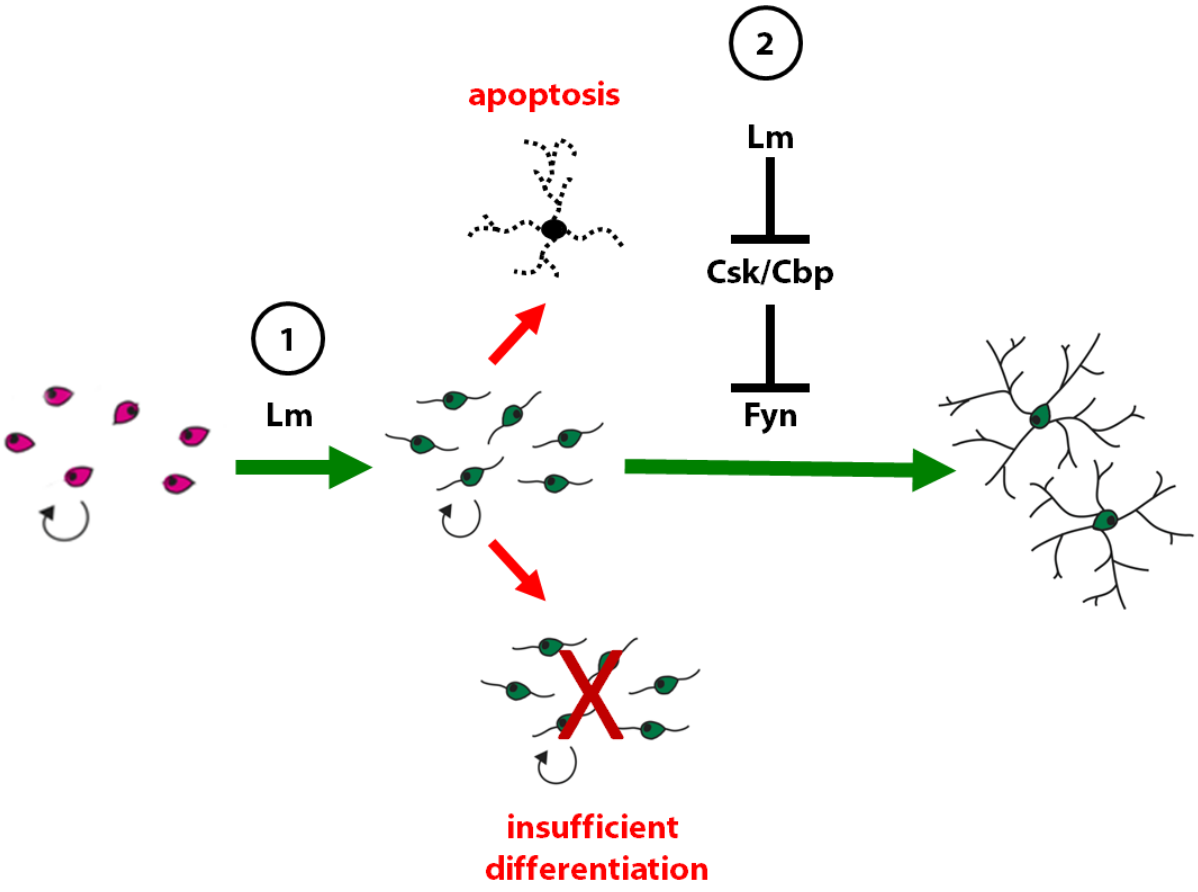
2
apoptosis
Lm
Csk/Cbp
1
Lm
Fyn
insufficient
differentiation

CHAPTER II: LAMININ ALTERS FYN REGULATORY MECHANISMS AND PROMOTES OLIGODENDROCYTE DEVELOPMENT*

ABSTRACT

Mutations in LAMA2, the gene for the extracellular matrix protein laminin-α2, cause a severe muscular dystrophy termed congenital muscular dystrophy type-1A (MDC1A). MDC1A patients have accompanying CNS neural dysplasias and white matter abnormalities for which the underlying mechanisms remain unknown. Here, I report that in laminin-deficient mice oligodendrocyte development was delayed such that oligodendrocyte progenitors accumulated inappropriately in adult brains. Conversely, laminin substrates were found to promote the transition of oligodendrocyte progenitors to newly-formed oligodendrocytes. Laminin-enhanced differentiation was Src Family Kinase–dependent and resulted in the activation of the Src Family Kinase Fyn. In laminin-deficient brains, however, increased Fyn repression was accompanied by elevated levels of the Src Family Kinase negative regulatory proteins, C-terminal Src kinase (Csk) and its transmembrane adaptor, Csk-binding protein (Cbp). These findings indicate that laminin deficiencies delay oligodendrocyte maturation by causing dysregulation of signaling pathways critical for oligodendrocyte development, and suggest that a normal role for CNS

* Reprinted with permission from "Laminin alters fyn regulatory mechanisms and promotes oligodendrocyte development" by Relucio, J., I.D. Tzvetanova, W. Ao, S. Lindquist, and H. Colognato. 2009. *J Neurosci*. 29(38):11794-11806, Copyright 2009 by the Society for Neuroscience.

laminin is to promote the development of oligodendrocyte progenitors into myelin-forming oligodendrocytes via modulation of Fyn regulatory molecules (Relucio et al., 2009).

INTRODUCTION

Children born with mutations in LAMA2, the gene that encodes the α2-subunit of the extracellular matrix protein laminin, have defects in the size and shape of the forebrain and cerebellum along with white matter abnormalities (Chun et al., 2003; Colognato et al., 2005). These abnormalities accompany severe muscular dystrophy and are collectively termed congenital muscular dystrophy type-1A (MDC1A). In the peripheral nervous system, laminins and their receptors regulate the ability of Schwann cells to proliferate, survive, radially-sort axons, and, ultimately, to myelinate (Court et al., 2006). In contrast, little is known about how laminins influence the development of oligodendroglia, the myelinating cells of the CNS. One study, however, has reported that α2-laminin-deficient mice have less forebrain myelin (Chun et al., 2003). While oligodendroglia lack basement membranes, structures in which laminin-mediated signal transduction has been defined classically, integrin and dystroglycan adhesion receptors have been implicated in oligodendrocyte laminin signaling using culture models (Baron et al., 2005; Colognato et al., 2007). Thus one possibility to account for MDC1A CNS abnormalities is that laminin deficiencies disrupt signaling pathways that contribute to oligodendrocyte lineage progression and/or oligodendrocyte function. However, it is not known whether laminins modulate oligodendrocyte lineage progression in the brain, and if so, through what signaling pathways.

Insights into the influence of α2-laminins on oligodendrocyte development have, however, been provided by *in vitro* studies. For example, oligodendrocytes cultured on laminin show enhanced process extension and myelin membrane expansion (Buttery and ffrench-

Constant, 1999; Howe, 2006). Laminins also enhance oligodendrocyte survival, at least in part by modulating receptor tyrosine kinase signaling (Colognato et al., 2002; Frost et al., 1999). Laminin has furthermore been shown to activate both integrin-linked kinase (ILK) and the Src-family-kinase Fyn in cultured oligodendrocytes (Chun et al., 2003). The link between laminin and Fyn may be particularly relevant to oligodendrogenesis since Fyn is required for normal CNS myelination (Kramer et al., 1999; Sperber et al., 2001; Umemori et al., 1994). These studies, together with reports of CNS abnormalities in laminin-deficient mice and people, suggest the hypothesis that laminin-mediated signaling guides the onset of oligodendrocyte differentiation in the developing CNS.

Here, α2-laminin-deficient mice were used to investigate the *in vivo* influence of laminins on oligodendrogenesis. Laminin-deficient brains were found to have a developmental delay in oligodendrocyte maturation accompanied by an accumulation of oligodendrocyte progenitor cells (OPCs). I furthermore identified several signaling abnormalities to account for these delays. Laminin-deficient brains showed dysregulated Fyn and elevated levels of C-terminal Src kinase (Csk) and Csk-binding-protein (Cbp), proteins that suppress Fyn activity. Laminin substrates were furthermore found to modulate Fyn regulation and to promote the transition of cultured oligodendrocyte progenitors to newly-formed oligodendrocytes in a Fyn-dependent manner. These findings indicate that the dysregulation of signaling pathways required for normal oligodendrocyte development may contribute to CNS abnormalities observed in MDC1A, and identify novel mechanisms by which laminins regulate gliogenesis in the developing brain.

MATERIALS AND METHODS

Animals

Dystrophic *dy/dy* mice were shown to have a severe decrease in expression of the laminin α2 protein, but to date the precise genetic mutation is thought to lie outside the LAMA2 coding region and has not been identified, therefore genotyping is not possible (Sunada et al., 1994). However, *dy/dy* mice exhibit a severe dystrophic phenotype that is readily apparent by ~2 weeks (weakness and hind leg paralysis). By 3 weeks *dy/dy* mice show characteristic hindlimb muscle atrophy, weakness, paralysis, and sporadic contractures and were separated from their wildtype littermates (homozygous +/+ and *dy/+*). To ensure that all *dy/dy* mice were identified correctly, we only evaluated brains at 3 weeks of age and older. Many dy/dy mice die prematurely between 4-6 weeks and therefore we restricted our analysis to mice at 6 weeks of age. Heterozygous 129P1/ReJ *dy/+* mice were obtained from The Jackson Laboratory (Bar Harbor, ME). All procedures were performed in accordance with the NIH Guide for the Care and Use of Laboratory Animals and approved by the Stony Brook University Institutional Animal Care and Use Committee.

Cell culture

Disassociated neonatal cortices from P0-P2 rats were cultured (37° C, 7.5% CO_2) in high glucose DMEM with 10% fetal calf serum (FCS) on poly-D-lysine (PDL)-coated flasks.

Medium was changed every 3-4 days. By day 10-14, mixed glial cultures consisting of oligodendrocyte precursor cells (OPCs) and microglia on an astrocyte monolayer were obtained. Purified OPCs were isolated from mixed glial cultures using a modification of the mechanical dissociation and differential adhesion method described by McCarthy and de Vellis (McCarthy and de Vellis, 1980). To evaluate protein expression and protein phosphorylation in response to substrate conditions, OPCs were suspended in modified SATO's medium and added to Nunclon dishes coated with PDL or laminin-2 (human placental laminin, Sigma). To coat dishes, PDL or laminin-2 at 10 μg/ml were incubated for 4 hours at 37° C. Following coating, surfaces were blocked with 10 μg/ml heat-inactivated, endotoxin-free BSA for 30 minutes at 37° C and washed with PBS. At indicated time points, cells were lysed in extraction buffer (1% SDS, 20 mM Tris pH 7.4 containing protease and phosphatase inhibitor cocktails (Calbiochem) added immediately prior to use) and heated to 95° C for 5 minutes.

Antibodies

The following antibodies were used for immunocytochemistry: rat monoclonal IgG against laminin α2 subunit, clone 4H82 (Sigma); rabbit polyclonal IgG against laminin-1 (Sigma); mouse monoclonal IgG against neurofilament (NF) (Sigma); rat monoclonal IgG against PDGFRα (BD Biosciences); rat monoclonal IgG against myelin basic protein (MBP) (Serotec); mouse monoclonal IgG against APC (CC1) (Calbiochem). FITC-, Texas Red-, Cy3- and biotin-conjugated donkey antibodies against rat, rabbit, and mouse IgG were used as secondary antibodies (Jackson Immuno). Texas Red-conjugated strepavidin (Jackson Immuno) was used to detect biotinylated secondary antibodies. The following antibodies were used for

Western blotting: rabbit polyclonal IgG against NG2 (a generous gift from Dr. Joel Levine, Stony Brook University, NY); mouse monoclonal IgG against CNP (Sigma); rat monoclonal IgG against MBP (Serotec); mouse monoclonal IgG against Kip1/p27 (BD Transduction Laboratories); rabbit monoclonal IgG against the quaking homolog KH domain RNA-binding protein (QKI) (Bethyl Laboratories); rabbit polyclonal IgG against cleaved caspase-3 (Asp175) (Cell Signaling Technology); rabbit polyclonal IgG against Fyn (Santa Cruz Biotechnology); rabbit polyclonal IgG against phospho-Tyr418 of Src family kinases (Calbiochem); rabbit polyclonal IgG against phospho-Tyr529 of Src family kinases (Calbiochem); rabbit polyclonal IgG against Csk (C-20) (Santa Cruz Biotechnology); rabbit polyclonal IgG against Cbp (generously provided by Jon Lindquist, Otto-von-Guericke-University, Magdeburg); rabbit polyclonal IgG against phospho-Tyr317-Cbp (Tyr314-Cbp in mouse, raised against phospho-peptide KEISAMpYSS); and mouse monoclonal IgG against β-actin (Sigma).

Western blot analysis

Cerebral cortices and cerebella were collected from 3- and 6-week old *dy/dy* and wildtype littermates. Following addition of extraction buffer (1 mL buffer per 200 mg tissue), tissues were incubated at 95° C for 10 minutes with occasional trituration. Homogenates were then centrifuged at 14,000 rpm to remove insoluble material. Protein concentration was determined (detergent compatible protein assay, BioRad) and the lysates were boiled for 5 minutes in Laemmli Solubilizing Buffer (LSB) with 4% β-mercaptoethanol (βME). Proteins were separated by SDS-PAGE using 7.5, 10, 12, or 15% acrylamide minigels and transferred onto 0.45 µm nitrocellulose. Membranes were blocked in 0.1 % Tween-20, and Tris buffered saline (TBS-T)

containing either 4% bovine serum albumin (BSA) or 1% non-fat milk (blocking buffer) for 1 hour, followed by primary antibodies in blocking buffer overnight at 4° C. Membranes were washed in TBS-T, incubated for 1 hour in HRP-conjugated secondary antibodies (Amersham) diluted 1:1000 in blocking buffer, washed in TBS-T, then developed using enhanced chemiluminescence (Amersham). Relative densitometries were determined using the NIH ImageJ Processing and Analysis Program.

Fluorescent immunocytochemistry using fresh frozen sections

Tissues were embedded in Tissue-Tek OCT (Sakura Finetek) and cryosectioned to a thickness of 25 μm. Fresh frozen sections were fixed in methanol for 5 minutes at -20° C. After washing in PBS, sections were blocked for 1 hour in PBS containing 10% donkey serum (DS; Sigma), followed by overnight incubation with primary antibodies in block buffer at 4° C. Sections were then washed in PBS and incubated in Texas Red-, CY3-, or FITC-conjugated secondary antibodies for 1 hour, then washed again in PBS. Sections were incubated in 10 μg/mL DAPI in PBS for 10 minutes to counterstain nuclei and mounted using Slowfade Gold antifade reagent (Invitrogen).

Fluorescent immunocytochemistry using perfused tissue

Mice were anesthetized with Avertin and perfused intracardially with a saline solution, followed by 4% paraformaldehyde (PFA) in PBS. Brains were harvested, post-fixed for 1 hour in PFA, and incubated overnight in 30% sucrose at 4° C. Tissues were embedded in Tissue-Tek

OCT (Sakura Finetek) and cryosectioned to a thickness of 25 μm. For MBP immunocytochemistry, sections were post-fixed in ethanol: acetic acid (95:5) for 20 minutes at -20° C. After quick washes in PBS, sections were incubated in 10% DS with 0.05% Triton X-100 for 1 hour before labeling with anti-MBP primary antibodies. FITC-conjugated secondary antibodies were incubated in 10% DS for 1 hour.

Alternatively, 50 μm floating sections were prepared. Briefly, cryosections were placed in chilled tissue stock solution (30% glycerol: 30% ethylene glycol: 10% 0.2 M phosphate buffer) to remove the remaining OCT. For immunodetection of OPCs, floating sections were post-fixed for 15 minutes in 4% PFA then washed 3 times in PBS with 0.2% Triton X-100 (PBST). After blocking in 1% DS in PBST for 30 minutes, the sections were incubated in anti-PDGFRα primary antibody overnight at room temperature. Sections were then washed once with PBST and incubated in fluorescent secondary antibody for 1 hour. Finally, floating sections were washed 3 times with PBST, followed by 3 washes with 0.1M phosphate buffer. All sections were incubated in 10 μg/ml DAPI in PBS for 10 minutes to visualize nuclei before finally being mounted with SlowFade Gold antifade reagent.

Oligodendrocyte cell density and survival

To determine whether the laminin-α2 deficiency in *dy/dy* mice affects oligodendrocyte cell density, fresh frozen cortical, cerebellar, and brain stem sections (25 μm) were fixed in 4% PFA for 15 minutes at room temperature. Following washes with PBS, sections were incubated in 10% DS with 0.5% Triton X-100 for 1 hour at room temperature. Immunocytochemistry using anti-APC (CC1; a marker expressed in mature oligodendrocytes) or anti-PDGFRα primary

antibody was carried out overnight at 4°C. Sections were washed 4 times in PBS then incubated in Cy3-conjugated secondary antibody for 1 hour, before washing again in PBS. In the cerebral cortex, CC1(+) oligodendrocytes and PDGFRα(+) OPCs were counted in the corpus callosum, lateral septum, and anterior commissure. Along the corpus callosum, oligodendroglia found at the fornix and at fixed distances of 0.8, 1.0, and 1.7 mm from the midline were scored in matching sections of wildtype and *dy/dy* brains. CC1(+) and PDGFRα(+) cell densities were also determined in the proximal white matter of the cerebellum, white matter of cerebellar folia, and ventral regions of the brain stem.

To identify apoptotic oligodendroglia, the CC1- and PDGFRα-immunostained sections were subjected to a TUNEL assay according to the manufacturer's instructions (Apoptag). Sections were then counterstained with 10 μg/ml DAPI and mounted with SlowFade Gold antifade reagent. TUNEL-positive cells per unit area, as well as the percentage of TUNEL-positive, CC1-positive cells (or TUNEL-positive, PDGFRα-positive cells) were determined.

Fluorescence microscopy and image acquisition

Sections were visualized using a Zeiss Axioplan inverted fluorescence microscope fitted with 10X eyepiece magnification using 5X (0.16 N.A.), 10X (0.3 N.A.), 20X (0.5 N.A.), 40X (0.75 N.A.), and 63X (1.4 N.A., oil) objectives. Images were acquired using a Zeiss Axiocam MRM digital camera and Zeiss AxioVision imaging software. For thick sections (50 microns) imaged using 63X oil immersion, Z-stacks of 0.25 micron increments were captured and maximal image projections were obtained.

Electron microscopy and morphometric analysis

Mice were perfused with 4% paraformaldehyde/ 2.5% glutaraldehyde in 0.1 M phosphate buffered saline. The brains were postfixed overnight in the same fixative and then individual structures were cut in the appropriate plane on a Leica VT-1000 vibratome at 50-60 µm. Vibratomed sections were processed using standard transmission electron microscopy techniques. Briefly, vibratomed sections were placed in 2% osmium tetroxide in 0.1M phosphate buffer, washed in 0.1M phosphate buffer and dehydrated in a graded series of ethyl alcohol. Sections were then vacuum infiltrated in Durcupan resin (Drurcupan ACM Epoxy, Electron Microscopy Sciences) overnight, flat embedded between two pieces of ACLAR film (Ted Pella) and placed in a 60^{o} C oven for 48-72 hours to polymerize. Areas to be sampled were blocked and ultrathin sections were cut at approximately 70-80 nm on a Rechert-Jung Ultracut E ultra-microtome. Ultrathin sections were placed on formvar coated copper slot grids and counterstained with uranyl acetate and lead citrate. Samples were viewed with a FEI Tecnai BioTwinG^2 transmission electron microscope. Digital images were acquired with an AMT XR-60 CCD digital camera system and compiled and analyzed using Adobe Photoshop and ImageJ (NIH). The g-ratio of myelinated axons was determined by dividing the axon diameter by the myelin diameter. A minimum of 300 axons per genotype was measured for each region.

Statistics

Statistical significance of data sets was determined using the Student's two-tailed, paired *t*-test. Raw values were then normalized to each wildtype littermate control (wildtype of the pair set at 100%). Graphs depict the mean values, with error bars depicting standard error of the

mean. Statistical analysis on overall g-ratio was performed using the Mann-Whitney Rank Sum Test (SigmaStat). Student's t-test was performed on binned g-ratios where normal distribution and equal variance was determined; mean g-ratio and S.E.M. is depicted (SigmaStat).

RESULTS

Laminin-deficient brains show delayed oligodendrocyte maturation.

Human laminin deficiencies result in a variety of CNS developmental defects that may in part reflect altered gliogenesis. Indeed, hypomyelination has been reported in the corpus callosum and optic nerve of 5 week-old *dy/dy* mice, a dystrophic mouse model in which laminin α2 subunit expression is severely reduced but not absent (Chun et al., 2003). To determine whether laminins influence the progression of oligodendrogenesis, I evaluated both oligodendrocytes and oligodendrocyte progenitors in dy/dy brains at two different ages. First, I evaluated mature oligodendrocytes by counting the number of cells positive for CC1, a marker for oligodendrocyte cell bodies (Fig. II-1). In 3 week old corpus callosum, I found a significant reduction in the number of CC1(+) cells per mm^2 in *dy/dy* animals compared to wildtype littermates (Fig. II-1A & II-1B, and Table 1; 1100.1 ± 54.0 versus 1404.6±103.0, respectively, n=3, p= 0.0287). By 6 weeks, however, the density of CC1(+) cells in the corpus callosum of both wildtype and *dy/dy* animals had increased; these increases were greater in *dy/dy* animals such that by 6 weeks *dy/dy* and wildtype corpus callosum had similar levels of CC1(+) cells (Fig. II-1A and Table 1; 1828.5± 268.6 CC1(+) cells per mm^2 in wildtype animals; 1640.8±234.5 in *dy/dy* littermates, n=3, p=0.2804). This result suggested that, in the corpus callosum, oligodendrocyte differentiation is delayed, but not prevented.

To determine whether oligodendrocyte differentiation was delayed in other brain regions, I evaluated CC1(+) cell density in cerebellum and brain stem (Fig. II-1C & II-1D). In the proximal white matter of 3 week old cerebella, I found similar levels of CC1(+) positive cells in

wildtype and dy/dy littermates (Fig. II-1C; n=5, p=0.3438). In wildtype mice, however, between 3 weeks and 6 weeks the CC1(+) cell density significantly increased (Fig. II-1C and Table 1; 978.2±196.7 versus 1840.8±70.5, n=5, p=0.0074) whereas in *dy/dy* mice CC1(+) cell density did not significantly change (Fig. II-1C and Table 1; n=5; p=0.3284). It should be noted that between 3 weeks and 6 weeks there was not a significant *decrease* in CC1(+) density in *dy/dy* cerebella; instead, oligodendrocytes in dy/dy cerebella failed to keep pace with the increase in density that was observed in wildtype animals. In brain stem (Fig. II-1D) a similar phenomenon occurred: similar CC1(+) cell density was observed in wildype and *dy/dy* brain stems at 3 weeks of age, but by 6 weeks, CC1(+) cell density had significantly increased in wildtype brain stem (Fig. II-1D and Table 1; 1405.1±-64.9 cells per mm^2 up from 988.5±104.7 cells per mm^2 at 3 weeks, n=5, p=0.0159) but did not significantly increase in dy/dy brain stem (Fig. II-1D and Table 1; 1054.4±47.6 compared to 1084.6±104.1 at 3 weeks, n=5, p=0.9369). Again, CC1(+) cell density did not significantly drop in *dy/dy* brain stem between 6 weeks and 3 weeks, suggestive of a slow or stalled differentiation rather than a loss of cells. In addition to the brain structures reported in Fig. II-1, several different cortical regions were evaluated (lateral septum and anterior commissure) as well as total cerebellar white matter, spinal cord, and optic nerve (see Table 1). In each region, CC1(+) cell density was either similar or lower in *dy/dy* animals compared to wildtype littermates, at both 3 weeks and 6 weeks. In all cases CC1(+) density increased in wildtype regions between 3 weeks and 6 weeks, whereas in some regions e.g. corpus callosum, *dy/dy* CC1(+) density caught up to wildtype density by 6 weeks, but in some regions e.g. cerebellum, it did not. These differences suggest different regional variation in the role of laminin in modulating timely development of appropriate oligodendrocyte numbers.

I then evaluated levels of myelin basic protein (MBP) in *dy/dy* brains versus wildtype littermates (Figs. II-1E and II-1F). In agreement with a previous study by Chun and colleagues (Chun et al., 2003) less MBP protein was observed in *dy/dy* cerebral cortices compared to wildtype cerebral cortices (Fig. II-1F; 69.8 ± 8.3% of protein in wildtype littermate cerebral cortices, n=3, p=0.049). I also monitored the expression of 2', 3'-cyclic nucleotide 3'-phosphodiesterase (CNP) and found reduced CNP levels in *dy/dy* cerebral cortices compared to wildype littermates (73.3 ± 10.6%, n=3, p=0.047, not shown). In addition, the overall organization of white matter tracts was visualized using MBP immunoreactivity, with *dy/dy* MBP(+) tracts appearing grossly normal but often appearing more sparse compared to wildtype counterparts (Fig. II-1E).

Correlation between delayed oligodendrocyte differentiation and myelination abnormalities in dy/dy brains.

Given that delayed oligodendrocyte differentiation showed a differential time course in *dy/dy* cerebella compared to that in cerebral cortices, we sought to determine whether the degree of myelination in the *dy/dy* cerebella correlated with its differentiation delay. Overall, the gross organization of white matter appeared normal in *dy/dy* cerebellum, as reflected by MBP and neurofilament immunoreactivity (Fig. II-2A). However, *dy/dy* cerebella showed a small, but significant, reduction in MBP levels relative to that found in wildtype littermates (Fig. II-2B; 84.1 ± 0.12%, n=4, p=0.025). It should also be noted that at 3 weeks of age *dy/dy* cerebellar white matter regions showed low level laminin α2 immunoreactivity, particularly associated with blood vessels (Fig. II-2C). This *dy/dy* laminin α2 immunoreactivity, however, was substantially less than in wildtype littermates, and by 6 weeks *dy/dy* cerebella did not show any residual

laminin α2 reactivity that was detectable above that in negative controls (Fig. II-2C). Next, we assessed myelin ultrastructure using transmission electron microscopy and found that *dy/dy* cerebellar axons, relative to their wildtype littermates, exhibited thinner myelin at 6 weeks of age; representative micrographs are shown in Fig. II-2D. Individual cerebellar g-ratios were plotted as a function of axon diameter (Fig. II-2E); a significant trend ($p<0.001$) was observed such that the median g-ratio was larger in *dy/dy* cerebella (0.874) compared to that in wildtype cerebella (0.832). Cerebellar g-ratios were also grouped by axon diameter to reveal that *dy/dy* cerebellar axons of all sizes showed significantly thinner myelin (Fig. II-2F). Thus in the cerebellum, delayed oligodendrocyte maturation correlated with dysmyelination (i.e., thinner myelin).

We proceeded to evaluate whether the optic nerve, previously reported to show myelin abnormalities (Chun et al., 2003), also showed delayed oligodendrocyte maturation (Fig. II-3). CC1 immunoreactivity revealed fewer mature oligodendrocytes per area in *dy/dy* optic nerves relative to those in wildtype littermates (Figs. II-3A and II-3B; Table 1). We also confirmed that *dy/dy* optic nerves at 6 weeks of age were dysmyelinated relative to wildtype littermates using transmission electron microscopy (Figs. II-3C and II-3D). In particular, significantly increased g-ratios were observed in a subset of axons larger than 1.0 microns in diameter (Fig. II-3E). We then analyzed a variety of brain regions using transmission electron microscopy to determine whether in general, delays or deficits in oligodendrocyte maturation corresponded with abnormal myelination **(**Fig. II-4**)**. We observed significant increases in g-ratio, indicative of thinner myelin, in cerebellum (Fig. II-2), optic nerve (Fig. I-3), and a subset of small caliber axons in the brain stem (Fig. II-4E). In contrast, however, the anterior commissure and corpus callosum showed no significant change in g-ratio but showed increased percentages of unmyelinated axons (Figs. II-

2A to II-2D). We noted that, overall, the degree of regional abnormalities in oligodendrocyte maturation at 6 weeks in general correlated with the degree of myelin abnormalities at 6 weeks (Figs. II-1, II-2, II-3, II-4, and Table 1).

Delayed differentiation of oligodendrocyte progenitors in dy/dy brains.

An observed decrease in mature oligodendrocytes at 3 weeks could result from a decreased availability of oligodendrocyte progenitors in future white matter target regions. Alternatively, oligodendrocyte progenitors may be available in target regions, but may differentiate poorly or on a slower time scale. A third possibility is that progenitors differentiate in a timely manner and in appropriate numbers, but that these newly-matured oligodendrocytes are then selectively eliminated via cell death. To distinguish between these possibilities, I first investigated whether *dy/dy* brains contained an adequate supply of oligodendrocyte progenitors in the correct locations by examining the numbers of PDGFRα(+) cells per area in the same 8 regions that were analyzed for the presence of mature oligodendrocytes (Table 2). Lineage tracing studies have shown that PDGFRα(+) cells in the developing and adult CNS white matter primarily give rise to oligodendrocytes (>90%), and generate very few astrocytes and/or neurons (He et al., 2009; Rivers et al., 2008; Sim et al., 2009; Tripathi et al., 2010). At 3 weeks, I found that levels of oligodendrocyte progenitors differed significantly between *dy/dy* brains and their wildtype littermates (Fig. II-5). In 3 week old corpus callosum, I found a significant increase in the number of PDGFRα(+) cells per mm^2 in *dy/dy* animals compared to wildtype littermates (Fig. II-5A, and Table 2; 1098.7±107.0 versus 763.4±65.5, respectively, n=3, p= 0.0193). By 6 weeks, however, the density of PDGFRα(+) cells in the corpus callosum of both wildtype and *dy/dy* animals had decreased, although *dy/dy* corpus callosum still had an increased density of

PDGFRα(+) oligodendrocyte progenitors relative to wildtype littermates (Fig. II-5A and Table 2; 917.4±78.9 cells per mm^2 in *dy/dy* versus 413.5±59.1 in wildtype, n=3, p=0.0212).

To investigate whether increased numbers of PDGFRα(+) oligodendrocyte progenitors occurred regionally versus globally, I evaluated progenitor numbers in cerebellum, brain stem, spinal cord, and in a variety of additional brain regions in which reduced numbers of mature oligodendrocytes had been observed (Fig. II-5 and Table 2). I first noted that the central white matter of the cerebellum had a similar pattern of elevated numbers of PDGFRα(+) cells such that *dy/dy* cerebella at 3 weeks showed significantly higher numbers of PDGFRα(+) cells per mm^2 compared to wildtype littermates (Fig II-5C; 622.6±129.6 versus 255.7±18.0, respectively, n=3, p=0.0486). By 6 weeks, however, PDGFRα(+) cell density in wildtype cerebella remained unchanged compared to 3 week levels, whereas PDGFRα(+) cell density in *dy/dy* cerebella remained significantly elevated (Fig. II-5C and Table 2; 534±40.0 cells per mm^2 versus 364.2±12.4, n=3, p=0.0367). In *dy/dy* brain stem, however, we did not observe any change in PDGFRα(+) cell density (Fig. II-5D and Table 2; 259.4±34.1 cells per mm^2 in *dy/dy* versus 259.7±13.6 in wildtype, n=3, p=0.9953), which may reflect the fact that the brain stem is one of the earliest regions to myelinate and thus oligodendrocyte development may have normalized by 3 weeks.

In addition to elevated numbers of oligodendrocyte progenitors, *dy/dy* brain lysates were observed to have elevated levels of NG2 (Figs. II-5E and II-5F; 183.5 ± 28.9%, n=4, p=0.022, at 6 weeks), a chondroitin sulfate proteoglycan expressed in oligodendrocyte progenitors but not in mature oligodendrocytes (Nishiyama et al., 1996; Stallcup, 1981). NG2 immunostaining confirmed that *dy/dy* cerebral cortices had a higher degree of NG2 immunoreactivity in the cerebellum and in the corpus callosum compared to wildtype littermates (not shown). Overall,

the decreased expression of maturation markers i.e. CC1 and MBP, accompanied by accumulation of progenitor markers i.e. PDGFRα and NG2, indicates that the timing of oligodendrocyte maturation could be altered in laminin-α2-deficient brains.

The Src Family Kinase Fyn is dysregulated in dy/dy brains.

The Src family kinase (SFK) Fyn is required for normal myelination such that mice lacking Fyn, as well as mice expressing a catalytically-inactive Fyn, have myelination defects (Osterhout et al., 1999; Sperber et al., 2001; Umemori et al., 1994). Fyn activity is tightly regulated by phosphorylation at several highly conserved tyrosines: an autophosphorylation site at tyrosine 418, and an inhibitory site at the C-terminal tyrosine 529. Because Fyn has been shown to be activated downstream of laminin in cultured oligodendrocytes (Colognato et al., 2004), I examined Fyn in laminin-deficient brains. Western blot analysis of *dy/dy* cortical lysates, however, revealed no significant differences in levels of Fyn protein compared to wildtype littermates (Fig. II-6A and II-6B; 114.7 ± 1.7%, n=3). I then evaluated the regulation of Fyn using antibodies against the SFK phosphorylation sites at Y418 (catalytic) and Y529 (regulatory). Oligodendrocytes express two SFKs, Fyn and Lyn, but Lyn protein and Lyn activity is virtually undetectable in myelin by 2 weeks of age (Kramer et al., 1999). By three weeks of age, Fyn and its kinase activity are elevated and correlate with the period of active myelination (Kramer et al., 1999; Lu et al., 2005). Using Western blots, I observed that levels of phosphorylated Y529 (relative to total Fyn levels) were increased by almost 2-fold in 3 week old *dy/dy* cortices compared to wildtype cortices (Figs. II-6A and II-6B; 190.9 ± 36.5%, n=3, p=0.0022), and remained elevated at 6 weeks of age, albeit with increased variability (174.9 ±

102.6%, *n*=6, *p*=0.24; not shown). The increased levels of phosphorylated Y529 indicated that Fyn was dysregulated in laminin-deficient mice.

Similar to *dy/dy* cortices, the cerebella of *dy/dy* mice expressed normal levels of Fyn (Figs. II-6C and II-6D*;* 103.3 ± 8.7% at 3 weeks, *n*=3; 95.5 ± 35.2% at 6 weeks, not shown). Levels of phosphorylated Y529 (relative to total Fyn), however, were higher in *dy/dy* cerebella than in wildtype cerebella (Figs. II-6C and II-6D; 147.3 ± 17.1%, *n*=3, *p*=0.026), although the degree of elevation was not as strong as in the cortex (190.9 ± 36.5% in the cortex, versus 147.3 ± 17.1% in the cerebellum). In contrast to cerebral cortices, however, the levels of phosphorylated Y529 in laminin-deficient cerebella returned to normal at 6 weeks (111.1 ± 34.6%, *p*=0.56, not shown). Taken together, these results indicate that Fyn is dysregulated in the brains of laminin-deficient mice, however, the cortex and cerebellum exhibited regional variation in terms of how much Fyn dysregulation occurred. It should be noted, however, that no significant changes in Fyn protein, Fyn phosphorylation, or Csk protein were observed between the cerebellum and cerebral cortex of wildtype mice (n=3; not shown). The observed Fyn dysregulation in laminin-deficient mice indicates that similar signaling abnormalities may contribute to the CNS pathology seen in MDC1A.

dy/dy brains contain elevated levels of Csk and Cbp, negative regulators of Fyn.

Based on the observations that Fyn was regulated inappropriately in laminin-deficient brains, I proceeded with examining the expression of known negative regulators of Fyn and other Src Family Kinases. The protein C-terminal Src kinase (Csk), shown previously to be expressed in oligodendrocytes, has been shown to be the principal kinase to regulate Fyn via

phosphorylation of the inhibitory Y529 site (Colognato et al., 2004; Takeuchi et al., 1993). And, in the presence of laminin-2, cultured oligodendrocytes were previously found to have decreased levels of phosphorylated Fyn Y529, suggesting that Csk activity can be affected by laminin (Colognato et al., 2004). In conjunction with elevated levels of Y529 phosphorylation, *dy/dy* cortices and cerebella at 3 weeks of age showed increased Csk protein compared to wildtype littermates (Figs. II-6A and II-6B, Csk in *dy/dy* cortices, 180.7 ± 30.3%, n=3, p=0.027; Fig. II-6D, 154.6 ± 31.5%, p=0.134 in cerebella; Csk normalized to actin levels in each lysate). By 6 weeks, Csk levels decreased in both wildtype and *dy/dy* cortices, compared to their respective levels at 3 weeks (not shown).

Csk binding protein (Cbp) is required for normal Csk function. This transmembrane adaptor protein is found in lipid raft microdomains and has been shown to recruit Csk to the membrane where myristoylated molecules such as Fyn are located (Kawabuchi et al., 2000; Takeuchi et al., 2000). I found that Cbp levels in the cortices of 3 week old *dy/dy* mice were significantly elevated compared to wildtype levels (Figs. II-6A and II-6B; 147.8 ± 34.9%, n=4, p=0.029). Cbp levels in *dy/dy* cerebella were also elevated relative to Cbp in wildtype cerebella (Fig. II-6D; 163.8 ± 68.5%, n=3, p=0.18). By 6 weeks, Cbp levels in *dy/dy* cortices and cerebella remained somewhat elevated, but only by ~28% of wildtype levels (128.7 ± 35.9%, n=3, p=0.31 in cortices; and 128.6 ± 54.5%, n=3, p=0.65 in cerebella). Csk is known to bind to a phosphorylated tyrosine 317 on Cbp; this binding both activates Csk and increases Csk affinity for Fyn (Matsuoka et al., 2004). In *dy/dy* cortices, I observed levels of Cbp Y317 phosphorylation (relative to total Cbp) that were similar to wildtype levels at all time points and regions investigated (not shown). Taken together, the elevated expression of both Csk and Cbp in

laminin-deficient *dy/dy* cerebral cortices suggests that these molecules may contribute to Fyn dysregulation.

Laminin promotes oligodendrocyte progenitor cell differentiation.

While I observed changes in Fyn regulation in vivo, it remained unclear whether these changes were occurring in oligodendrocyte progenitors or oligodendrocytes failing to make appropriate laminin contact. To determine whether the loss of laminin altered Fyn phosphorylation in oligodendrocyte progenitor cells, I placed isolated rat oligodendrocyte progenitor cells (OPCs) in contact with laminin-2 substrates and monitored Fyn Y529 phosphorylation (Fig. II-7). I found that on laminin substrates Fyn phosphorylation at Y529 was decreased substantially (Figs. II-7A and II-7B; 37.44± 5.8% relative to phosphorylation levels on poly-D-lysine (PDL) substrates, p=0.0045). This laminin-mediated suppression of Fyn phosphorylation in cultured rodent OPCs suggested that the abnormally high degree of phosphorylation of Fyn Y529 in *dy/dy* brains may be due to loss of appropriate laminin contact.

The decreased numbers of mature oligodendrocytes and increased numbers of oligodendrocyte progenitors that were together observed in laminin-deficient brains indicated that laminin contact with oligodendrocyte progenitors might be able to promote or change the timing of differentiation into newly-formed oligodendrocytes. We sought to determine whether laminin contact could promote oligodendrocyte progenitor cell differentiation. We placed oligodendrocyte progenitors on laminin versus PDL substrates for 24 hours and evaluated the percentage of cells that expressed CNP, a protein expressed by newly-formed oligodendrocytes but not oligodendrocyte progenitors (Figs. II-7C and II-7D). We found that oligodendrocyte

progenitors grown on laminin showed an approximately 2-fold increase in the percentage of cells expressing CNP after 24 hours (Fig. II-7D; n=3, p=0.0128). In contrast, cells treated with PP2, a Src Family Kinase inhibitor, did not show any laminin-mediated enhancement of oligodendrocyte progenitor differentiation (Fig. II-7D; n=3, p=0.9801). Together these results suggest that laminin promotes the transition from oligodendrocyte progenitor cell to newly-formed oligodendrocyte and this laminin-mediated effect depends on Src Family Kinase activity. After 4 days on laminin or PDL substrates, however, we did not observe any substrate-mediated difference in the percentage of CNP(+) cells (not shown), suggesting that laminin may accelerate differentiation but is not required for it per se. This finding would be consistent with *in vivo* observations in which laminin-deficient animals at 3 weeks show delays in differentiation that are partially or fully remedied by 6 weeks, depending on the region (Figs. II-1, II-2, and II-5; Tables 1 and 2).

Dysregulation of p27 occurs in the dy/dy cerebellum.

Because the timing of oligodendrocyte differentiation is altered in laminin-deficient brains, I examined the expression of the cyclin-dependent kinase inhibitor, p27, a protein known to exert temporal control over oligodendrocyte development. p27 is known to be upregulated progressively as OPCs undergo cell division, and p27 protein levels peak with the onset of active myelination (reviewed in Nguyen et al., 2006). There were small decreases in p27 levels in both the *dy/dy* cerebral cortex (85.2 ± 22.3%, n=*3*, *p*=0.38) and *dy/dy* cerebellum (93.7 ± 32.5%, *n*=3, *p*=0.93) compared to their wildtype littermates at 3 weeks (not shown). By 6 weeks, however, p27 levels were substantially higher in both brain regions of *dy/dy* mice relative to that in wildtype littermates (Figs. II-8A and II-8B; 298.4 ± 223.1%, *n*=3, *p*=0.12 in the cortex; 224.0 ±

127.2%, *n*=3, *p*=0.047 in the cerebellum). Interestingly, I also observed increased levels of the RNA binding protein, QKI, in the cerebella of *dy/dy* brains (183.0 ± 73.2% of wildtype levels, *n*=4, *p*=0.035, not shown). QKI is a downstream target of Fyn and has been shown to stabilize mRNAs critical to the myelination process including p27 and MBP transcripts (Larocque and Richard, 2005; Lu et al., 2005). Finally, my collaborators also monitored oligodendrocyte progenitor p27 protein levels at 2 hours and 24 hours post-exposure to laminin (Figs. II-8C and II-8D). At 2 hours post-attachment, no differences were observed in p27 levels between laminin and PDL substrates. We found that by 24 hours, however, cells grown on laminin showed lower levels of p27 (67.3± 8.5%) than cells grown on PDL (Fig. II-8D; n=3, p=0.0442).

Oligodendrocyte survival is unchanged in adult laminin-deficient mice.

Cultured oligodendrocytes have been shown to die more readily in the presence of antibodies that block the laminin receptor α6β1 integrin (Colognato et al., 2002; Frost et al., 1999), and newly-formed oligodendrocytes show increased cell death in the developing brain stem of α6-integrin knockout mice (Colognato et al., 2002). These findings prompted me to ask whether in laminin-deficient brains, the decrease in mature oligodendrocyte numbers could be the result of increased cell death. To determine whether white matter tracts showed normal levels of death, I performed TUNEL on wildtype and *dy/dy* littermate brains at 3 weeks and 6 weeks (Fig. II-9 and Table 3). I evaluated 9 separate fields within the corpus callosum of each animal and found no difference in TUNEL(+) cells per area between wildtype and *dy/dy* animals (Fig. II-9A and Table 3; p=0.6100, n=4 at 3 weeks; p=0.8863, n=4 at 6 weeks). To determine whether mature oligodendrocytes were dying selectively in *dy/dy* brains, I performed TUNEL in conjunction with CC1, an antibody that labels the cell bodies of mature oligodendrocytes. I

found very few dying CC1(+) cells within the corpus callosum (less than 1% in all animals evaluated), and did not find any change in TUNEL in the CC1-positive cell population of *dy/dy* brains at either 3 or 6 weeks (Figs. II-9A and II-9C, and Table 3; n=3; p=0.6991 for 3 weeks; p=0.7336 for 6 weeks). We also determined the percentage of TUNEL(+) in the PDGFRα(+) population and in this case observed virtually no overlap between TUNEL and PDGFRα(+) cells (Table 3; 0.3±0.3% in wildtype and none in *dy/dy*, n=3).

I furthermore evaluated overall TUNEL(+) cells per area, the percentage of TUNEL(+) cells within the CC1(+) population, and the percentage of TUNEL(+) cells within the PDGFRα(+) population in two additional brain regions: the cerebellar white matter and the brain stem (Table 3). In the cerebellar white matter, a minimum of 10 fields were evaluated per animal (n=3) and in the brain stem a minimum of 3 different fields were evaluated per animal (n=3). Overall very little death was observed, with no significant differences between wildtype and *dy/dy* at either 3 weeks or 6 weeks (Table 3). *dy/dy* animals showed increased death within the CC1(+) cell population of cerebellar white matter at 3 weeks, however, this increase was not statistically significant (Table 3; 0.3±0.3% in wildtype versus 1.5±0.8% in *dy/dy*, n=3, p=0.1835). Likewise, *dy/dy* animals had increased death within the PDGFRα(+) cell population of cerebellar white matter at 3 weeks, however this increase was not statistically significant (Table 3; 0.6±0.6% in wildtype versus 1.4±0.2% in dy/dy, n=3, p=0.2586). These findings indicate that, at least at 3 weeks of age and beyond, preferential death of cells in the oligodendrocyte lineage is unlikely to play a major role in altering the numbers of oligodendrocytes and oligodendrocyte progenitors. It remains possible, however, that oligodendrocyte death at earlier time points could occur and contribute to the decrease in oligodendrocyte numbers observed at 3 weeks.

DISCUSSION

In the CNS of laminin-α2-deficient *dy/dy* mice, oligodendrocyte progenitors accumulate due to delayed differentiation. By 6 weeks, however, oligodendrocyte development begins to catch up across multiple regions of the *dy/dy* brain and spinal cord. In several regions, however, elevated numbers of oligodendrocyte progenitors persist in conjunction with fewer mature oligodendrocytes and abnormal myelination. These findings indicate that laminin-α2-deficiency stalls or delays oligodendrocyte lineage progression, and, while widespread, the degree of developmental delay varies regionally. Fyn signaling abnormalities were furthermore identified in dy/dy brains, which may, at least in part, account for perturbed oligodendrocyte lineage progression (Model, Fig. II-10). In particular, Fyn was inappropriately phosphorylated at its inhibitory tyrosine; this dysregulation was accompanied by an increase in Csk and Cbp, oligodendrocyte proteins that suppress Fyn activity. These findings provide new insight into the molecular mechanisms by which α2-containing laminins regulate oligodendrocyte progenitor maturation.

The *dy/dy* mouse model for muscular dystrophy is the result of laminin α2-deficiency. While the mutation has not been identified, it has been linked to the LAMA2 locus (Sunada et al., 1994). Vartanian and colleagues reported that 5 week old *dy/dy* mice have CNS myelination abnormalities that include less MBP protein in the forebrain, and fewer mature oligodendrocytes and myelinated axons in the corpus callosum and optic nerve (Chun et al., 2003). In this study, I observed that in 3 week old mice a similar decrease in mature oligodendrocytes exists in the corpus callosum, as well as in many other brain regions. By 6 weeks, however, the density of

CC1(+) cells had risen in most brain regions but still remained lower than in wildtype littermates. In addition to decreased numbers of oligodendrocytes, I found that *dy/dy* brains, in almost all regions examined, showed significant increases in the number of oligodendrocyte progenitors. The presence of excess progenitors suggested that the observed reduction in oligodendrocytes is neither due to a failure of oligodendrocyte progenitors to be generated from germinal zones, nor due to a failure of progenitors to arrive at white matter tracts. Instead, oligodendrocyte differentiation may be stalled or delayed such that progenitors accumulate at their target destinations.

Laminin-deficient brains showed delayed differentiation in almost all regions evaluated. The timing of this delay, however, varied regionally. In the cerebellum, for instance, oligodendrocyte density was relatively normal at 3 weeks but lagged behind at 6 weeks both in terms of oligodendrocyte density (Fig. II-1, Table 1) and thinner myelin as evidenced by increased g-ratios (Fig. II-2). Conversely, delays in oligodendrocyte differentiation in the corpus callosum, while pronounced at 3 weeks, were no longer significant at 6 weeks and corresponded with relatively normal myelin thickness, albeit with an approximately 37% increase in unmyelinated axons (Figs. II-1, II-4, and Table 1). In almost every region, therefore, an inverse relationship between increased numbers of oligodendrocyte progenitors and decreased numbers of mature oligodendrocytes was observed (Tables 1 and 2). Some exceptions to this correlation were found; in particular, the brain stem contained decreased numbers of mature oligodendrocytes without a corresponding increase in the numbers of oligodendrocyte progenitors (Tables 1 and 2) or significant changes in myelination (Fig. II-4). It is possible, therefore, that early myelinating regions such as the brain stem either are not influenced by laminin or have compensatory changes that occur by 3 weeks of age.

Laminin-deficient MDC1A patients also show regional differences in brain abnormalities. In one study, white matter signals were abnormal to varying degrees in the cerebral cortex of all patients, whereas the cerebellum and the brain stem showed T2 abnormalities in only approximately 20% of patients (Leite et al., 2005b). These findings indicate that laminin's influence on CNS development may be different in different brain regions, or, alternatively, that development in different brain regions may be differentially modulated by other factors that in turn influence their response to laminins. Another possibility is that differential compensation by additional laminin heterotrimers may take place in different brain regions e.g. the loss of α2-laminins is compensated for in the cerebellum but not the cortex. This is observed in the peripheral nervous system, where α2-laminin-deficiencies cause myelination abnormalities; these animals show upregulated laminin-α2 expression, but only in selected regions (Patton et al., 1997; Yang et al., 2005). In the current study, I found that residual laminin α2 immunoreactivity was detectable in the cerebellum and brain stem of 3 week old *dy/dy* brains but was undetectable by 6 weeks (Figs. II-2, II-11, and II-12). These findings suggest that variable degrees of laminin-α2 expression could also account for the different degrees of oligodendrocyte differentiation delay observed regionally in *dy/dy* brains.

Besides a differentiation delay, another possible explanation to account for fewer mature oligodendrocytes is increased cell death. Laminin substrates are known to promote the survival of newly-formed oligodendrocytes *in vitro* (Colognato et al., 2002; Frost et al., 1999). Loss of the laminin receptor α6β1 integrin, on the other hand, causes increased death in premyelinating axon tracts in both the brain stem and the cerebellum (Benninger et al., 2006; Colognato et al., 2002). At 3 weeks, however, *dy/dy* mice did not show increased death in either oligodendrocytes or oligodendrocyte progenitors (Fig. II-9 and Table 3). A small increase in both the percentage of

TUNEL-positive-CC1(+) cells and TUNEL-positive-PDGFRα(+) cells was observed in laminin-deficient cerebellar white matter (Table 3), but these increases were not statistically significant. Therefore, these cell-specific TUNEL data from *dy/dy* mice provide no evidence to support a role for death in the diminished numbers of mature oligodendrocytes at 3 weeks. Decreased survival of oligodendrocytes at earlier time points, however, cannot be ruled out. Unfortunately *dy/dy* mice cannot be identified at earlier ages (see Methods). I instead used laminin α2 knockout mice to investigate the consequence of laminin loss on cell survival earlier in the developing brain (see Chapter III).

What are the potential signaling mechanisms by which laminins regulate the transition from oligodendrocyte progenitor to myelinating oligodendrocyte? Several signaling molecules are influenced by laminins in oligodendrocyte cultures, including ILK, Fyn, FAK, MAPK, and PI3K (Baron et al., 2003; Chun et al., 2003; Colognato et al., 2002; Colognato et al., 2004; Hoshina et al., 2007). In the current study, we examined whether Fyn was regulated by laminins *in vivo* and found that phosphorylation of the Fyn negative regulatory tyrosine was enhanced in *dy/dy* brains (Fig. II-6). We also found that oligodendrocyte progenitor cell attachment to laminin caused a *decrease* in phosphorylation of this same negative regulatory tyrosine (Fig. II-7). Together these findings suggest that laminin regulates the transition from oligodendrocyte progenitor to oligodendrocyte, at least in part, by modulating Fyn regulation. Fyn activity peaks during active myelination, and Fyn knockout mice have less forebrain myelination. These findings thus suggest that changes in Fyn regulation could alter the timing of oligodendrocyte development (Sperber et al., 2001; Umemori et al., 1994). Fyn null mice also show changes in the ratio of exon2-containing MBP isoforms such that the 21.5 kDa isoform is decreased relative to other isoforms (Lu et al 2005). In laminin-deficient mice, the ratio of the 21.5 kDa MBP

isoform was also decreased such that the percentage of 21.5 kDa MBP protein (relative to total MBP protein) drops by approximately 50% (6.2±7.1% total MBP protein in the wildtype versus 3.1±0.8% in dy/dy cerebral cortex at 3 weeks). The 21.5 kDa isoform is highly associated with active myelination therefore a trend towards less of the 21.5 kDa MBP isoform is consistent with the hypothesis that laminin-deficiency leads to a delayed developmental progression. Due to high variability however these trends were not statistically significant (n=3, p=0.4916).

In T-cells, Fyn activity is tightly regulated by Csk, the C-terminal Src Kinase (Palacios and Weiss, 2004). Csk in turn is regulated by its ability to bind to the transmembrane adapter molecule Cbp. Csk is the principal kinase that phosphorylates Fyn and other Src family kinases (SFKs) at SFK negative regulatory tyrosines and has thus been shown to suppress the ability of Fyn to phosphorylate downstream targets. Csk expression is normally highest in the developing embryonic brain, when Fyn activity is low (Inomata et al., 1994). During myelination, Csk levels decrease substantially compared to those in the embryonic brain. Here, I show that elevated levels of Csk and Cbp found in dy/dy brains correlate with increased phosphorylation of the Fyn negative regulatory tyrosine, providing a potential molecular basis for Fyn dysregulation in laminin-deficient brains. It cannot be ruled out, however, that increased levels of Csk and Cbp may also be found in non-oligodendrocyte lineage cells.

Evidence from this part of the dissertation indicates that the inappropriate accumulation of oligodendrocyte progenitors could reflect a dysregulation of the signaling mediators that control the timing of oligodendrocyte development. The timing of cell cycle exit regulates myelination onset, although the precise mechanisms that dictate when and where oligodendrocytes initiate the final phases of myelination remain to be elucidated. Several cyclin-dependent-kinase inhibitors, such as p27 and p57, however, are known to regulate the

withdrawal of oligodendrocyte progenitors from the cell cycle (Nguyen et al., 2006). The levels of p27 in particular have been shown to peak with the onset of myelination. Here I report that (1) laminin contact with OPCs suppresses p27 accumulation and (2) p27 is increased in laminin-deficient brains (Fig. II-8). Overexpression of p27 has been shown to block both oligodendrocyte progenitor division and differentiation, and thus results in a stalled progenitor phenotype (Tang et al., 1999). Here I noted that increased p27 coincided in some cases with the accumulation of OPCs, raising the possibility that laminin normally promotes OPC differentiation through p27. In support of this, integrin engagement by extracellular matrix has been shown to regulate p27 by activating signaling pathways that control p27 protein degradation (Fu et al., 2007).

p27 levels are also regulated by mRNA stability. The RNA binding protein, QKI, enhances the stability of p27 mRNA in developing oligodendrocytes (Larocque et al., 2005). QKI is in itself an essential molecule for myelination: *quaking viable* mice have a mutation that causes the loss of particular QKI isoforms important for MBP mRNA stability, causing these mice to have severe myelination defects (Larocque and Richard, 2005). I found that QKI levels in laminin-deficient brains were elevated (not shown), providing a possible mechanism for the observed increase in p27. Fyn is known to phosphorylate QKI and regulate its ability to stabilize and traffic MBP mRNA (Lu et al., 2005), thus providing a potential link between Fyn dysregulation, QKI/p27 dysregulation, and delayed oligodendrocyte differentiation observed in laminin-deficient animals.

In summary, we have shown that laminins promote the transition from oligodendrocyte progenitor cell to oligodendrocyte and do so, at least in part, by modulating Fyn signaling. These findings suggest that dysregulated Fyn signaling may contribute to the CNS pathology in

MDC1A laminin deficiencies and offer new insight into how laminins regulate oligodendrocyte development.

Figure II-1. Delayed oligodendrocyte maturation in *dy/dy* brains.

(A) Mature CC1(+) oligodendrocytes per mm^2 in the corpus callosum were measured in wildtype (white bars, wt) and *dy/dy* (black bars, dy) littermates at 3 weeks (3W) and 6 weeks (6W) of age. Graphs depict mean (± sem) counts obtained from 7 different areas of the corpus callosum (n=3; *p<0.05). **(B)** Representative images of CC1(+) oligodendrocytes (green) in the corpus callosum of 3 week old wildtype (wt) and *dy/dy* (dy) brains. Nuclei are visualized using DAPI (blue). Scale bar = 50 microns. **(C)** Mature CC1(+) oligodendrocytes per mm^2 in the proximal cerebellar white matter were measured in wildtype (white bars, wt) and *dy/dy* (black bars, dy) littermates at 3 weeks (3W) and 6 weeks (6W) of age. Graphs depict mean (± sem) counts obtained from 6 different areas of the proximal cerebellar white matter (n=5; *p<0.05 for comparison between 3W wt and 6W wt). **(D)** Mature CC1(+) oligodendrocytes per mm^2 in the brain stem were measured in wildtype (white bars, dy) and *dy/dy* (black bars, dy) littermates at 3 weeks (3W) and 6 weeks (6W) of age. Graphs depict mean (± sem) counts obtained from 3 different areas of the brain stem (n=5; *p<0.05 for comparisons between 3W wt and 6W wt, and, between 6W wt and 6W dy). **(E)** Top panels: representative images of MBP immunocytochemisty (green) in the corpus callosum of 3 week old wildtype (wt) and *dy/dy* (dy) brains. Scale bar = 200 microns. Middle panels: representative images of MBP (green) and NF (red) immunocytochemisty in the corpus callosum of 3 week old wildtype (wt') and *dy/dy* (dy') brains. Scale bar = 25 microns. Lower panels: representative images of MBP (green) and neurofilament (NF; red) immunocytochemisty in the corpus callosum of 3 week old wildtype (wt'') and *dy/dy* (dy'') brains. Scale bar = 10 microns. **(F)** Lysates from 3 week old cerebral cortices were evaluated by Western Blot to detect myelin basic protein (MBP). MBP isoforms 21.5, 18.5, 17.2 and 14.0 kDa are indicated. Actin blots are shown as a loading control. Figure modified from Relucio et al., 2009.

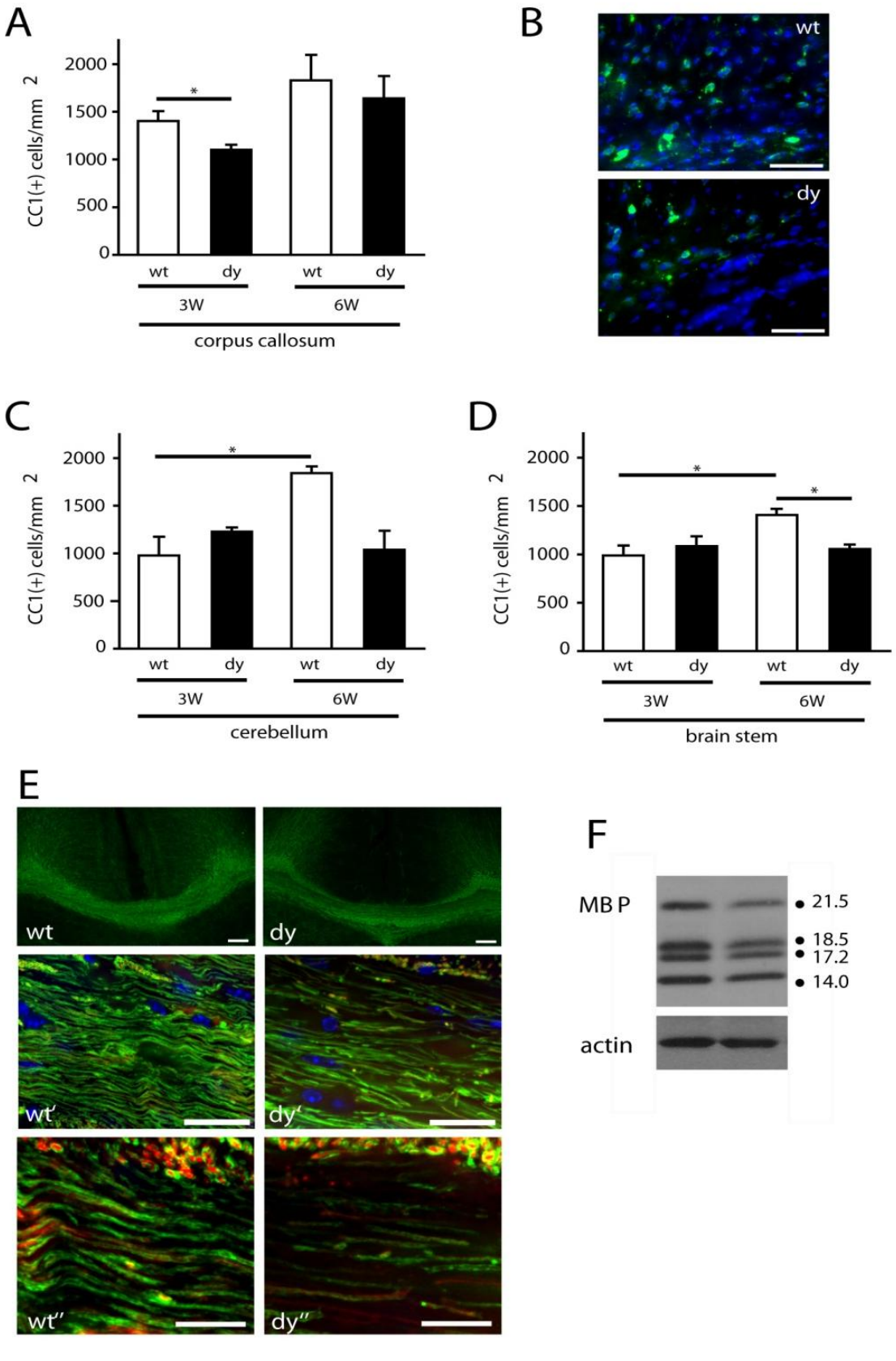
A
CC1(+) cells/mm 2
2000
1500
1000
500
0
*
wt
dy
wt
dy
3W
6W
corpus callosum
B
wt
dy
C
CC1(+) cells/mm 2
2000
1500
1000
500
0
*
wt
dy
wt
dy
3W
6W
cerebellum
D
CC1(+) cells/mm 2
2000
1500
1000
500
0
*
*
wt
dy
wt
dy
3W
6W
brain stem
E
wt
dy
wt'
dy'
wt''
dy''
F
MB P
21.5
18.5
17.2
14.0
actin

Figure II-2. Myelin abnormalities in *dy/dy* cerebella.

(A) Immunocytochemistry to visualize MBP (green) and neurofilament (NF; red) in wildype (wt) and *dy/dy* (dy) 3 week-old cerebella. Sections are counterstained with DAPI (blue) to visualize nuclei. Scale bar = 200 microns. **(B)** Lysates from 3 week old cerebella were evaluated by Western Blot to detect myelin basic protein (MBP) relative to actin as a loading control. MBP isoforms 21.5, 18.5, 17.2 and 14.0 kDa are indicated. **(C)** Laminin α2 subunit immunoreactivity in wildtype (wt) and *dy/dy* (dy) cerebellar white matter at 3 weeks (3w) and 6 weeks (6w). Low intensity laminin α2 immunoreactivity was observed in 3 week old *dy/dy* cerebella but this residual immunoreactivity was absent at 6 weeks. Scale bars = 50 microns**. (D)** EM analysis of the cerebellum revealed thinner myelin. Representative electron micrographs of central cerebellar sagittal sections from 6 week old mice; scale bars of 2 microns are shown in both low and high magnification images. **(E)** Cerebellar g-ratios were plotted as a function of axon diameter for wildtype (open circles) and dy/dy (black triangles); increased median g-ratios were observed overall in dy/dy cerebella (0.832 in wildtype versus 0.874 in dy/dy cerebella, $p<0.001$). **(F)** Cerebellar g-ratios grouped by axon diameter revealed significantly thinner myelin in *dy/dy* cerebellar axons of all sizes. Mean g-ratio ± S.E.M are shown (***$p<0.001$). Figure modified from Relucio et al., 2009.

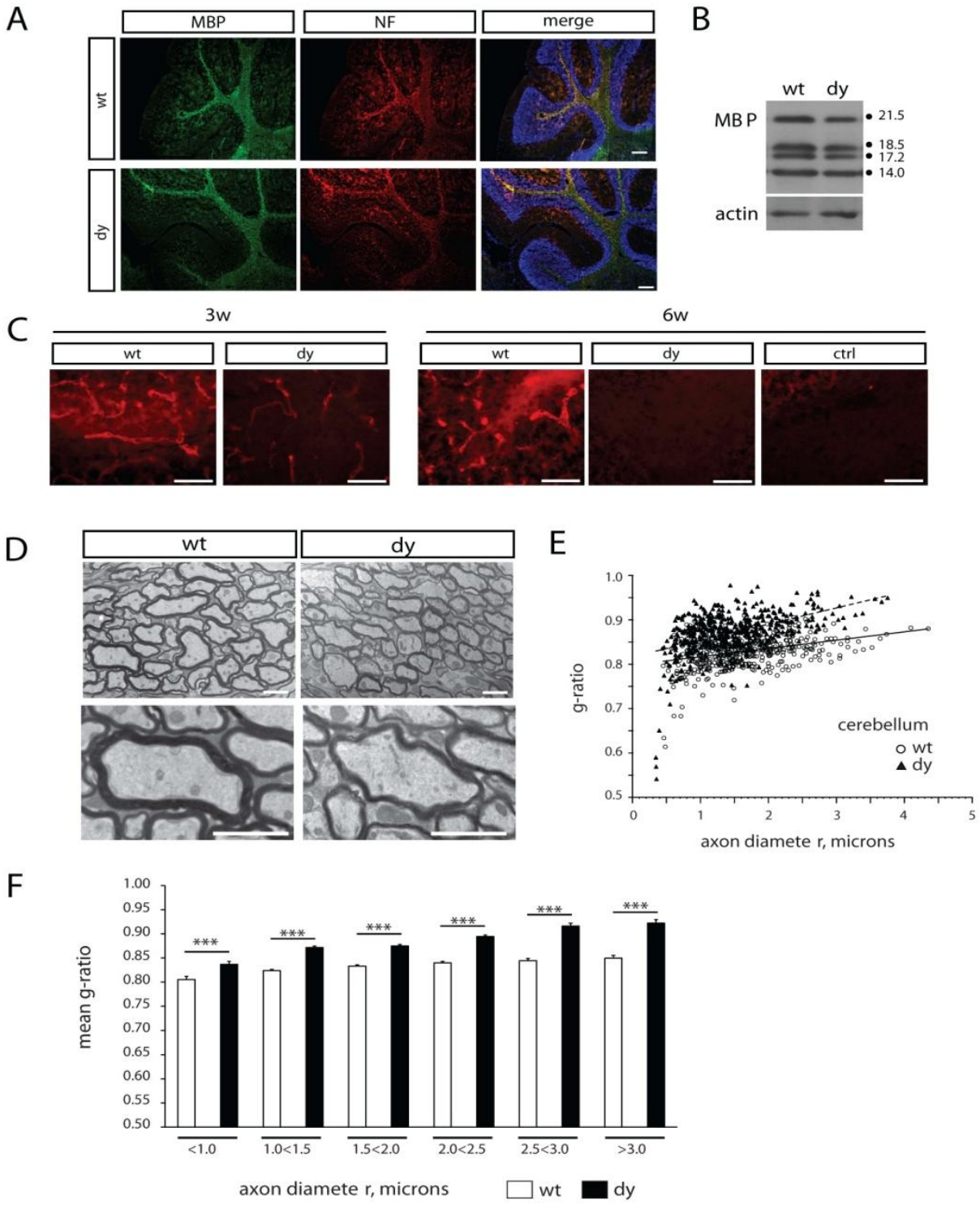
A
MBP
NF
merge
wt
dy
B
wt
dy
MB P
21.5
18.5
17.2
14.0
actin
C
3w
6w
wt
dy
wt
dy
ctrl
D
wt
dy
E
g-ratio
cerebellum
wt
dy
axon diamete r, microns
F
mean g-ratio
***
<1.0
1.0<1.5
1.5<2.0
2.0<2.5
2.5<3.0
>3.0
axon diamete r, microns
wt
dy

Figure II-3. Oligodendrocyte progenitor differentiation and myelination are altered in the optic nerves of *dy/dy* mice.

(A) Representative images of CC1(+) oligodendrocytes (green) in transverse sections from 6 week old wildtype (wt) and *dy/dy* (dy) optic nerves. Nuclei are visualized using DAPI (blue). Scale bar = 25 microns. **(B)** PDGFRα immunocytochemistry (to detect OPCs) and CC1 immunocytochemistry (to detect oligodendrocytes) was used to measure cell density in the optic nerves of wildtype (white bars, wt) and *dy/dy* (black bars, dy) littermates at 6 weeks of age. Graphs are mean (±sem) counts obtained from 4 different sections of optic nerve and bars (n=2; $p=0.0766$ for PDGFRα(+) cells and $p=0.0335$ for CC1(+) cells; $*p<0.05$). **(C)** EM analysis of optic nerve reveals thinner myelin in larger *dy/dy* axons. Representative electron micrographs of optic nerve cross-sections from 6 week old mice; scale bars of 1 micron (low magnification images) and 0.5 microns (high magnification images) are shown. **(D)** Optic nerve g-ratios were plotted as a function of axon diameter for wildtype (open circles) and *dy/dy* (black triangles); a small overall increase in median g-ratios were observed in *dy/dy* optic nerves (0.845 in wildtype versus 0.852 in dy/dy) however these changes were not significant. No change was observed in the *dy/dy* optic nerve as to the degree of unmyelinated axons. **(E)** Optic nerve g-ratios grouped by axon diameter revealed significantly thinner myelin in larger *dy/dy* optic nerve axons (>1.0 micron diameter). Mean g-ratio ± S.E.M are shown ($***p<0.001$). Figure modified from Relucio et al., 2009.

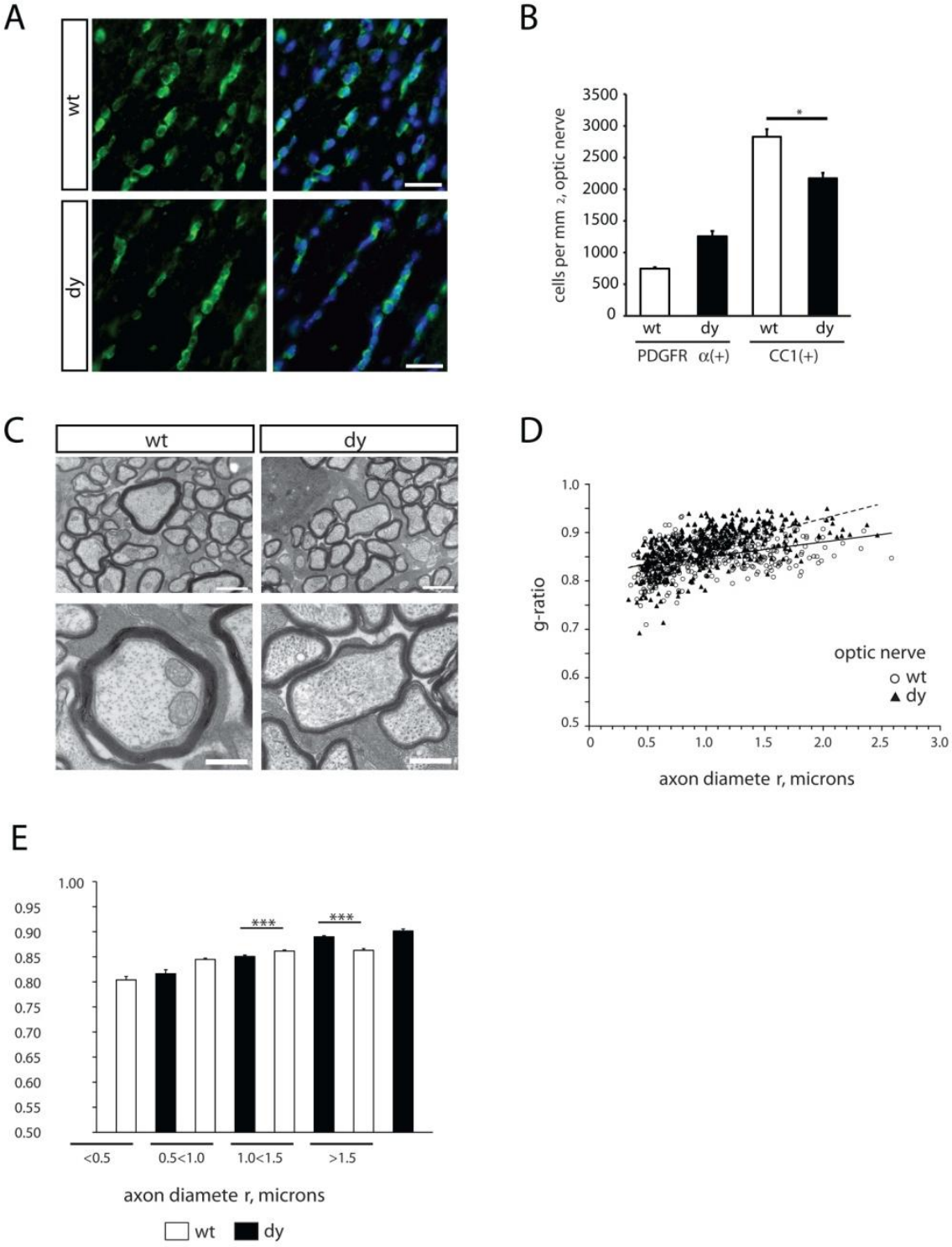
A
wt
dy
B
cells per mm 2, optic nerve
3500
3000
2500
2000
1500
1000
500
0
*
wt
dy
wt
dy
PDGFR α(+)
CC1(+)
C
wt
dy
D
g-ratio
1.0
0.9
0.8
0.7
0.6
0.5
optic nerve
wt
dy
0
0.5
1.0
1.5
2.0
2.5
3.0
axon diamete r, microns
E
mean g-ratio
1.00
0.95
0.90
0.85
0.80
0.75
0.70
0.65
0.60
0.55
0.50
***
***
<0.5
0.5<1.0
1.0<1.5
>1.5
axon diamete r, microns
wt
dy

Figure II-4. Myelination abnormalities in laminin-deficient *dy/dy* brains show regional variation.

(A) EM analysis of anterior commissures revealed no significant change in *dy/dy* myelin thickness. Representative electron micrographs of anterior commissure sagittal sections from 6 week old mice; scale bars of 1 micron (low magnification images) and 0.5 microns (high magnification images) are shown. Instead, the percentage of unmyelinated axons was increased in *dy/dy* anterior commissure relative to wildtype (29% unmyelinated in *dy/dy* versus 16.9% in wildtype). **(B)** EM analysis of corpus callosum revealed no significant change in dy/dy myelin thickness. Representative electron micrographs of corpus callosum sagittal sections from 6 week old mice; scale bars of 1 micron (low magnification images) and 0.5 microns (high magnification images) are shown. Instead, the percentage of unmyelinated axons was increased in *dy/dy* corpus callosum relative to wildtype (36.8% unmyelinated in *dy/dy* versus 26.9% in wildtype). **(C)** Anterior commissure g-ratios were plotted as a function of axon diameter for wildtype (open circles) and *dy/dy* (black triangles) 6 week old mice. Overall median g-ratios were not significantly different (0.827 in wildtype versus 0.840 in *dy/dy*). **(D)** Corpus callosum g-ratios were plotted as a function of axon diameter for wildtype (open circles) and *dy/dy* (black triangles) 6 week old mice. Overall median g-ratios were not significantly different (0.855 in wildtype versus 0.849 in *dy/dy*). **(E)** Brain stem g-ratios were plotted as a function of axon diameter for wildtype (open circles) and *dy/dy* (black triangles) 6 week old mice. Overall median g-ratios were not significantly different (0.838 in wildtype versus 0.846 in *dy/dy*). Significantly thinner myelin was, however, observed in *dy/dy* brain stem axons of <0.5 micron diameter (*dy/dy* mean ± SEM of 0.812±0.014, versus wildtype 0.748±0.017; $p<0.01$) whereas medium and large caliber axons showed no change (not shown). No change was observed in the brain stem as to the degree of unmyelinated axons. Figure modified from Relucio et al., 2009.

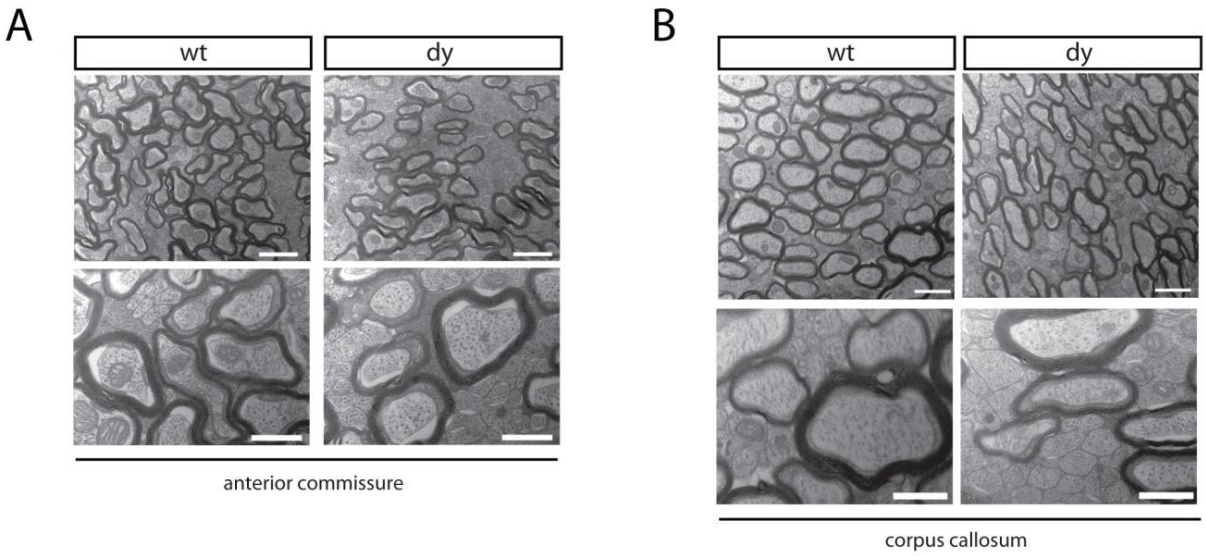
A
wt
dy
anterior commissure
B
wt
dy
corpus callosum

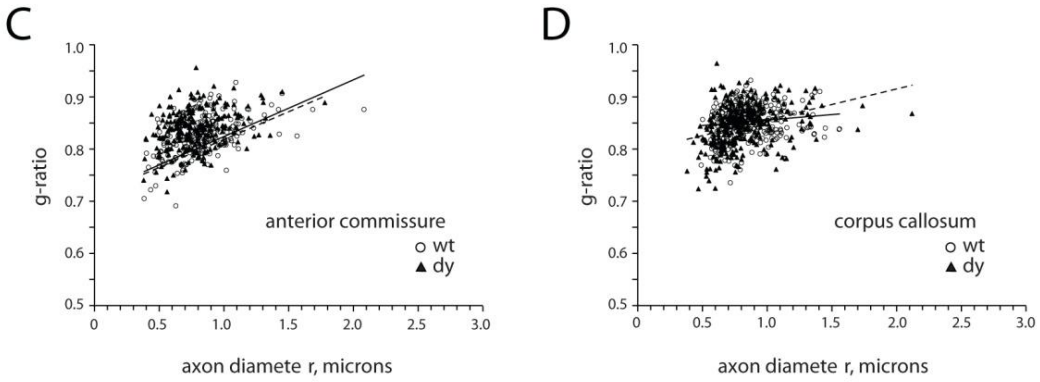
C
g-ratio
anterior commissure
wt
dy
axon diamete r, microns
D
g-ratio
corpus callosum
wt
dy
axon diamete r, microns

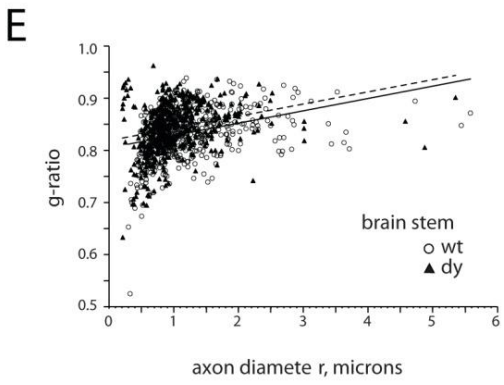
E
g-ratio
brain stem
wt
dy
axon diamete r, microns

Figure II-5. Oligodendrocyte progenitors accumulate in *dy/dy* brains.

(A) Oligodendrocyte progenitor cells per mm^2 in the corpus callosum were measured in wildtype (white bars, wt) and *dy/dy* (black bars, dy) littermates at 3 weeks (3W) and 6 weeks (6W) of age using PDGFRα immunocytochemistry. Graphs are mean (±sem) counts obtained from 7 different areas of the corpus callosum (n=3; **p*<0.05). **(B)** Top panels: representative images of PDGFRα(+) oligodendrocyte progenitors (red) in the corpus callosum of 3 week old wildtype (wt) and *dy/dy* (dy) brains. Nuclei are visualized using DAPI (blue). Scale bar = 100 microns. Lower panels: representative images of PDGFRα(+) oligodendrocyte progenitors (red; indicated by *) in the corpus callosum of 3 week old wildtype (wt') and *dy/dy* (dy') brains obtained at higher magnification. Scale bar = 25 microns. **(C)** Oligodendrocyte progenitor cells per mm^2 in the proximal cerebellar white matter were measured in wildtype (white bars, wt) and *dy/dy* (black bars, dy) littermates at 3 weeks (3W) and 6 weeks (6W) of age. Graphs are mean (±sem) counts obtained from 6 different areas of the proximal cerebellar white matter (n=3; **p*<0.05). **(D)** Oligodendrocyte progenitor cells per mm^2 in the brain stem were measured in wildtype (white bars, wt) and dy/dy (black bars, dy) littermates at 3 weeks (3W) and 6 weeks (6W) of age. Graphs are mean (±sem) counts obtained from 3 different areas of the brain stem (n=3; n.s, not significant). **(E)** Lysates from 6 week old cerebella were evaluated by Western Blot to detect NG2 protein relative to actin as a loading control. A representative blot from a wildtype (wt) and *dy/dy* (dy) littermate is shown. **(F)** Relative densitometry of NG2 protein levels at 3 weeks (3W) and 6 weeks (6W) in *dy/dy* cerebella compared to paired littermate wildtype (wt) cerebella (*n*=4, **p*<0.05). Figure modified from Relucio et al., 2009.

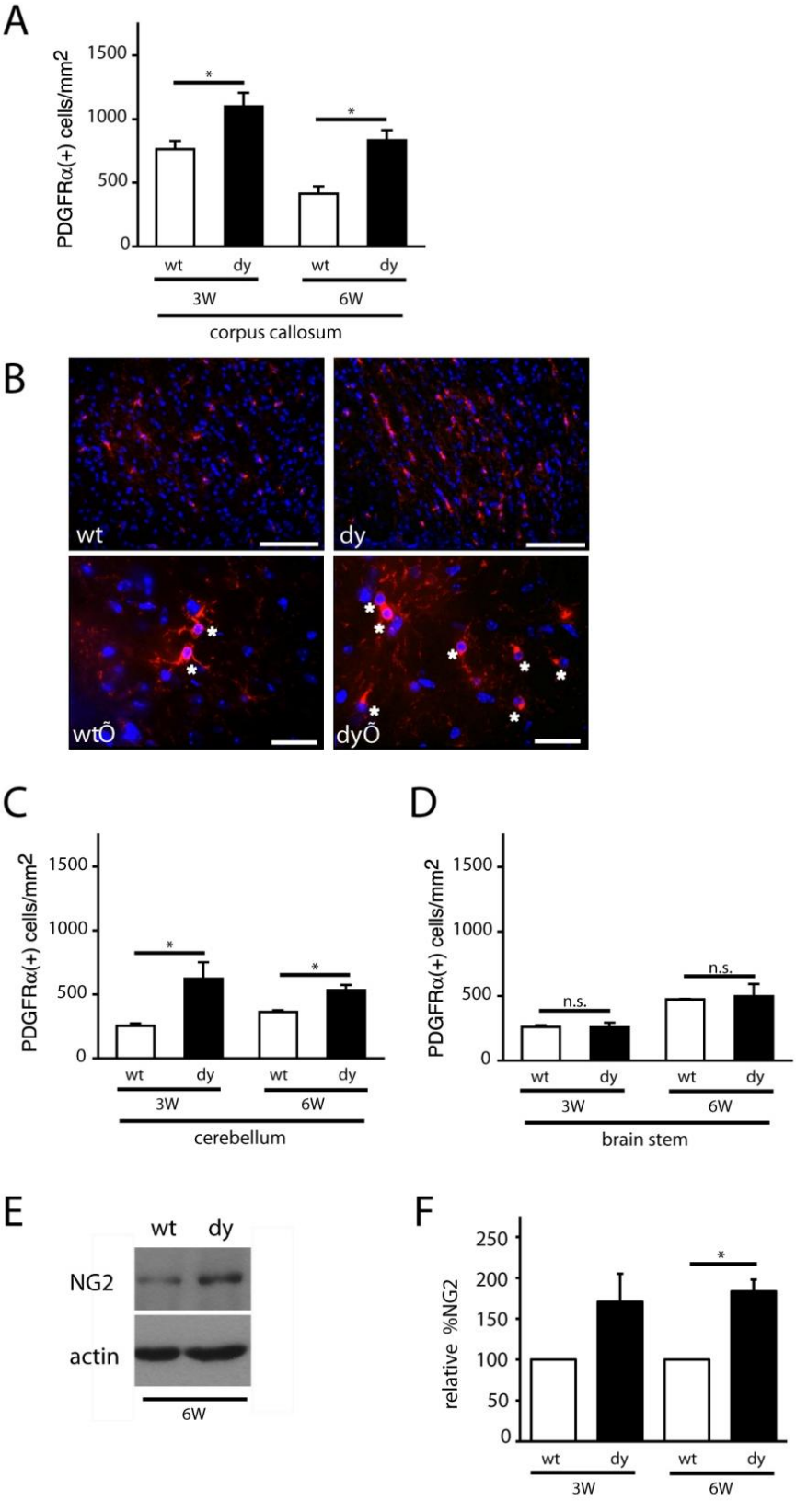
A
PDGFRα(+) cells/mm2
1500
1000
500
0
*
*
wt
dy
wt
dy
3W
6W
corpus callosum
B
wt
dy
wtÕ
dyÕ
C
PDGFRα(+) cells/mm2
1500
1000
500
0
*
*
wt
dy
wt
dy
3W
6W
cerebellum
D
PDGFRα(+) cells/mm2
1500
1000
500
0
n.s.
n.s.
wt
dy
wt
dy
3W
6W
brain stem
E
wt
dy
NG2
actin
6W
F
relative %NG2
250
200
150
100
50
0
*
wt
dy
wt
dy
3W
6W

Figure II-6. Fyn is dysregulated in *dy/dy* brains.

(A) Lysates from 3 week old cerebral cortices (CTX) were evaluated by Western Blot to detect Fyn, phosphorylated tyrosine 529 (pY529), Csk, Cbp, and actin. Representative blots from 3 week old wildtype (wt) and *dy/dy* (dy) littermates are shown. **(B)** Densitometric analysis of Fyn, phospho-Fyn, and Fyn regulatory proteins Csk and Cbp: mean Fyn protein, mean phospho-Y529 immunoreactivity normalized to total Fyn protein, mean Csk protein, and mean Cbp protein are shown (n=3; **$p<0.01$; *$p<0.05$). Fyn, Csk, and Cbp protein levels were normalized to actin protein levels. **(C)** Lysates from 3 week old cerebella (CB) were evaluated by Western Blot to detect Fyn, phosphorylated tyrosine 529 (pY529), Csk, Cbp, and actin. Representative blots from 3 week old wildtype (wt) and *dy/dy* (dy) littermates are shown. **(D)** Densitometric analysis of Fyn, phospho-Fyn, and Fyn regulatory proteins Csk and Cbp: mean Fyn protein, mean phospho-Y529 immunoreactivity normalized to total Fyn protein, mean Csk protein, and mean Cbp protein are shown (n=3; *$p<0.05$). Fyn, Csk, and Cbp protein levels were normalized to actin protein levels. Figure modified from Relucio et al., 2009.

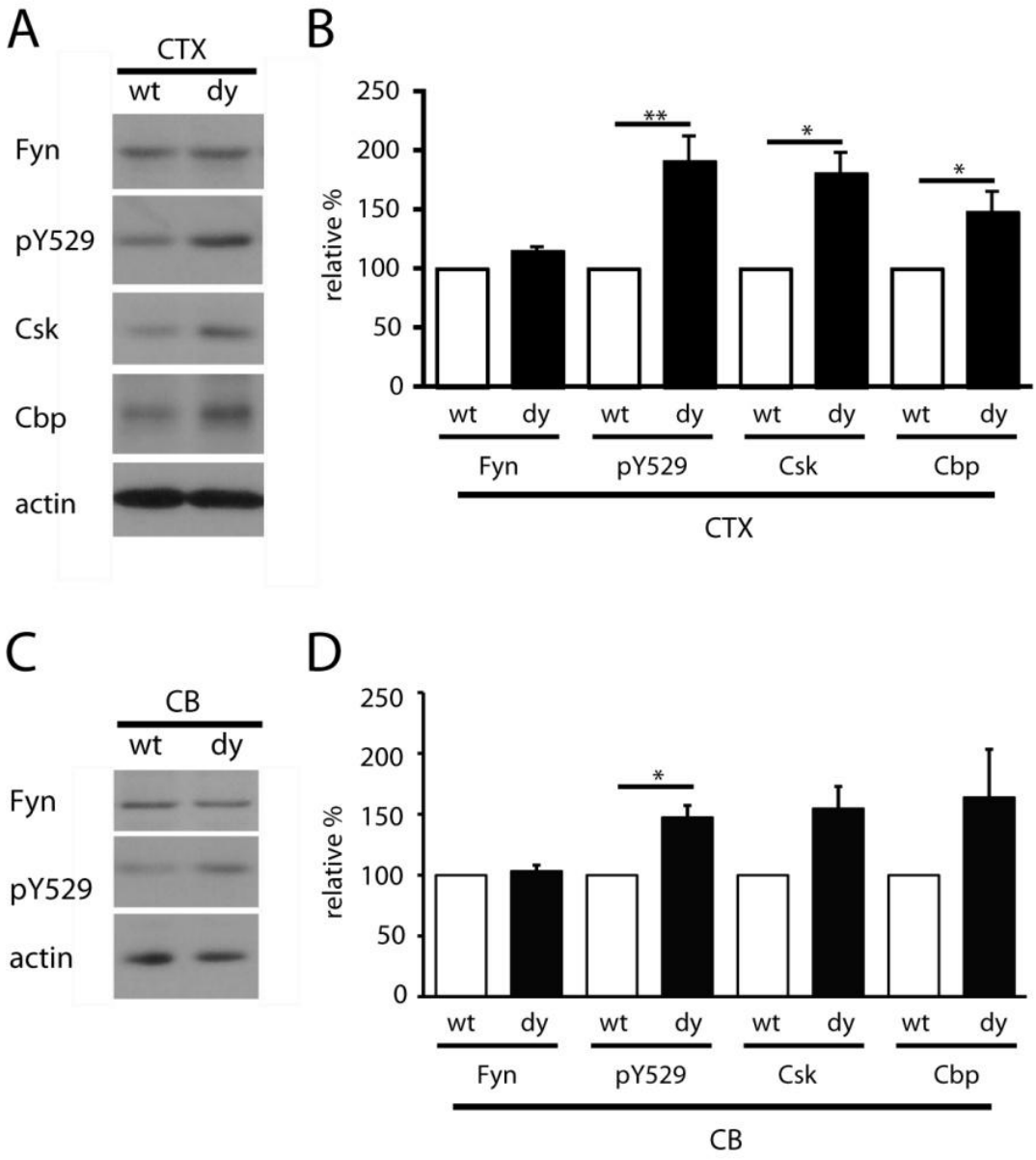
A
CTX
wt
dy
Fyn
pY529
Csk
Cbp
actin
B
relative %
250
200
150
100
50
0
**
*
*
wt
dy
Fyn
pY529
Csk
Cbp
CTX
C
CB
wt
dy
Fyn
pY529
actin
D
relative %
250
200
150
100
50
0
*
wt
dy
Fyn
pY529
Csk
Cbp
CB

Figure II-7. Laminin promotes the differentiation of oligodendrocyte progenitors using a Fyn-dependent mechanism.

(A) Oligodendrocyte progenitor cells added to poly-D-lysine (PDL) or laminin-2 (Lm) substrates for 2 hours were lysed and evaluated by Western blot to detect phospho-Y529 relative to total Fyn. **(B)** Graph depicts mean pY529 phosphorylation, relative to total Fyn levels, on laminin-2 substrates (Lm) relative to PDL substrates (**p<0.01, n=3). **(C)** Oligodendrocyte progenitor cells were added to PDL or laminin-2 (Lm) substrates for 24 hours in minimal medium, in the presence of 1 μM PP2 or equivalent volume of DMSO vehicle as a control (ctrl). CNP immunoreactivity (green) was performed to visualize newly-formed oligodendrocytes, in conjunction with DAPI to view total nuclei (blue). Scale bar = 50 microns. **(D)** Graph depicts the mean percentage of cells that show CNP immunoreactivity per field, in 3 independent experiments (n=3; *p<0.05 for comparisons between PDL and Lm under control conditions, and, between control and PP2 conditions on Lm). Figure modified from Relucio et al., 2009.

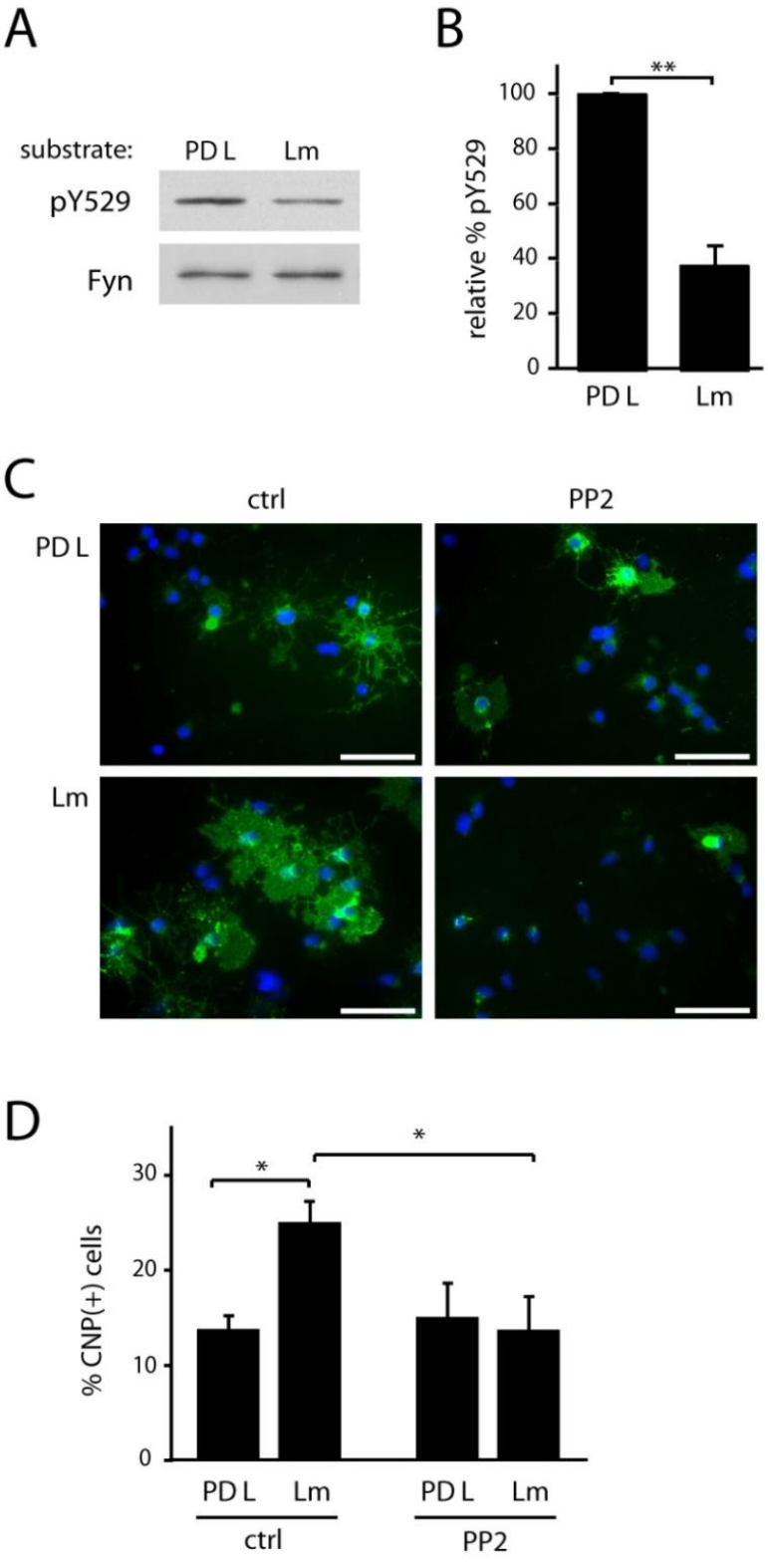
A
substrate:
PD L
Lm
pY529
Fyn
B
**
100
80
60
40
20
0
relative % pY529
PD L
Lm
C
ctrl
PP2
PD L
Lm
D
*
*
30
20
10
0
% CNP(+) cells
PD L
Lm
PD L
Lm
ctrl
PP2

Figure II-8. Laminin regulates p27 protein levels.

(A) Cerebellar lysates were evaluated by Western Blot to detect p27 or actin. Representative blots from 6 week old wildtype (wt) and a *dy/dy* (dy) littermates are shown. **(B)** Densitometric analysis was performed to evaluate p27 protein relative to actin at 6 weeks in *dy/dy* cerebella compared to paired wildtype (wt) littermates. (n=3, *$p<0.05$). **(C)** Oligodendrocyte progenitor cells on poly-D-lysine (PDL) or laminin-2 (Lm) substrates for 2 hours (2h) or 1 day (1d) were lysed and evaluated by Western blot to detect p27 relative to actin as a loading control. **(D)** Densitometric analysis was performed to evaluate p27 protein relative to actin after 1 day on each substrate. Oligodendrocyte progenitor cells showed 67.3±8.5% p27 protein compared to cells grown on PDL (n=3, *$p<0.05$). Figure modified from Relucio et al., 2009.

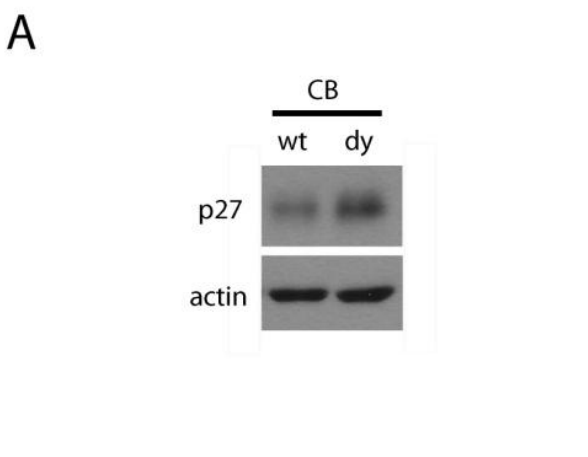
A
CB
wt
dy
p27
actin
B
relative % p27
300
200
100
0
*
wt
dy
CB
C
2h
1d
substrate:
PD L
Lm
PD L
Lm
p27
actin
D
relative % p27
100
80
60
40
20
0
*
substrate:
PD L
Lm

Figure II-9. Oligodendrocyte death in *dy/dy* adult brains.

(A) The mean number of TUNEL-positive cells per area (mm^2) is shown for wildtype (wt) and *dy/dy* (dy) corpus callosum at 3 weeks and 6 weeks (*n*=4). **(B)** The percentage of TUNEL-positive cells within the CC1(+) cell population is shown for wildtype (wt) and *dy/dy* (dy) corpus callosum at 3 weeks and 6 weeks (*n*=3). **(C)** CC1 immunocytochemistry (green) to visualize mature oligodendrocyte cell bodies was performed in combination with TUNEL to detect dying cells (red). Representative fields are shown from 3 week old wildtype (wt) and *dy/dy* (dy) corpus callosum. Arrows depict TUNEL-positive cells, scale bar denotes 100 microns. Figure modified from Relucio et al., 2009.

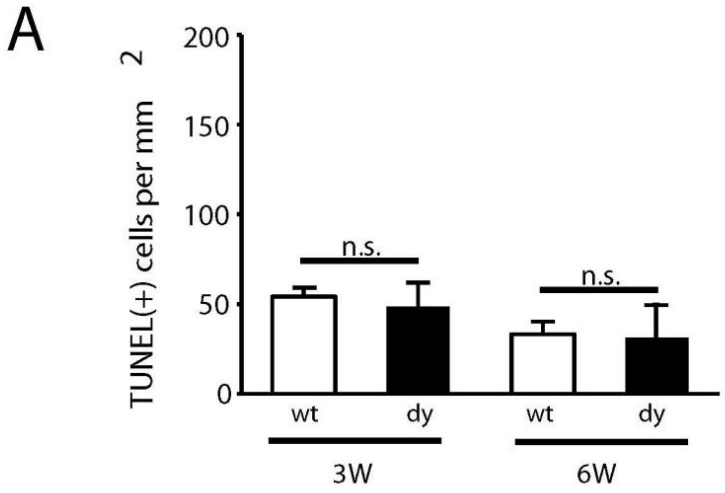
A
TUNEL(+) cells per mm 2
200
150
100
50
0
n.s.
n.s.
wt
dy
wt
dy
3W
6W

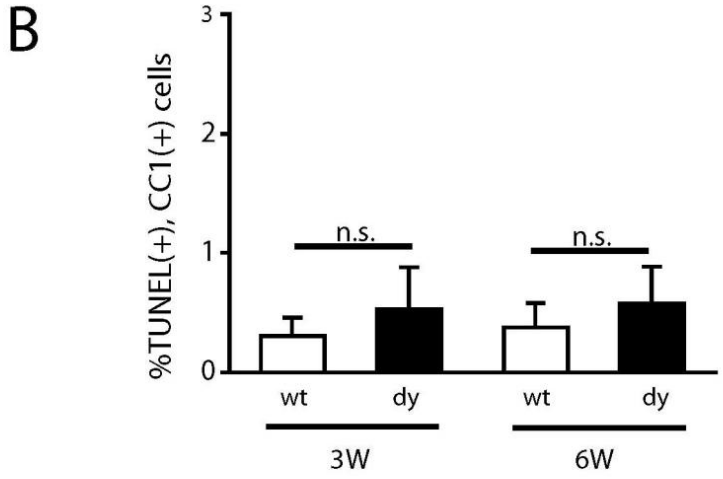
B
%TUNEL(+), CC1(+) cells
3
2
1
0
n.s.
n.s.
wt
dy
wt
dy
3W
6W

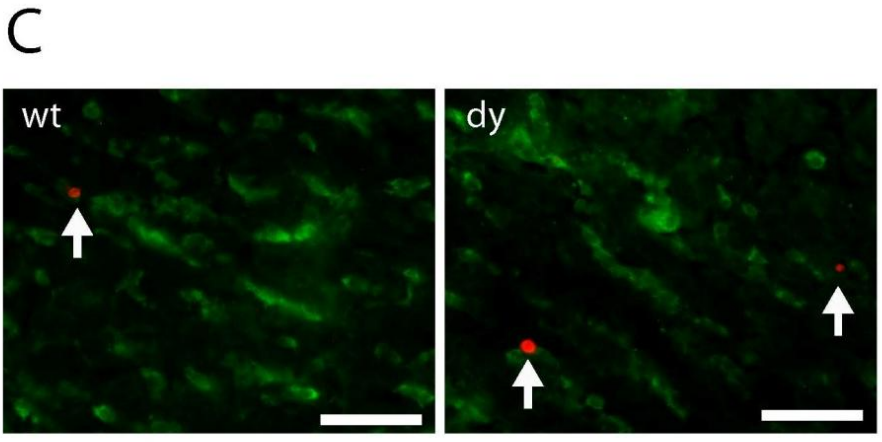
C
wt
dy

Figure II-10. Laminin and oligodendrocyte progenitor development.

Oligodendrocyte progenitor differentiation is inappropriately delayed in the brains of *dy/dy* laminin-deficient mice. Regulatory molecules that can suppress Fyn activity, Csk and Cbp, are elevated in laminin-deficient brains. A normal role of laminin is therefore to suppress Csk and Cbp, and thus promote Fyn activation and oligodendrocyte maturation. In addition, laminin may activate Fyn independent of Csk/Cbp suppression (Colognato et al., 2004). It remains unknown if laminin is able to promote oligodendrocyte differentiation through Fyn-independent mechanisms (dashed line). Figure modified from Relucio et al., 2009.

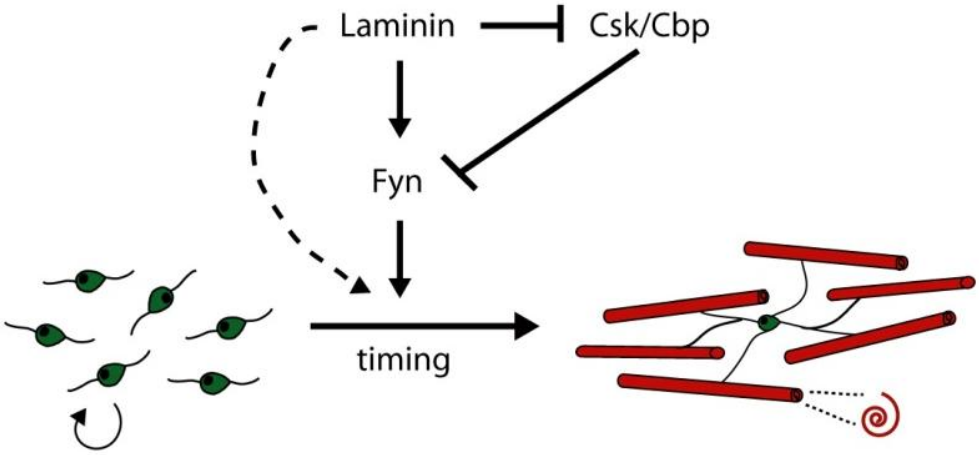
Laminin
Csk/Cbp
Fyn
timing

Figure II-11. *dy/dy* brains show selective loss of laminin α2.

To confirm that *dy/dy* brains were deficient in the laminin α2 subunit and evaluate whether other laminin chains remained unaffected, we performed immunocytochemistry on fresh frozen sections of cerebral cortices from 6 week old *dy/dy* mice and their wildtype littermates. **(A)** Laminin α2 subunit immunoreactivity (mouse monoclonal 4H8-2, red) was visualized in the basement membranes of the pia and vasculature of wildtype (wt) cortices, but appeared absent in *dy/dy* (dy) cortices **(B)** A polyclonal laminin-1 antibody that detects the α1, β1, and γ1 laminin subunits was used to detect a wide variety of laminin heterotrimers found within the brain's pial and blood vessel basement membranes (Jucker et al., 1996); prominent laminin immunoreactivity is confined largely to these basement membrane sites in the adult brain. Laminin-1 immunoreactivity (red) was observed in the pial and vascular basement membranes of both wildtype (wt) and *dy/dy* (dy) cortices. DAPI nuclear stain is shown in blue; scale bar = 100 microns. Incubation with secondary alone was performed on wildtype brains to identify non-specific background staining (2° alone). Immunoreactivity to the laminin α2 subunit was seen in the basement membranes of the pia and vasculature in wildtype cortices, but was absent in *dy/dy* cortices. In contrast, laminin subunits recognized by an anti-laminin-1 antibody had a similar pattern and intensity in both wildtype and *dy/dy* basement membranes. It should be noted that the majority of all laminin heterotrimers contain the laminin-γ1 subunit and are thus readily detected by the polyclonal laminin-1 antibody. Figure modified from Relucio et al., 2009.

A

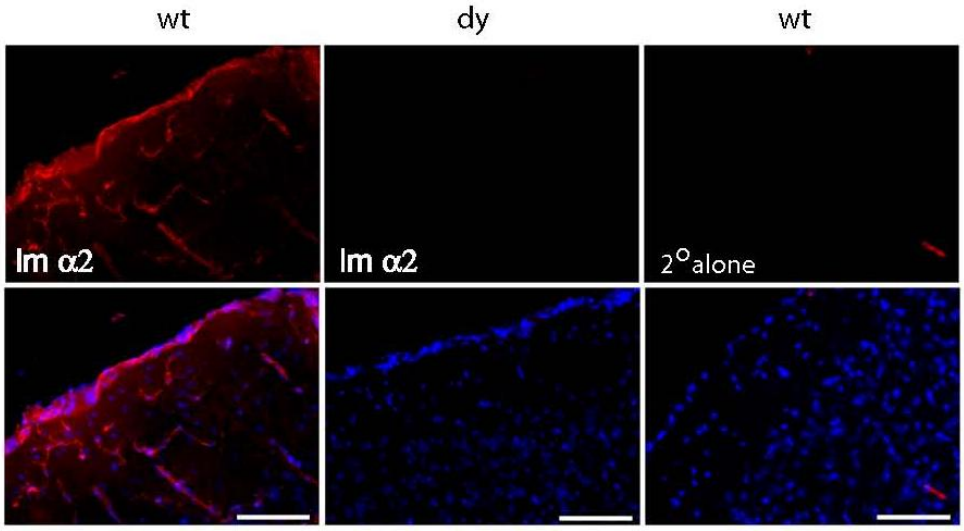

B

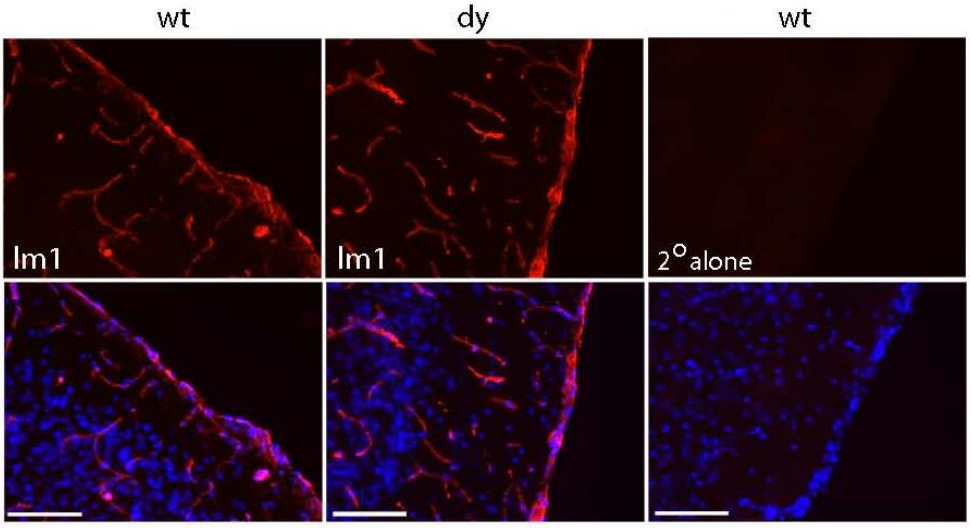

Figure II-12. Regional and temporal variation in residual *dy/dy* laminin α2 expression.

Varying degrees of residual laminin α2 expression has been reported in *dy/dy* mice, as they are hypomorphs and not true nulls (Sunada et al., 1994). To determine potential residual expression of laminin α2 immunocytochemistry was performed on fresh frozen sections from 3 and 6 week old *dy/dy* mice and their wildtype littermates from a variety of brain regions. **(A)** Laminin α2 subunit immunoreactivity in wildtype (wt) brains at 3 weeks of age was most prominent in the basal lamina of the cerebral cortex (ctx BL) and cerebellum (cb BL) as well as in the vasculature of the cortical (ctx WM), striatum (str), and brain stem (bs). In contrast laminin α2 subunit immunoreactivity in *dy/dy* (dy) brains at 3 weeks of age was variable: it was virtually absent in *dy/dy* cerebral cortices yet apparent in cerebellum and brain stem. Overall, *dy/dy* cerebellum and brain stem showed less laminin α2 immunoreactivity than wildtype structures, but more than negative control wildtype sections (ctrl; CY3-labelled secondary antibody alone). Scale bars = 50 microns. **(B)** Laminin α2 subunit immunoreactivity in wildtype (wt) brains at 6 weeks of age was still prominent in the cerebellum (cb BL) as well as in the brain stem (bs) yet was virtually undetectable in *dy/dy* structures. Scale bar = 50 microns. Figure modified from Relucio et al., 2009.

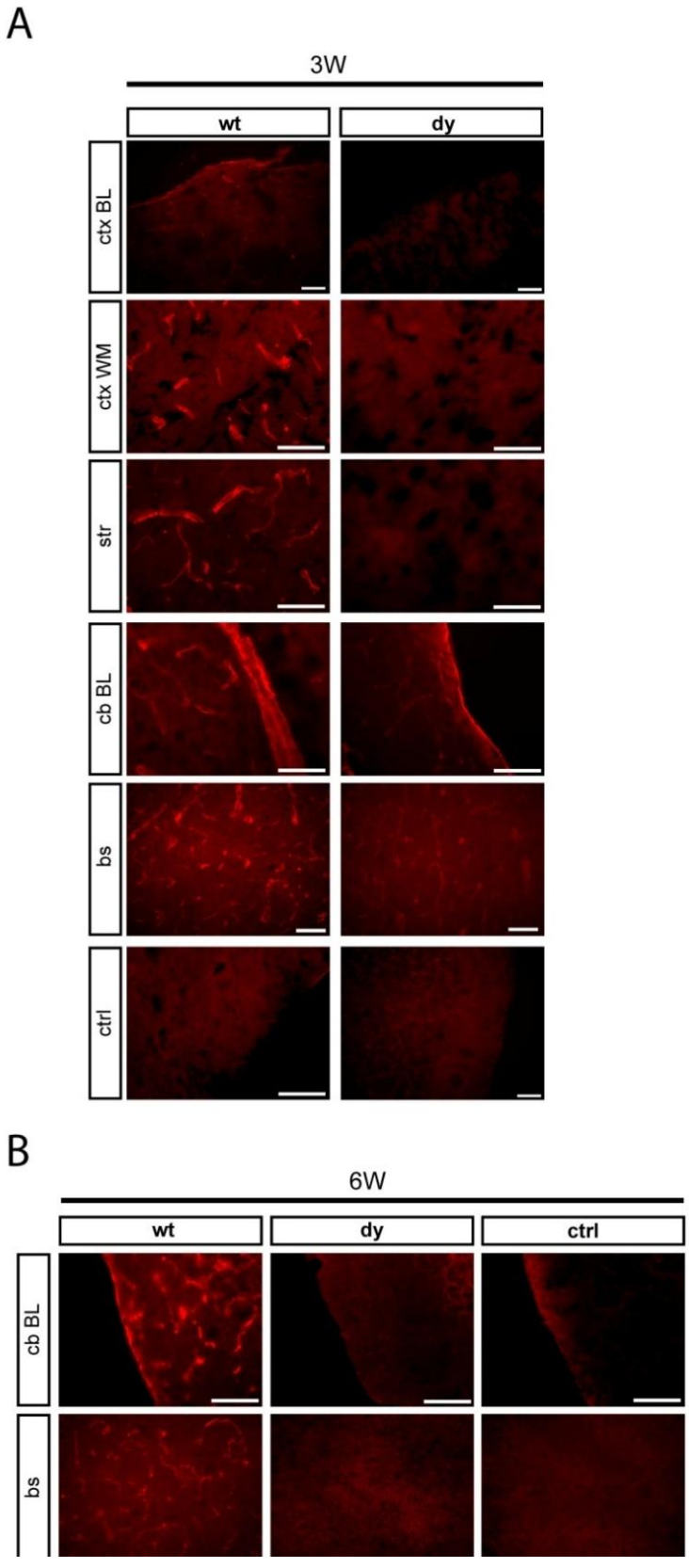
A
3W
wt
dy
ctx BL
ctx WM
str
cb BL
bs
ctrl
B
6W
wt
dy
ctrl
cb BL
bs

Table 1. CC1(+)cells per mm^2.

Table modified from Relucio et al., 2009.

		3 weeks			6 weeks			3wk v. 6 wk	
	region	wt	dy	p value wt v. dy	wt	dy	p value wt v. dy	p value wt	p value dy
1	corpus callosum	1404.6±103.0	1100.1±54.0	0.0287 *	1828.5±268.6	1640.8±234.5	0.2804	0.3686 n.s.	0.2017 n.s.
2	lateral septum	1217.7±169.0	875.3±144.3	0.3042 n.s.	1713.8±443.3	1315.2±617.9	0.1183	0.4091 n.s.	0.7103 n.s.
3	anterior commissure	1347.1±32.7	1081.3±18.6	0.0097 **	1769.3±328.0	1558.8±213.2	0.4976	0.2962 n.s.	0.1707 n.s.
4	cortex, all	1359.9±66.6	1061.9±34.8	0.0139 *	1785.0±286.4	1531.9±183.9	0.2383	0.3466 n.s.	0.1619 n.s.
5	cerebellum, central	978.2±196.7	1228.9±43.5	0.3438 n.s.	1840.8±70.5	1037.5±199.7	0.1085	0.0074 **	0.3284 n.s.
6	cerebellum, all	1473.9±76.3	1604.0±82.2	0.0263 *	1840.8±70.5	1389.6±105.6	0.0473 *	0.0107 *	0.1471 n.s.
7	brain stem	988.5±104.7	1084.6±104.1	0.0026 **	1405.1±64.9	1054.4±47.6	0.0166 *	0.0159 *	0.9369 n.s.
8	spinal cord	-	-	-	1333.8±103.4	1413.3±52.8	0.7000 n.s.	-	-
9	optic nerve	-	-	-	2923.1±124.2	2245.5±88.5	0.0335 *	-	-

Table 2. PDGFRα(+)cells per mm^2.

Table modified from Relucio et al., 2009.

		3 weeks			6 weeks			3wk v. 6 wk	
	region	wt	dy	p value wt v. dy	wt	dy	p value wt v. dy	p value wt	p value dy
1	corpus callosum	763.4±65.5	1098.7±107.0	0.0193 *	413.5±59.1	917.4±78.9	0.0212 *	0.0540 n.s.	0.0265 *
2	lateral septum	735.6±107.4	982.4±109.2	0.3624 n.s.	449.2±127.6	547.1±62.5	0.3690 n.s.	0.3074 n.s.	0.0124 *
3	anterior commissure	868.3±80.0	1307.6±73.5	0.0993 n.s.	501.1±125.9	726.7±42.1	0.1630 n.s.	0.2112 n.s.	0.0229 *
4	cortex, all	790.9±50.9	1136.4±73.6	0.0045 **	439.4±19.7	823.1±39.7	0.0137 *	0.0294 *	0.0166 *
5	cerebellum, central	255.7±18.0	622.6±129.6	0.1108 n.s.	364.2±12.4	534.3±40.0	0.0367 *	0.0134 *	0.5860 n.s.
6	cerebellum, all	333.6±28.7	636.3±100.9	0.1317 n.s.	407.6±19.8	593.5±21.6	0.0340 *	0.1478 n.s.	0.7600 n.s.
7	brain stem	259.7±13.6	259.4±34.1	0.9953 n.s.	475.7±1.4	499.2±95.4	0.8305 n.s.	0.0032 **	0.1239 n.s.
8	spinal cord	-	-	-	478.1±165.4	706.8±169.1	0.0104 *	-	-
9	optic nerve	-	-	-	745.8±22.0	1256.9±83.8	0.0766 n.s.	-	-

Table 3. TUNEL(+)cells per mm^2.

Table modified from Relucio et al., 2009.

		3 weeks			***6 weeks***		
		wt	*dy*	*p value*	*wt*	*dy*	*p value*
TUNEL(+) cells per mm^2	corpus callosum	54.2±4.9	48.4±13.4	0.6100 (n=4)	33.2±7.0	31.2±18.3	0.8863 (n=4)
	cerebellar white matter	60.1±16.0	56.2±12.5	0.6221 (n=4)	39.7±8.6	26.5±5.7	0.1437 (n=3)
	brain stem	42.2±12.5	44.2±8.9	0.8528 (n=4)	38.9±9.4	41.4±9.0	0.6904 (n=4)
%TUNEL(+) of CC1(+)	corpus callosum	0.3±0.2	0.5±0.4	0.6991 (n=3)	0.4±0.2	0.6±0.3	0.7336 (n=3)
	cerebellar white matter	0.3±0.3	1.5±0.8	0.1835 (n=3)	0.6±0.6	0.3±0.3	0.7664 (n=3)
	brain stem	0.3±0.3	0.0±0.0	N.A. (n=3)	0.0±0.0	0.8±0.5	N.A. (n=3)
%TUNEL(+) of PDGFRα(+)	corpus callosum	0.3±0.3	0.0±0.0	N.A. (n=3)	0.2±0.2	0.0±0.0	N.A. (n=3)
	cerebellar white matter	0.6±0.6	1.4±0.2	0.2586 (n=3)	0.3±0.3	0.6±0.4	0.5647 (n=3)
	brain stem	1.3±0.7	1.6±0.8	0.8396 (n=3)	0.0±0.0	0.6±0.6	N.A. (n=3)

CHAPTER III: LAMININ REGULATES POSTNATAL OLIGODENDROGENESIS

ABSTRACT

Members of the laminin family of extracellular matrix proteins are found throughout the cortical plate during corticogenesis, and are also highly enriched at the ventricular and pial surfaces, i.e. sites of radial glial attachment. Later, laminins adopt a more restricted distribution in the adult brain where laminin-containing fractone structures are found in the neural stem cell niche of the subventricular zone (SVZ). During mouse embryogenesis, laminin loss-of-function leads to detachment and misplacement of radial glia, which in turn causes disturbances in neuronal progeny and cerebral cortical development. It is not known, however, if laminins regulate the wave of oligodendrogenesis that occurs in the neonatal and postnatal brain. Here, I report that *Lama2*, the gene that encodes the laminin α2 subunit, regulates postnatal oligodendrogenesis. During early postnatal development, mice that lack LAMA2 expression (LAMA2KO) develop significantly fewer oligodendrocyte progenitor cells (OPCs), both in the dorsal aspect of the SVZ, as well as in an adjacent developing white matter tract, the corpus callosum. Progenitor cell organization is disturbed in the SVZ of LAMA2KO mice, in conjunction with selective OPC death. Later, LAMA2KO mice lag in developing mature oligodendrocytes, thus accumulating elevated levels of oligodendrocyte progenitors. These deficits lead to axonal dysmyelination in the corpus callosum by postnatal day 21. Together these

data suggest that laminin-cell interactions in the developing postnatal brain regulate the timing or ability of oligodendrogenesis to occur appropriately.

INTRODUCTION

In the developing CNS, two anatomically-defined germinal regions maintain the neural stem cells (NSCs) that give rise to the majority of neurons and glia of the forebrain (Brazel et al., 2003; Marshall et al., 2003). The early germinal niche, the pseudostratified ventricular zone (VZ), appears at embryonic day 8 (E8) and serves as the primary site of NSC expansion and neurogenesis until E17 (Parnavelas, 1999; Takahashi et al., 1995). As NSCs migrate out of the VZ and cause this niche to decline, a second pool of progenitors expands to form the subventricular zone (SVZ). By E19, the SVZ becomes the major germinal zone and primarily generates glial lineage cells during postnatal development (Levison et al., 1993; Lewis and Lai, 1974; Marshall et al., 2005; Zerlin et al., 1995). Cells of neuronal and glial lineage are thus generated in a sequential fashion, with the peak of neurogenesis occurring first and overlapping with the development of the first astrocytes; and oligodendrocyte formation beginning later in embryonic development and continuing until postnatal timepoints (Bayer and Altman, 1991; Levison et al., 1993; Miller and Gauthier, 2007; Sauvageot and Stiles, 2002; Zerlin et al., 1995).

During lineage specification, the behavior of NSCs can be influenced by the microenvironment of its niche. While much insight has been gained on how extrinsic signals regulate neurogenesis *in vitro* and in the embryonic VZ (Kang et al., 2009; Machon et al., 2003; Yu et al., 2007), the extrinsic factors that regulate postnatal SVZ oligodendrogenesis remain largely uncharacterized. Components of the stem cell niche that could potentially play functional roles during oligodendrocyte formation are the members of the laminin family of extracellular matrix molecules.

Previous studies have determined roles for one type of laminin, the laminin-α2 subunit, in regulating cortical neurogenesis (Lathia et al., 2007; Loulier et al., 2009). Several laminin chains, including laminin α2, are found in association with the VZ/SVZ proliferative zones during embryonic development. The laminin-α2 receptor β1 integrin is expressed on the surface of NSCs in the germinal niche, suggesting possible requirements for laminin ligand/integrin receptor interactions in the regulation of NSC functions (Lathia et al., 2007). Patients with mutations leading to deficient expression of the laminin-α2 gene are born with a form of congenital muscular dystrophy (type 1A; MDC1A) that is accompanied by delayed motor milestones, cognitive defects, and abnormal white matter in the brain (Allamand and Guicheney, 2002; Buteică et al., 2008; Fujii et al.; Miyagoe-Suzuki et al., 2000). An animal model of MDC1A, the laminin α2-deficient *dy/dy* mouse, also exhibits defects in oligodendrocyte maturation and myelination at 3 and 6 weeks of age (Chun et al., 2003; Relucio et al., 2009). The potential roles that laminin-α2 may play during postnatal oligodendrogenesis, however, remain uncharacterized.

In this study, I used the laminin α2-knockout mouse (LAMA2KO) as a model to determine if α2-containing laminins regulate SVZ oligodendrogenesis in the neonatal and early postnatal brain. A previous study has shown that LAMA2KO mice exhibit abnormal embryonic NSCs phenotype, resulting in dysregulated NSC proliferation and altered cleavage plane orientation in the developing cortical plate (Loulier et al., 2009). I found that laminin α2 is expressed in the pial basal lamina and within the SVZ during early postnatal development. LAMA2KO mice initially had less oligodendrocyte progenitor cells (OPCs), both in the germinal SVZ and in an adjacent developing white matter tract. These mutant mice also had a disorganized radial glial scaffold and proliferating NSCs/intermediate progenitor cells found in

ectopic locations. Later, LAMA2KO mice had defective oligodendrocyte maturation, such that by 3-weeks of age they had fewer mature oligodendrocytes than their wildtype littermates, along with increased numbers of OPCs. These deficits correlated with thinner myelin in the axons of the LAMA2KO corpus callosum. Our findings suggest that laminin-α2 regulates oligodendrogenesis in the developing brain and that early dysregulation of gliogenic niches may contribute to the CNS abnormalities observed in MDC1A.

MATERIALS AND METHODS

Animals

Laminin α2 chain-null mice (LAMA2KO) have been described previously (Miyagoe et al., 1997). Heterozygous *lama2* (+/-) mice were bred to obtain homozygous mutant animals. Genotyping was performed on tail DNA to detect the *lama2* wildtype (WT) and mutant allele (Iwao et al., 2000). The primers used to detect the WT allele were: 5'–CCAGATTGCCTACGTAATTG–3' and 5'– CCTCTCCATTTTCTAAAG–3'. PCR was carried out using the primer pair 5'–CTTTCAGATTGCATTGCAAGC–3' and 5'–TCGTTTGTTCGGATCCGTCG–3' to detect the KO allele. Homozygous wildtype (+/+) and heterozygous littermates were used as age-matched controls. All procedures were performed in accordance with the National Institutes of Health Guide for the Care and Use of Laboratory Animals and approved by the Stony Brook University Institutional Animal Care and Use Committee.

Antibodies

The following antibodies were used for immunocytochemistry: rat monoclonal IgG against the laminin α2 subunit clone 4H82 (Sigma); rabbit polyclonal IgG against laminin-1 (Sigma); rat monoclonal IgG against the laminin γ1 subunit clone A5 (Chemicon); mouse monoclonal IgG against nestin (BD Pharmingen); rabbit polyclonal IgG against NG2 (Chemicon); rat monoclonal IgG against CD140a (PDGFRα) (BD Pharmingen); rat monoclonal

IgG against myelin basic protein (Serotec); rabbit polyclonal IgG against Sox2 (Millipore); rabbit polyclonal IgG against Olig2 (Immuno-Biological Laboratories); mouse monoclonal IgG against PCNA (Cell Signaling Technology); mouse monoclonal IgG against APC (CC1) (Calbiochem); and mouse monoclonal IgG against neurofilament 200 (Sigma). The following antibodies were used for western blotting: rabbit polyclonal IgG against NG2 (Chemicon); mouse monoclonal IgG against CNPase (Sigma); rat monoclonal IgG against myelin basic protein (Serotec); and mouse monoclonal IgG against β-actin (Sigma).

Fluorescent immunocytochemistry using frozen sections

Cerebral cortices were collected from age-matched *lama2ko* mutant and wildtype control littermates. Tissues were frozen, embedded in Tissue-Tek OCT (Sakura Finetek), and cryosectioned to a thickness of 18 to 40 µm. Frozen sections were fixed in methanol for 5 min at –20°C and washed with PBS afterwards. Sections were blocked for 1 h in PBS containing 10% donkey serum (DS; Sigma), and incubated overnight with anti-laminin α2 primary antibodies in block buffer at 4°C. Following washes in PBS, CY3-conjugated secondary antibodies were applied to sections for 1 h at room temperature. After PBS washes, nuclei were counterstained with 10 µg/ml DAPI in PBS for 10 minutes and sections were mounted using Slowfade Gold antifade reagent (Invitrogen).

Fluorescent immunocytochemistry using PFA-perfused sections

Cerebral cortices were collected from wildtype and *lama2ko* littermates at postnatal days 1, 5, and 8. Tissues were submerged for 16-24 hours in 4% paraformaldehyde (PFA) in PBS at 4°C to allow fixation. Older animals (i.e., at least 2 weeks postnatal) were anesthetized with Avertin and perfused intracardially with a saline solution, followed by 4% PFA in PBS. Brains were harvested from perfused animals, postfixed for 1 h in PFA, and equilibrated in 30% sucrose at 4°C before they were cryosectioned to generate coronal sections (thickness of 18 to 25 µm). Tissue sections were blocked in 10% DS with 0.1% Triton X-100 for 1 h before labeling with primary antibodies overnight at 4°C. This was followed by incubation with secondary antibodies in 10% DS for 1 h before nuclear counterstaining and mounting with Slowfade Gold reagent.

Alternatively, 40 µm free-floating sections were prepared. Briefly, cryosections were placed in chilled tissue stock solution (30% glycerol: 30% ethylene glycol: 10% 0.2 M phosphate buffer). For immunodetection using antibodies against laminins and oligodendrocyte lineage markers, floating sections were washed 3 times in PBS with 0.2% Triton X-100 (PBST). After blocking in 1% DS in PBST for 30 min, the sections were incubated in primary antibody overnight at room temperature. Sections were washed with PBST and incubated in fluorescent secondary antibody for 1 h. Finally, floating sections were washed 3 times with PBST, followed by 3 washes with 0.1 M phosphate buffer. All sections were incubated in DAPI for 10 min and then mounted with SlowFade Gold antifade reagent.

Analysis of Sox2$^+$ intermediate progenitor cells in the dorsal subventricular zone

To determine the organization, proliferation, and survival of intermediate progenitor cells (iPCs) in the dorsal SVZ region juxtaposing the corpus callosum, immunocytochemistry with progenitor cell type-specific antigens was performed in conjunction with cell proliferation and apoptosis markers. For anti-Sox2 immunostaining, PFA-fixed coronal sections from mutant and wildtype brains were pretreated with 0.3% Triton X-100 detergent in PBS for 15 min at room temperature. To allow co-detection of Sox2 with nestin (a marker expressed in radial glia) or PCNA (a marker expressed in proliferating cells), sections were immersed in 1X Target Retrieval Solution citrate buffer (pH 6.0, DakoCytomation) and heated at 95-99°C for 20 min. Slides were removed from the water bath and allowed to cool for 20 min at room temperature. After several washes with PBS, sections were blocked in 10% DS with 0.1% Triton X-100 for 1 h. Immunocytochemistry using anti-Sox2 antibodies in combination with either anti-nestin or anti-PCNA primary antibody was performed overnight at 4°C. Sections were washed with PBS then incubated in fluorescence-conjugated secondary antibodies for 1 h, before counterstaining with DAPI and mounting with SlowFade Gold. TUNEL assays (ApopTag^{TM} In Situ Apoptosis Detection Kit, Chemicon) were also performed on Sox2-stained sections to determine cell survival in the iPC population. Sections were visualized and imaged using a Zeiss LSM 510 Meta confocal microscope with 10x eyepiece magnification using 40x [1.3 numerical aperture (NA), oil], 63x (1.4 NA, oil), and 100x (1.4 NA, oil) objectives. The density of Sox2$^+$-progenitor cells in the dorsal SVZ, along with the numbers of proliferating (i.e., PCNA$^+$) Sox2$^+$-cells and apoptotic (i.e., TUNEL$^+$) Sox2$^+$-cells, were determined using the *Axio Vision Rel. 4.8* software (Carl Zeiss, Microimaging GmbH, Germany). Morphometric analyses of the thickness of the dorsal SVZ and the distances of Sox2$^+$- and PCNA$^+$Sox2$^+$-stained nuclei from the ventricular

surface were done on matching sections of wildtype and *lama2ko* cerebral cortices using Axio Visions Interactive Measurement Wizard modules.

Analysis of oligodendrocyte density, survival, and proliferation

To determine oligodendrocyte lineage cell density in the dorsal SVZ and the corpus callosum during development, frozen and PFA-fixed cortical sections (18-25 µm in thickness) were blocked in 10% DS with 0.1% Triton X-100 for 1 h at room temperature. Immunocytochemistry using anti-Olig2 (a marker expressed during all stages of the oligodendrocyte lineage) in conjunction with either anti-PDGFRα (a marker expressed in oligodendrocyte progenitors) or anti-APC (CC1; a marker expressed in mature oligodendrocytes) primary antibody was performed overnight at 4°C. Sections were washed 4 times in PBS, then incubated in fluorescence-conjugated secondary antibodies for 1 h, before washing again in PBS. The numbers of $Olig2^+$, $PDGFR\alpha^+Olig2^+$ and $CC1^+Olig2^+$ cells in the corpus callosum and the dorsal SVZ were scored in matching sections of wildtype and *lama2ko* cerebral cortices.

To determine oligodendroglial proliferation and survival, cortical sections stained with stage-specific antibodies (e.g., anti-NG2 or with anti-CC1 primary antibody) were co-stained to detect either $PCNA^+$ proliferating cells or apoptotic cells (ApopTag^{TM} In Situ Apoptosis Detection Kit). Sections were visualized using Zeiss LSM 510 Meta confocal microscope and a Zeiss Axioplan inverted fluorescence microscope fitted with 10x eyepiece magnification using 5x [0.16 numerical aperture (NA)], 10x (0.3 NA), 20x (0.5 NA), 40x (0.75 NA), and 63x (1.4 NA, oil) objectives. The corpora callosa and the dorsal SVZ of matching sections of wildtype

and mutant cortices were analyzed to determine the percentages of proliferating OPCs ($PCNA^+NG2^+$ cells) and apoptotic oligodendrocytes ($TUNEL^+$ $NG2^+$ and $TUNEL^+$ $CC1^+$ cells).

Western blot analysis

Cerebral cortices collected from age-matched wildtype and mutant littermates were lysed in extraction buffer (1% SDS, 20 mM Tris pH 7.4 with protease and phosphatase inhibitor cocktails (Calbiochem), used at 1 ml buffer per 200 mg tissue). Tissues were incubated at 95°C for 10 min with occasional trituration. Following sample centrifugation at 14,000 rpm, the supernatant was collected and used to determine total protein concentration (detergent compatible protein assay, Bio-Rad). Tissue lysates were boiled for 5 min in Laemmli solubilizing buffer (LSB) with 4% β-mercaptoethanol (βME). Proteins were separated by SDS-PAGE using 7.5, 12, or 15% acrylamide minigels and transferred onto 0.45 µm nitrocellulose. Membranes were blocked in 0.1% Tween 20, and Tris buffered saline (TBS-T) containing either 4% bovine serum albumin (BSA) or 1% nonfat milk (blocking buffer) for 1 h, followed by primary antibodies in blocking buffer overnight at 4°C. Membranes were washed in TBS-T, incubated for 1 h in HRP-conjugated secondary antibodies (Amersham) diluted 1:3000 in blocking buffer, washed in TBS-T, and then developed using enhanced chemiluminescence (Amersham). Relative densitometries were determined using the NIH ImageJ Processing and Analysis Program.

Electron microscopy and morphometric analysis

Five three-week old littermate mice were processed for electron microscopy (three were *lama2ko* and two wild type). Mice were perfused intracardially with 4% paraformaldehyde/2.5% glutaraldehyde in 0.1 M phosphate buffered saline. Brains were postfixed overnight at 4°C and individual structures were cut in sagittal plane on a Leica VT-1000 Vibratome at 50–60 µm. Vibratomed free-floating sections were processed using standard transmission electron microscopy techniques. Briefly, sections were placed in 2% osmium tetroxide in 0.1 M phosphate buffer, washed in 0.1 M phosphate buffer and dehydrated in a graded series of ethyl alcohol. Sections were then vacuum-infiltrated in Durcupan ACM embedding agent (Electron Microscopy Sciences) overnight, flattened between two pieces of ACLAR film (Ted Pella) and placed in a 60°C oven for 48–72 h to polymerize. Regions of interest were blocked and ultrathin sections (70-80 nm) were generated using a Reichert-Jung 701704 Ultracut E ultramicrotome. Ultrathin sections were placed on formvar-coated copper slot grids and counterstained with uranyl acetate and lead citrate. Samples were viewed with a Tecnai^{TM} Spirit BioTwin G^2 transmission electron microscope (FEI Company). Digital images were acquired with an AMT XR-60 CCD Digital Camera System (Advanced Microscopy Techniques, Corp.) and compiled and analyzed using Adobe Photoshop and ImageJ (NIH). The g-ratio of myelinated axons was determined by dividing the axon diameter by the myelin diameter. A minimum of 333 axons was measured for the corpus callosum of each mouse.

Statistical analysis

Statistical significance of data sets was determined using the Student's two-tailed, paired t test. Graphs depict the mean values, with error bars depicting SEM. Student's t test was performed on binned g-ratios where normal distribution and equal variance was determined; mean g-ratio and SEM is depicted.

RESULTS

Laminin expression patterns in the postnatal cerebral cortex.

To help determine potential roles for laminins during oligodendrogenesis, oligodendrocyte development, and myelination, I characterized the spatial and temporal patterns of laminin expression during early postnatal timepoints of CNS development. Previous studies have shown that laminins are widely expressed in neurogenic regions of the CNS during embryonic development (Lathia et al., 2007; Libby et al., 2000; Liesi, 1985). In contrast, the adult brain exhibits restricted laminin expression largely confined to the basal lamina of the pia and cerebral vasculature (Villanova et al., 1997b). Transitional changes in the distribution and expression levels of laminins as myelination proceeds, however, remain largely uncharacterized.

I first performed immunohistochemistry using a polyclonal laminin-1 antibody to detect the β1 and γ1 chains that are widely distributed among different types of laminins in the developing CNS. In postnatal day 1 cerebral cortices, strong expression levels of laminin were detected in the basement membranes of the pia and the vasculature (Fig. III-1A, top panels). Additionally, I also observed moderate pericellular staining on presumptive neuronal cell bodies found in the marginal zone and other cortical layers underlying the pial basal lamina. By postnatal day 8, levels of laminin immunoreactivity in the pia and blood vessels remained comparable to levels observed at P1 (Fig. III-1A, top panels). The pericellular staining on neuronal cell bodies seemed to be less frequent at P8 compared to P1 (Fig. III-1A).

I next examined laminin expression in the postnatal SVZ (Fig. III-1A, bottom panels). Pronounced laminin immunoreactivity was detected in the blood vessels of the SVZ at P1 (Fig. III-1A, bottom panels). There were also pronounced extravascular laminin immunoreactive

structures reminiscent of fractones, particularly near the ventricular surface, although these were also detected to a lesser extent outside the SVZ. By P8, laminin immunoreactivity became restricted to the vasculature and the detection of extravascular laminin structures was markedly decreased. Concurrently, ependymal cells lining the apical surface of lateral ventricles began exhibiting immunoreactivity to the pan-laminin antibody (Fig. III-1A, bottom panels).

Since radial glia can be found in association with the lateral ventricle through their apical and basal processes during early postnatal development, I therefore performed laminin immunostaining in conjunction with antibodies against the intermediate filament protein nestin (a protein expressed in radial glial cells) (Fig. III-1B). During oligodendrogenesis, laminin immunoreactivity was seen in proximity to nestin(+) radial glial fibers (Fig. III-1B**)**, where laminin may be able to influence intermediate progenitor cell (iPC) populations and/or nestin(+) radial glial cells.

Since the postnatal SVZ is the major source of glial progenitors in the developing postnatal brain, I performed immunostaining for the laminin γ1 subunit in conjunction with the oligodendrocyte progenitor marker NG2 (Fig. III-1C). Laminin γ1-immunoreactivity was seen in the P1 SVZ (Fig. III-1C, top panels). Cells expressing NG2 were found to associate with these laminin γ1(+) structures in the SVZ (Fig. III-1C, top panels). I also looked at laminin expression in the major white matter tract overlying the SVZ, the corpus callosum. In the corpus callosum of mice at P1, NG2(+) OPCs were also found in association with blood vessels that exhibited laminin γ1 basement membrane expression. (Fig. III-1C, bottom panels) When I performed co-immunostaining with the polyclonal laminin antibody and MBP (a marker of myelinating oligodendrocytes), I found that laminins are expressed in the vascular basal lamina and neuronal cell bodies in the white matter tracts at P1 and at P8 (Fig. III-1D). No detectable levels of MBP

were found in the P1 corpus callosum (Fig. III-1D, left panel). During P8, when cortical myelination is normally initiated, MBP(+) oligodendrocytes can be found in proximity to both laminin(+) vasculature and laminin(+) cell bodies, particularly near the cingulum and external capsule of the corpus callosum (Fig. III-1D, right panel). These findings suggest that the distribution and expression of laminins in the SVZ and corpus callosum could allow them to influence stem cells, basal progenitors, and oligodendrocyte lineage-committed cells during early postnatal development.

SVZ cell numbers and organization are abnormal in postnatal LAMA2KO mice

Immunostaining with laminin α2 (4H82) monoclonal antibody was used to determine spatial patterns of laminin α2 protein in postnatal cerebral cortices, and to verify loss of laminin α2 protein in LAMA2KO mice (Figs. III-2A and III-2B). Wildtype mice had high levels of laminin α2 protein in the basal lamina of the cerebral cortices at P1 (Fig. III-2A). Laminin α2 protein was also found within the subventricular zone, although at lower levels compared to that seen at the pial basal lamina levels (Fig. III-2B). Cortical sections from LAMA2KO mice did not exhibit immunoreactivity, indicating specificity of the detected laminin α2 chain in wildtype sections (Figs. III-2A and III-2B).

To determine if loss of laminin α2 disrupted the oligodendrogenic niche, I first characterized the organization of a subset of the resident cell types of the subventricular zone (SVZ). Morphological analysis of the cell-dense SVZ by DAPI nuclear staining showed a significant reduction in the thickness of the postnatal dorsal SVZ in laminin α2-knockout mice (61.0±6.2 μm in laminin α2-nulls versus 84.3±12.5 μm in wildtype; n=4; p=0.0357). Immunohistochemistry using antibodies against the intermediate filament protein nestin (a

protein expressed in radial glia) was performed in conjunction with the neural progenitor cell transcription factor, Sox2 (Fig. III-2C). In wildtype animals, radial glia were found in their stereotypical palisade arrangement, with their corresponding apical attachments terminating near the lateral ventricle and their basal attachments reaching the pial basement membrane. In mutant mice, however, the density of nestin(+) radial glial fibers appears reduced (Fig. III-2C, inset). Upon closer examination, their organization also appears disrupted, particularly at their apical ends, suggesting disrupted radial glial adhesion to structures within the SVZ gliogenic niche (Fig. III-2C, inset).

Since radial glia have dual functions, as both scaffolds for migrating progenitor cells and as a source of neural progenitors for the developing brain, I proceeded to examine whether disruption of radial glial organization would also affect the resident pool of Sox2(+) neural progenitors in the niche (Fig. III-2D). Analysis of the Sox2(+) cell density at P1 revealed no significant difference, however, between the density of neural progenitors in the SVZ of wildtype and LAMA2KO (Fig. III-2D; 1754037.6±145429.4 cells/mm^3 versus 1774479.4±184591.2, respectively, n=3, p=0.919), suggesting that laminin α2 mutants are able to generate appropriate numbers of NSCs/iPCs. There were also no significant differences in Sox2(+) cell density between the wildtype and LAMA2-/- SVZ at both P5 (Fig. III-2D; 1469273.6±328582.9 cells/mm3 compared to 1177243.6±8616.6, respectively, n=3, p=0.347) and P8 (Fig. III-2D; 609679.1±32939.8 cells/mm3 in wildtype versus 661025.9±139808.7 in LAMA2-/- SVZ, n=3, p=0.856), indicating that appropriate numbers of NSCs/iPCs are maintained in the mutant SVZ during these developmental timepoints.

To determine if oligodendrogenesis is affected by the loss of laminin α2, I performed immunostaining with the OPC protein NG2 and determined the density of NG2(+) OPCs in the

SVZ (Figs. III-2E and III-2F). At P1, I observed that the numbers of NG2(+) OPCs per volume of LAMA2KO SVZs were ~40% of wildtype values (Figs. III-2E and III-2F; 138346.1±2807.0 cells/mm^3 versus 86196.0±4682.1, respectively, n=4, p=0.0178). By postnatal day 8, however, the numbers of NG2(+) OPCs were significantly increased in the SVZ of mutant mice relative to control animals (Fig. III-2E; 185024.0±28982.2 cells/mm^3 in LAMA2KO compared to 125971.1±24673.5 in wildtype, n=3, p=0.0163). These findings suggest that proper oligodendrogenesis becomes dysregulated in the absence of α2-containing laminins.

Ectopic Sox2(+) intermediate progenitors in the LAMA2KO SVZ

Cell adhesion to the ECM has been shown to regulate both the positioning and proliferation of neural progenitors. Genetic deletion of the nidogen-binding site of the laminin γ1 chain caused basement membrane disruption, leading to radial glial endfeet retraction and ectopic positioning of radially-migrating neurons (Halfter et al., 2002). In the adult SVZ where proliferating NSCs associate closely with laminin-rich blood vessels, the administration of integrin blocking antibodies disrupted NSC adhesion to the vascularized niche, altering both NSC position and proliferation *in vivo* (Shen et al., 2008). Loss of laminin α2 function in mutant cerebral cortices could cause cell proliferation and positioning in the SVZ to become disrupted.

I first examined if the intermediate and oligodendrocyte progenitors generated in the LAMA2KO mice were more or less proliferative than the OPCs and iPCs generated in wildtype animals. Previous studies have provided evidence that laminin can regulate the proliferation of various progenitor cell types in the CNS. Cultured OPCs exhibited enhanced proliferation when grown on laminin substrates in combination with soluble neuregulin. In mice where β1 integrin has been removed in the CNS, cerebellar granule cell precursors exhibited reduced proliferation

(Blaess et al., 2004). To examine if OPC proliferation is affected by the loss of laminin α2, I determined the percentage of proliferative OPCs in the SVZ of wildtype and knockout animals through immunohistochemistry with NG2 in conjunction with the proliferation marker PCNA. (Fig. III-3A). Although mutant mice have fewer resident OPCs in the P1 SVZ, I found no significant differences in the proportion of PCNA(+) proliferating cells in the NG2(+) progenitor populations of control and mutant animals (Fig. III-3A, left panel; 37.1±6.9% versus 48.8±14.9%, respectively, n=3, p=0.328). Analysis of later timepoints also showed no significant differences in OPC proliferation between control and mutant animals (Fig. III-3A; at P5, 27.1±4.1% in controls versus 33.5±7.0% in mutants, n=3, p=0.576; at P8, 48.5±1.5% in controls compared to 34.6±12.8% in mutants, n=3, p=0.394). For intermediate progenitors at P1, proliferation in the LAMA2KO SVZ was also similar to that seen in control animals, as determined by the percentage of PCNA(+) cells within the Sox2(+) progenitor pool (Fig. III-3A, right panel; 51.7±17.6% in controls versus 54.9±3.6% in LAMA2KO mice; n=3; p=0.870). Analysis of later time points (P5 and P8) also showed no significant change in Sox2+ cell proliferation in the LAMA2-/- SVZ (Fig. 3A; at P5, 41.2±1.5% in controls versus 31.1±2.3% in mutants, n=3, p=0.335; at P8, 33.0±5.6% in controls compared to 24.7±3.9% in mutants, n=3, p=0.138)

The emergence of oligodendrocytes from specific sites in the CNS is due in part to highly localized extrinsic signals, such as morphogens (Sonic Hedgehog, Shh) and growth factors (e.g., PDGF) (Bongarzone, 2002). The location of a progenitor cell within the niche could then possibly influence its cell fate choices. To determine whether the loss of laminin α2 would alter the position of progenitors in the SVZ, I used the Measurement Pro module of the Zeiss Axiovision imaging software to measure the distances of Sox2(+) and PCNA(+)Sox2(+) cell

bodies from the ventricular surface (VS) (Figs. III-3B and III-3C). I observed a significant ($p<0.001$) increase in the mean and median distance of Sox2(+) cells from the ventricular surface in the laminin α2 knockout SVZ at P1 (mean distance of 43.40±1.18 μm from the VS, n=1378 Sox2+ cell bodies; median distance of 26.91 μm from the VS) compared to the wildtype SVZ (mean distance of 35.61±1.15 μm from the VS, n=1065 Sox2+ cell bodies; median distance of 13.68 μm from the VS). Similarly, the proliferating progenitors (PCNA+;Sox2+) in the LAMA2KO SVZ were also found at ectopic positions in the niche (Fig. III-3B). On average, LAMA2KO PCNA(+);Sox2(+) cells were found at a significantly ($p<0.001$) shorter distances from the VS (mean distance of 53.31±2.00 μm from the VS, n=788 PCNA+ Sox2+ cell bodies; median distance of 29.69 microns from the VS) compared to their wildtype counterparts (data not shown; mean distance of 31.15±1.56 μm from the VS, n=564 PCNA+; Sox2+ cell bodies; median distance of 14.74 μm from the VS). Individual measurements were also grouped into 6 abventricular bins (i.e., <20, 20-40, 60-100, 100-140, 140-180, and >180 μm from the VS) and revealed that an increased proportion (59.8%) of the proliferating progenitor (PCNA+ Sox2+) cell population in the LAMA2KO cerebral cortex can be found within 20 μm of the VS, compared to proportions observed in their wildtype littermates (40.2%). This change in location indicated that neural progenitors were abnormally found close to the LAMA2KO ventricles (Figs. III-3B and III-3C). At P1, the SVZ border can be found 61.0±6.2 μm from the VS in laminin α2-nulls, while the SVZ border in wildtype brain lies, on average, 84.3±12.5 μm from the VS.

Additionally, I also observed a significant ($p=0.00105$) increase in the mean and median distance of Sox2(+) cells from the ventricular surface in the laminin α2-knockout SVZ at P8 (mean distance of 26.07±2.29 μm from the VS, n=171 Sox2(+) cell bodies; median distance of

13.86 µm from the VS) compared to the wildtype SVZ (mean distance of 37.47±2.47 µm from the VS, n=219 Sox2+ cell bodies; median distance of 25.16 µm from the VS). Taken together, these data indicate that the loss of laminin α2 results in profound disruptions in the organization and cellular composition of the SVZ, such that radial glia structure is disorganized, and intermediate progenitor cells are found in abnormal distributions.

Increased oligodendrocyte progenitor cell death in the laminin α2-null SVZ.

The observed decrease in the numbers of NG2(+) OPCs found in the dorsal SVZ of postnatal LAMA2KO cerebral cortices could indicate that OPCs produced in laminin α2 mutant niches die more readily compared to those in their wildtype littermates. I therefore examined whether the loss of laminin α2 caused increased OPC death in the SVZ. Cortical sections from early postnatal wildtype and mutant mice were subjected to a TUNEL assay to allow detection of dying cells. This was done in conjunction with either NG2 (OPC marker) or Sox2 (intermediate progenitor marker) immunohistochemistry, to allow evaluation of cell death within these respective cell populations (Fig. III-4). I found a dramatic increase in the percentage of TUNEL(+) apoptotic cells within the NG2-expressing oligodendrocyte progenitor populations in LAMA2KO subventricular zones relative to wildtype at postnatal day 1 (Figs. III-4A and III-4B; 64.85±7.3% in mutant SVZ versus 31.4±3.3% in wildtype, n=3, p=0.0245). No significant differences in OPC death were detected at the later postnatal timepoints analyzed (Fig. III-4B). In contrast, I did not observe differences in Sox2(+) progenitor cell death at the timepoints analyzed (Fig. III-4C), suggesting that iPCs were not dying selectively in the LAMA2KO SVZ. Together, these findings indicated that preferential OPC death, not decreased OPC proliferation,

may play a major role in altering the numbers of oligodendrocyte progenitors in the SVZ of laminin α2 knockout mice.

Abnormal numbers of oligodendrocyte progenitors in the LAMA2KO corpus callosum.

Since loss of laminin α2 affected the numbers of oligodendrocyte progenitors at their site of genesis in the SVZ, I next examined whether the population of oligodendrocyte progenitors in the overlying white matter tract, the corpus callosum, also becomes affected in laminin α2-knockout animals. I first evaluated the number of oligodendrocyte progenitors in the corpus callosum by counting cells positive for NG2 immunoreactivity (Figs. III-5A and III-5B). Similar to my findings in the P1 SVZ, I also found significantly reduced numbers of NG2(+) cells per mm^3 in the developing corpus callosum of laminin α2-knockout mice compared to wildtype animals (Figs. III-5A and III-5B; 106363.9± 2807.0 cells per mm^3 in wildtype animals; 57227.5± 4346.6 cells per mm^3 in *lama2ko* animals; n=3; p= 0.00757). Levels of NG2 protein were also consistently reduced in cerebral cortical lysates of P1 knockout animals compared to wildtype, as determined by western blotting (Fig. III-5D). By postnatal day 5, the density of NG2(+) cells in both wildtype and LAMA2KO animals had increased. However, while wildtype animals only had an approximately 48% increase in NG2(+) cell numbers from postnatal day 1 to 5 (Fig. III-5A; 106363.9± 2807.0 cells per mm^3 at P1 compared to 157416.6 ± 13633.7 cells per mm^3 at P5; n=3; p=0.0469), LAMA2KO animals had an almost two-fold increase in NG2(+) cell numbers within the same developmental timepoints (Fig. III-5A; 57227.5± 4346.6 cells per mm^3 at P1; 110329.9± 4057.4 cells per mm^3 at P5; n=3; p=0.00338). By postnatal day 8, however, NG2(+) cell numbers were beginning to reach normal values but remained significantly decreased in the mutant corpus callosum versus control animals (Fig. III-5A; 133529.3 ± 13047.4 cells per mm^3

in wildtype versus 93890.4 ± 7317.2 cells per mm^3 in knockout; n=3; p=0.0447). These results indicated that the role of laminin α2 in regulating the timing of OPC production in the SVZ is critical for generating the correct numbers of oligodendrocyte progenitors that populate the corpus callosum early in postnatal development.

The observed decrease in oligodendrocyte progenitors during early postnatal timepoints could result from an overall reduction in the numbers of oligodendrocyte lineage cells residing in white matter target regions. Alternatively, oligodendrocyte lineage cells may be available in target regions, but may be generating oligodendrocyte progenitors less readily or on a slower time scale. To address these questions, I first quantified the total numbers of Olig2(+) oligodendrocyte lineage cells in the same regions of the corpus callosum that were analyzed for the presence of NG2(+) oligodendrocytes. At the timepoints analyzed, a slight but significant decrease in the density of Olig2(+) cells was only observed in the P5 mutant corpus callosum compared to wildtype (data not shown; 219398.3±6586.7 cells per mm^3 in wildtype; 199130.2±3925.4 cells per mm^3 in LAMA2KO animals; n=3; p=0.0376). No significant differences in the density of Olig2(+) cells were observed at either P1 or P8 (data not shown; n=3 and p=0.446 for P1; n=4 and p=0.615 for p8). These findings suggested that Olig2(+) oligodendrocyte-lineage cells are available in similar densities within the corpus callosum of wildtype and knockout littermates.

To determine whether the loss of laminin α2 affects the numbers of oligodendrocyte progenitors within the pool of total Olig2(+) oligodendrocyte lineage cells, I performed double immunohistochemistry using antibodies against Olig2 and PDGFRα (a cell marker expressed in oligodendrocyte progenitors) to determine the density of cells that are double-positive for PDGFRα and Olig2 in the corpus callosum (Fig. III-5C). During early postnatal development, I

found PDGFRα(+);Olig(2+) cell densities in the laminin α2 knockout corpus callosum to be consistently less than wildtype values (Fig. III-5C). At P5, mutant mice had ~33% less PDGFRα(+);Olig2(+) OPCs compared to control littermates (Fig. III-5C; 77288.8±10169.0 cells per mm^3 in wildtype animals versus 51664.1±2581.5 cells per mm^3 in mutants; n=3; p=0.0130). This significant reduction in numbers of PDGFRα(+);Olig2(+) OPCs in the knockout white matter persisted until P8 (Fig. III-5C; 66494.8±5720.4 cells per mm^3 in wildtype; 51866.7±2581.5 cells per mm^3 in LAMA2KO; n=3; p=0.0433). After this timepoint, however, the numbers of PDGFRα(+);Olig2(+) cells in the knockout animals began to increase significantly such that by 3 weeks of age, their oligodendrocyte progenitor numbers were two-fold of wildtype values (Fig. III-5C; 32469.9±1843.5 cells per mm^3 in wildtype compared to 67168.7±6608.6 cells per mm^3 in mutants; n=3; p=0.0365). By 4 weeks of age, the OPC numbers in the corpus callosum of both wildtype and mutants had decreased, although LAMA2KO corpus callosum still had more PDGFRα(+);Olig2(+) oligodendrocyte progenitors relative to their control littermates (Fig. III-5C; 37252.4±3006.7 cells per mm^3 in mutants compared to 21681.6±2015.6 cells per mm^3 in control; n=3; p=0.00438). The lower numbers of NG2(+) and PDGFRα(+)Olig2(+) progenitors during peak timepoints of cortical oligodendrogenesis, followed by progressively significant elevation of the numbers of these cells in the corpus callosum later during development, suggested that oligodendrocyte progenitor production is delayed in the laminin α2-knockout brain.

While the above results indicated that the laminin α2-knockout mice failed to generate the correct numbers of oligodendrocyte progenitor cells in a timely manner, I also wanted to determine if increased progenitor apoptosis and reduced OPC proliferation contribute to this phenotype. TUNEL assays were performed in conjunction with NG2 immunohistochemistry to

detect apoptotic progenitor cells in the corpus callosum of LAMA2KO and control animals (Figs. III-5E and III-5F). At P1, higher percentages of TUNEL+ OPCs were observed in LAMA2-/- mice compared to wildtype (Figs. III-5E and III-5F; 14.2± 2.3% in wildtype and 24.5± 3.4% in mutant animals; n=5; p= 0.0492). A small increase in OPC death was also found in the P5 LAMA2-/- corpus callosum relative to age-matched control mice (Fig. III-5E; 10.9± 0.9% in wildtype and 12.5± 1.0% in mutant animals; n=3; p= 0.0130). By P8, however, OPC death in both wildtype and LAMA2-/- corpus callosum was similar in both genotypes (Fig. III-5E; 14.8±0.8% in wildtype versus 12.8±4.7% in LAMA2-/- mice; n=3, p=0.742). These results suggest that selective OPC death also occurs in the white matter tracts of laminin α2 knockout animals at early postnatal timepoints, albeit at a lower magnitude than what was seen in the SVZ.

Proliferation was also analyzed in white matter OPCs through NG2 immunohistochemistry in conjunction with PCNA to determine the ratio of PCNA(+); NG2(+) proliferating OPCS within the total oligodendrocyte progenitor pool in the corpus callosum (Fig. III-5G). While fewer OPCs were found in the white matter tracts of LAMA2KO animals, the percentages of proliferating PCNA(+) OPCs in the corpus callosum of mutant animals were similar to controls (Fig. 5G; at P1, 37.0±7.9% in wildtype compared to 52.8±2.2% in mutant animals, p=0.200; at P5, 60.4±6.1% in control littermates versus 58.5±7.7% in LAMA2-/- mice, p=0.879; at P8, 50.5±2.2% in wildtype and 50.2±5.5% in knockout littermates; n=3).. This proliferation data indicates that a reduction of OPC proliferation in LAMA2KO brains is unlikely to contribute to the observed differences in OPC density. Overall, these results suggested that laminin α2 is critical for generating an adequate supply of oligodendrocyte progenitors to populate the developing corpus callosum.

Oligodendrocyte maturation is abnormal in laminin α2 knockout brains.

Given that laminin α2-knockout mice had inappropriate oligodendrocyte progenitor numbers throughout the timepoints we analyzed, I next examined oligodendrocyte maturation. First, I evaluated the density of mature oligodendrocytes by counting the number of cells that were double-positive for Olig2 and the mature oligodendrocyte marker CC1 (Figs. III-6A and III-6C). In P8 white matter, the densities of CC1(+);Olig2(+) cells in mutant mice were significantly reduced compared to their age-matched littermate controls (Fig. III-6C). At postnatal day 8, when mutant animals were previously found to have less OPCs than their wildtype littermates, numbers of CC1(+);Olig2(+) cells in the LAMA2KO corpus callosum were less than 50% of wildtype values (Fig. III-6A; 16706.5±2376.6 cells per mm^3 in laminin α2 knockout mice; 38059.1±4658.7 cells per mm^3 in wildtype littermates; n=3; p=0.0214). By 2 weeks of age, the numbers of CC1(+);Olig2(+) oligodendrocytes had increased in both wildtype and laminin α2 knockout animals (Fig. III-6A). These increases were greater in the knockout animals, such that by P14 there was no significant difference in the numbers of mature oligodendrocytes in wildtype and LAMA2KO corpus callosum (Fig. III-6A; 87475.9±5603.7 cells per mm^3 in wildtype compared to 75579.5±10254.0 cells per mm^3 in mutants; n=4; p=0.227). These findings indicated that reduced OPC numbers correlate with lower numbers of mature oligodendrocytes in the early postnatal laminin α2 knockout corpus callosum.

My findings indicated that by 3 weeks of age, LAMA2KO brains exhibited excess numbers of OPCs in the corpus callosum. I proceeded to quantify the density of CC1(+);Olig2(+) cells in 3-4 week old mutant animals to determine if oligodendrocyte differentiation at these later timepoints were also altered in LAMA2KO brains (Figs. III-6A and III-6C). In spite of elevated numbers of oligodendrocyte progenitors in the corpus callosum, the numbers of mature

oligodendrocytes remained significantly lower in three-week old LAMA2KO compared to controls (Fig. III-6C; 89705.9±24402.4 cells per mm^3 in mutants compared to 130612.84±22473.3 cells per mm^3 in controls; n=4; p=0.0184). I confirmed these changes through western blotting to detect levels of oligodendrocyte stage-specific protein markers in cortical lysates from 3-week old wildtype and laminin α2 knockout mice (Fig. III-6B). I found decreased levels of the differentiated oligodendrocyte proteins, myelin basic protein (MBP) and 2', 3'-cyclic nucleotide 3'-phosphodiesterase (CNP) in LAMA2KO cerebral cortices compared to wildype littermates (Fig. III-6B). Levels of the OPC protein NG2, on the other hand, were elevated in 3 week-old laminin α2 knockout cortices, compared to wildtype littermates (Fig. III-6B). By postnatal day 28, wildtype mice had 2.5-fold more CC1(+);Olig(2+) cells than their LAMA2KO littermates (Fig. III-6C; 167927.6±32167.5 cells per mm^3 in wildtype versus 65891.0±7728.7 cells per mm3 in knockout animals; n=3; p=0.0634).

Additionally, low levels of oligodendrocytes could reflect increased cell death in these cells. TUNEL assays in conjunction with CC1 immunohistochemistry revealed, however, that oligodendrocytes in LAMA2-/- white matter were no more likely to die than those in the white matter of littermate wildtype mice (not shown). Oligodendrocyte-specific death was very low in both genotypes at P21 (0.57±0.34% TUNEL(+) cells in the CC1(+) oligodendrocytes of wildtype animals and 1.29±0.73% TUNEL(+) oligodendrocytes in LAMA2-/- mutants; n=3, p=0.537). At P28, no TUNEL(+);CC1(+) cells were detected in both genotypes (n=3). Overall, the decreased numbers of mature oligodendrocytes, accompanied by abnormal numbers of oligodendrocyte progenitor cells, indicated that both oligodendrocyte progenitor development and oligodendrocyte maturation may be altered in laminin α2-knockout brains.

Myelination deficits in laminin α2-knockout brains.

Since I observed decreased numbers of mature oligodendrocytes in the 3 week-old laminin α2 knockout corpus callosum, I next characterized myelination within this white matter tract (Fig. III-7). Since immunoblotting revealed lower levels of the myelin protein MBP in cerebral cortical lysates of 3 week-old LAMA2KO mice relative to wildtype littermates, I performed MBP immunohistochemistry in conjunction with the axonal marker neurofilament to examine the gross organization of the myelinated axons in the corpus callosum of mutant and control animals (Fig. III-7A, top panels). At 3 weeks of age, the corpus callosum of laminin α2 knockout mice was thinner compared to their wildtype litermates (Fig. III-7A; 186.5±15.1 μm in LAMA2-/- compared to 242.4±9.4 μm in wildtype littermates; n=4; p=0.0240).. Higher magnification showed that the organization of MBP(+) fibers in the LAMA2KO corpus callosum, however, is comparable to wildtype, but often appeared sparser (Fig. III-7A, top panels). Axons also appeared grossly normal in their organization, as visualized through neurofilament immunocytochemistry (Fig. III-7A, top panels). I also evaluated myelin ultrastructure using transmission electron microscopy (Figs. III-7A, bottom panels, III-7B, and III-7C). Analysis revealed that axons in the corpus callosum of 3-week old laminin α2 knockout mice have thinner myelin compared to their wildtype counterparts (Figs. III-7A, III-7B, and III-7C). When individual g-ratios were plotted as a function of axon diameter (Fig. III-7C), I observed a significant ($p<0.001$) increase in the median g-ratio in the mutant corpus callosum (0.822; n=567 axons) compared to wildtype corpus callosum (0.755; n=476 axons). Axon g-ratios were also binned by axon diameter and revealed that axons of all sizes in the corpus callosum showed significantly thinner myelin (Fig. III-7B). Analyses of both overall axon density and axonal size distribution showed that there were no significant differences in these

parameters between the wildtype and laminin α2-knockout corpus callosum. This data thus shows that defects in oligodendrogenesis and oligodendrocyte maturation in the corpus callosum of laminin α2-knockout mice correlated with defects in myelination.

DISCUSSION

Previous findings in *dy/dy* mice revealed that low levels of laminin α2 expression resulted in delayed oligodendrocyte maturation in many regions of the adult CNS (Chun et al., 2003; Relucio et al., 2009). Since the precise mutation causing the laminin α2 deficiency in *dy/dy* mice remains unidentified (Sunada et al., 1994), analysis of oligodendrocyte lineage cells and myelin in *dy/dy* animals were restricted to timepoints when the animals displayed characteristic dystrophy that distinguished them from their wildtype littermates (homozygous +/+ and *dy*/+). Therefore, the role of laminin α2 in the developing brain remained unclear. In this study, I used mice that completely lacked laminin α2 expression (LAMA2KO) and determined that appropriate radial glia organization, intermediate progenitor cell positioning, and oligodendrogenesis in the postnatal subventricular zone depend on laminin α2. In the absence of laminin α2, the apical attachments of radial glia at the ventricular surface became disrupted such that radial glial processes appeared discontinuous and deviate from their normal palisade structure (Fig. III-2C). Loss of laminin α2 also led to abnormal distribution of Sox2(+) intermediate progenitors cells near the ventricular surface (Figs. III-3B and III-3C), a phenotype which may reflect the disruption in the radial glial scaffold of the LAMA2KO neocortex. Genetic deletion of laminin α2 also resulted in abnormal oligodendrocyte numbers in the gliogenic niche and white matter of the cerebral cortex (Figs. III-2E, III-2F, III-5, and III-6). LAMA2KO initially had fewer oligodendrocyte progenitors in the SVZ and corpus callosum due, in part, to selective OPC death observed during the neonatal period (Fig. III-4). As development progressed, however, laminin α2-null mice exhibited delayed oligodendrocyte maturation such that OPC accumulation and axonal dysmyelination became evident in the corpus

callosum (Figs. III-5C, III-6, and III-7). Together, these findings indicated roles for laminin α2 in regulating SVZ progenitor cells and oligodendrocytes in the developing cerebral cortex.

Laminin α2, radial glial cells, and intermediate progenitors.

Radial glial cells generate intermediate progenitors, neurons, and glia in the developing CNS (Fishell and Kriegstein, 2003; Götz and Barde, 2005; Götz et al., 2002; Sessa et al., 2008). Apical and basal attachments allow radial glia to span the developing cortical plate and provide discrete pathways for progenitors migrating out of the VZ/SVZ (Goldman, 1995; Marshall et al., 2003; Rakic, 2003). In the postnatal brain, laminin α2 is normally expressed both within the SVZ and the pial basal lamina (Figs. III-2A and III-2B), providing a rationale for laminin's potential influence on radial glia and their progeny during gliogenesis. Indeed, laminin α2-knockout brains exhibited disorganized radial glia at P1 (Fig. III-2C), a phenotype that initially arose during embryonic development (Loulier et al., 2009).

Analysis of the SVZ's proliferative intermediate progenitor population (identified as co-expressing Sox2 and PCNA) showed that the overall level of proliferation of these cells was not profoundly affected by the loss of laminin α2 (Fig. III-3A). Instead, these progenitors were found to be located abnormally close to the ventricular surface in the postnatal LAMA2KO niche (Figs. III-3B and III-3C). Thus at P1, a higher percentage of PCNA(+);Sox2(+) cells were found closer to the ventricular surface, compared to wildtype controls (Fig. III-3C). This finding suggested that intermediate progenitor migration may be impaired in the LAMA2KO SVZ, possibly due to the detachment of the apical radial glial processes that these progenitors normally utilize as a migration scaffold (Goldman, 1995; Levison et al., 1993; Marshall et al., 2003). Alternatively, because the disorganization of the radial glial cells reflects similar phenotypes seen in mice

lacking other basement membrane components (e.g., perlecan, α6 integrin, the nidogen binding site of laminin γ1), the underlying mechanism may also involve loss of appropriate signaling from the laminin α2-null pial basement membrane (Haubst et al., 2006).

During neurogenesis, the position of a dividing progenitor in the niche is thought to determine the identity of its daughter cells. Apical progenitors (APs) in contact with the ventricular surface generate another progenitor and a postmitotic daughter neuron. Basally located progenitors (BPs), on the other hand, do not contact the ventricle and, at least during cortical development, only generate neurons upon division (Cappello et al., 2006; Gotz and Huttner, 2005; Miyata et al., 2004; Noctor et al., 2004). Since LAMA2KO mice have fewer OPCs at this stage, does this aberrant positioning correlate with a failure in specification or with delayed lineage progression only within the oligodendrocyte lineage? Olig2(+) cell densities in the SVZ of knockout mice were comparable to numbers seen in wildtype mice (data not shown), suggesting that specification of cortical oligodendrocytes from NSCs may not be affected by the loss of laminin α2. The numbers of SVZ cells co-expressing PDGFRα(+) and Olig2(+), however, was increased significantly by at least 30% in knockout animals (data not shown), in spite of reduced numbers of cells expressing NG2(+). Since the onset of NG2 expression is slightly later than both PDGFRα and Olig2 in OPCs (Nishiyama, 2007; Nishiyama et al., 2009), this may reflect delayed lineage progression within the pool of oligodendrocyte precursors in the SVZ.

Laminin α2-mediated survival of OPCs in the SVZ.

Additional explanations that could account for decreased NG2(+) OPC numbers in laminin α2 knockout SVZs are: (1) decreased OPC proliferation, and (2) increased OPC death. Significant differences were not observed, however, between the fractions of proliferating (i.e.,

PCNA-positive) cells in the OPC populations of mutant and wildtype littermates (Figs. III-3A and III-5G). There was, however, significantly increased OPC death in the germinal niches of laminin α2-null (~65% TUNEL+) compared to wildtype mice (~31% TUNEL+) (Figs. III-4A and III-4B).

Appropriate developmental apoptosis is critical to establishing the correct numbers of progenitors in the NSC niche. For instance, in Bcl-X_L, caspase 3- and 9-null animal models, the genetic deletion of programmed cell death effectors resulted in the accumulation of supernumerary neurons, distortion of cortical structures, and premature lethality (Kuida et al., 1998; Kuida et al., 1996; Roth et al., 2000). On the other hand, even small increases in germinal niche cell death can also have profound effects on the developing brain. *In vivo* lineage tracing studies indicate that the death of a single SVZ cell potentially translates to the loss of hundreds of downstream lineage-restricted progenitors (Levison et al., 1999; Walsh and Cepko, 1988). In the laminin α2-knockout model, the two-fold increase in the mean percentage of dying OPCs in the germinal niche (Fig. III-4B) presents a compelling reason behind the decreased oligodendrocyte progenitor numbers in the SVZ and white matter tracts of these postnatal animals.

What may be causing OPCs in the laminin α2-knockout SVZ to die more readily? Later in development, laminin-mediated signaling has been shown to promote the target-dependent survival of oligodendrocytes in developing white matter tracts in response to limited amounts of trophic factors (Benninger et al., 2006; Colognato et al., 2002). In the SVZ, ECM-rich fractones lining the ventricular wall capture growth factors and regulate growth factor availability in the NSC niche (Kerever et al., 2007). Similarly, the β1integrin receptor for laminin has been implicated in the maintenance of neurospheres *in vitro* and in promoting neurosphere survival

(Campos et al., 2004; Leone et al., 2005). In postnatal LAMA2KO mice, I propose that these pro-survival signals between OPCs and their SVZ microenvironment may have become disrupted. Thus, selective oligodendrocyte progenitor death in the SVZ may be a result of altered trophic factor availability and/or direct adhesive interactions in the gliogenic niche.

Laminin α2 and oligodendrocyte development in white matter tracts.

In the postnatal corpus callosum, laminin α2-knockout mice initially had significantly decreased numbers of NG2(+) and PDGFRα(+);Olig2(+) OPCs (Figs. III-5A and III-5C). In addition, the LAMA2KO corpus callosum also had fewer mature CC1(+);Olig2(+) oligodendrocytes during these same early timepoints (Fig. III-6C). By three weeks, however, the loss of laminin α2 had led to excessive numbers of OPCs observed in the corpus callosum (Fig. III-5C). Mature oligodendrocyte numbers in both wildtype and LAMA2KO mice, however, increased between P8 and P21, although the density of CC1(+);Olig2(+) remained lower in the knockout corpus callosum at most timepoints analyzed (Fig. III-7C).

The early reduction in oligodendrocyte numbers may be due to decreased cell survival in conjunction with improper oligodendrogenesis from the germinal zones. Integrin-mediated signaling promotes the survival of oligodendrocytes in the myelinated regions of the brain, and this may be, at least in part, due to laminin-cell engagement (Benninger et al., 2006; Colognato et al., 2002). In this study, a small but significant increase in the percentage of TUNEL(+);NG2(+) cells was observed in the postnatal day 5 laminin α2-knockout corpus callosum (Fig. III-5E), but not in the mature CC1(+) oligodendrocyte population (data not shown). This is in contrast to the large and significant changes in OPC death that was observed in the SVZ.

In P21 animals, the increased numbers of oligodendrocyte progenitors in the corpus callosum indicated that the observed reduction in mature oligodendrocytes may be due to a delay in the generation of oligodendrocyte progenitors from germinal zones, and cannot be due to a failure of progenitors to arrive at their target white matter destination. And while this progenitor availability is therefore increased (at least by P14) in the LAMA2KO cerebral cortex, the numbers of mature CC1(+);Olig2(+) oligodendrocytes in the mutant corpus callosum remained lower than wildtype (Fig. III-6C). Thus, oligodendrocyte differentiation remains delayed, such that mature oligodendrocyte densities fail to achieve the levels observed in their corresponding wildtype littermates, and progenitors accumulate in the white matter. Concurrently, this delay in maturation correlates with thinner myelin on the axons of the corpus callosum, as indicated by an increase in axonal g-ratios (Fig. III-7).

In summary, by using the laminin α2 knockout animal model, we were able to reveal that α2-containing laminins regulate postnatal germinal niches and the oligodendrogenic process. This was significant in addressing the limitations encountered with the laminin α2-deficient *dy/dy* mouse, where the inability to identify mutant animals through genotyping and residual laminin α2 expression precluded oligodendrocyte analysis at timepoints earlier than 3 weeks of age (Relucio et al., 2009).

Figure III-1. Laminin expression patterns in the postnatal cerebral cortex.

(A) Top panels: immunohistochemistry with a pan-laminin (Lm) antibody on 40µm-floating sections of cerebral cortices reveals high levels of laminin expression (green) in the pia basal lamina (pia BL) and vasculature of the cerebral cortex at postnatal day 1 (P1) and 8 (P8). Moderate pericellular staining was also observed on cell bodies in the cortical layers underlying the pia BL. Scale bar = 100 microns. Bottom panels: laminin immunoreactivity (green) in the SVZ niche during postnatal gliogenesis. At P1 (bottom left panel), laminin expression is prominent near the ventricular surface and in the blood vessels of the SVZ. Extravascular laminin immunoreactive structures reminiscent of fractones were also detected near the ventricular surface. By P8 (bottom right panel), although laminin levels in the SVZ become markedly decreased relative to P1, laminin expression remains extensive in the vasculature. Ependymal cells lining the lateral ventricles also exhibit positive immunoreactivity to the pan-laminin antibody. Nuclei are visualized using DAPI (blue) Scale bar=50 microns. **(B)** Representative images of nestin (red) and laminin (green) immunocytochemistry in the postnatal day 1 (P1) SVZ. Nuclei are visualized using DAPI (blue). Scale bars=50 microns. **(C)** Immunocytochemistry for the laminin γ1 subunit (LmC1; red) in conjunction with the oligodendrocyte progenitor marker NG2 (green). Top panels: in the P1 SVZ, NG2-positive OPCs were found to associate with laminin γ1(+) structures. Bottom panels: representative images of the postnatal corpus callosum where NG2-positive OPCs (green) were found to associate with laminin γ1(+) (LmC1; red) structures. Scale bars denote 50 microns. Nuclei are visualized using DAPI (blue). **(F)** Representative images of the postnatal white matter tract, where immunodetection using anti-MBP (green) and anti-laminin (red) antibodies was performed. At P1, laminin immunoreactivity (red) was detected on vascular structures and cell bodies surrounding the corpus callosum, while MBP expression was not detectable. At the initiation of myelination at P8, MBP-positive oligodendrocytes (green) were found to associate with laminin(+) (red) structures. Nuclei are visualized using DAPI (blue). Scale bar denotes 50 microns.

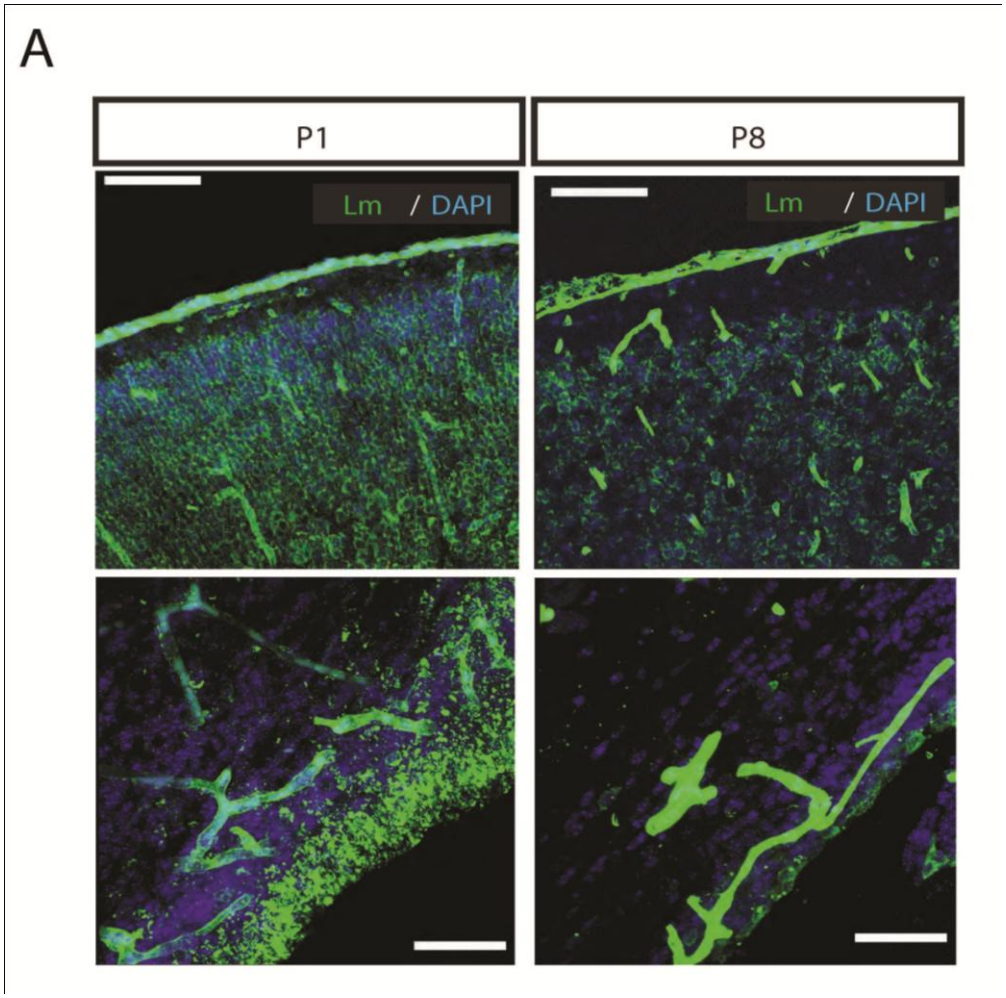
A
P1
P8
Lm / DAPI
Lm / DAPI

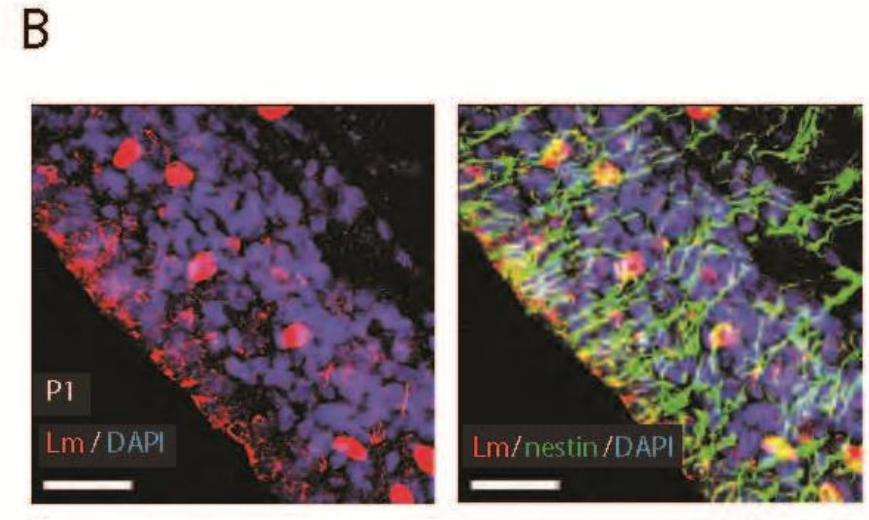
B
P1
Lm / DAPI
Lm/nestin /DAPI

C

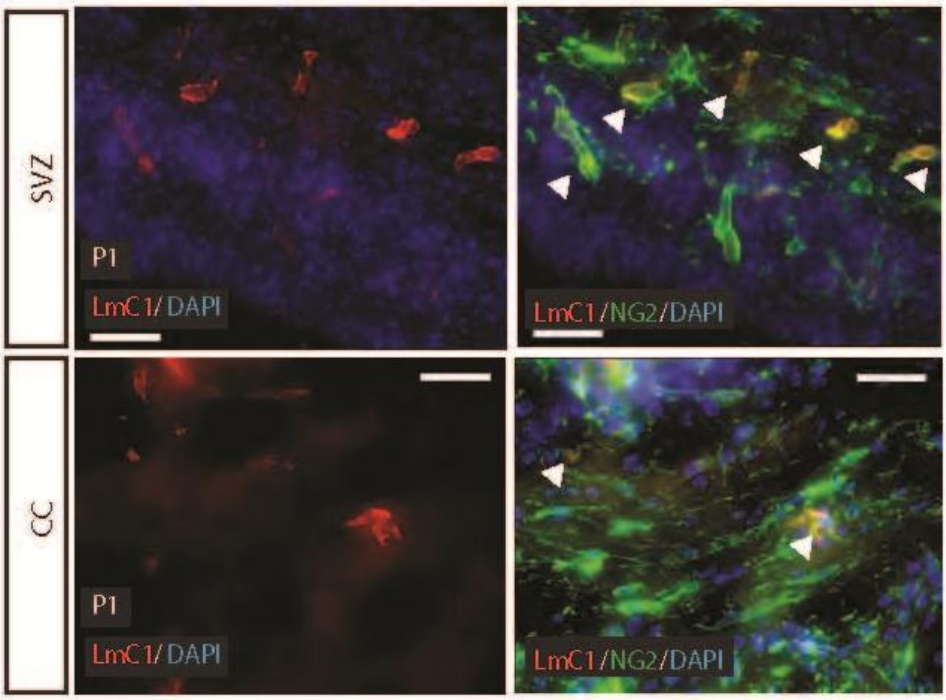
SVZ
P1
LmC1/DAPI
LmC1/NG2/DAPI
CC
P1
LmC1/DAPI
LmC1/NG2/DAPI

D

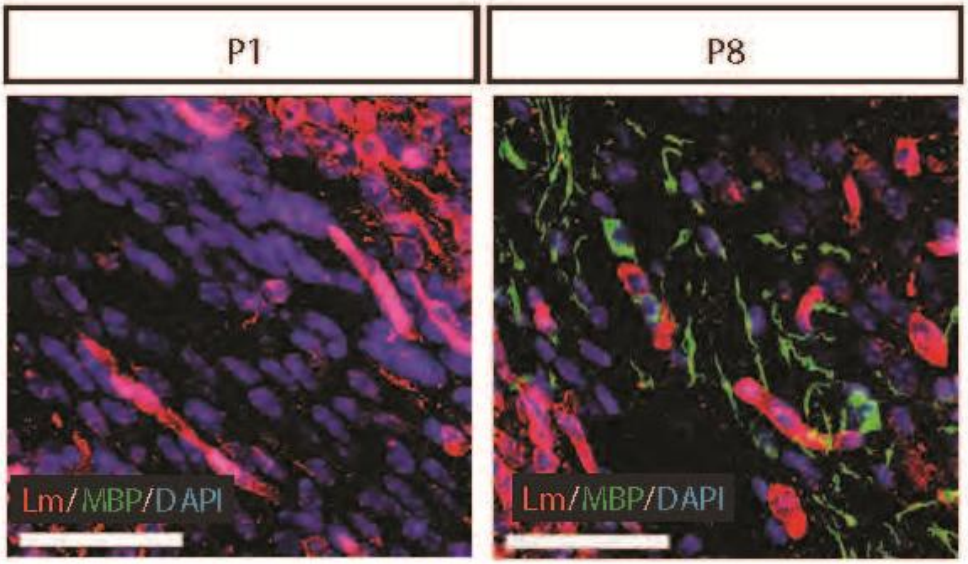
P1
P8
Lm/MBP/DAPI
Lm/MBP/DAPI

Figure III-2. Abnormal progenitor cell organization and numbers in the postnatal SVZ of laminin α2-knockout mice.

(A) Laminin α2 (Lma2) immunoreactivity (green) was observed in the pia basal lamina surrounding wildtype (WT) cortices, but was absent in laminin α2-knockout (LAMA2KO) cortices. Scale bar=500 microns. **(B)** Laminin α2 expression (Lma2; green) was detected in the subventricular zone (SVZ) of wildtype mice (WT) at P1, but not in mutant (LAMA2KO) SVZ. Scale bar=50 microns. **(C)** Using IH on floating 40 micron sections, radial glial cells (nestin+, red) and NSC/IPC nuclei (Sox2+, green) were visualized in the SVZ of LAMA2KO mice or wildtype (WT) littermates at P0. Radial glial cells appeared disorganized in LAMA2KO mice (inset, right). Scale bar=50 microns. Right panels: representative images of nestin (red) and Sox2 (green) immunocytochemistry in wildtype (WT) and mutant (LAMA2KO) SVZ obtained at higher magnification. Scale bars=20 microns**. (D)** Sox2(+)progenitor cells per mm^3 in the SVZ were measured in wildtype (white bars, WT) and mutant (black bars, LAMA2KO) littermates at ages postnatal day 0/1 (P0/1), P5, and P8 using Sox2 immunocytochemistry. Graphs are mean (±sem) counts obtained from 3 different areas of the dorsal SVZ (n=3). **(E)** Oligodendrocyte progenitor cells per mm^3 in the dorsal SVZ were measured in wildtype (white bars, WT) and laminin α2-knockout (black bars, LAMA2KO) littermates at ages P0/1, P5, and P8 using NG2 immunocytochemistry. Graphs are mean (±sem) counts obtained from 3 different areas of the dorsal SVZ (n=4; $*p<0.05$). **(F)** Representative images of NG2 (red) immunocytochemistry in the postnatal SVZ of wildtype (WT) and mutant (LAMA2KO) mice. Compared to wildtype (WT), LAMA2KO mice have fewer NG2(+) cells in the SVZ at P1. Scale bar=50 microns. Nuclei are visualized using DAPI (blue).

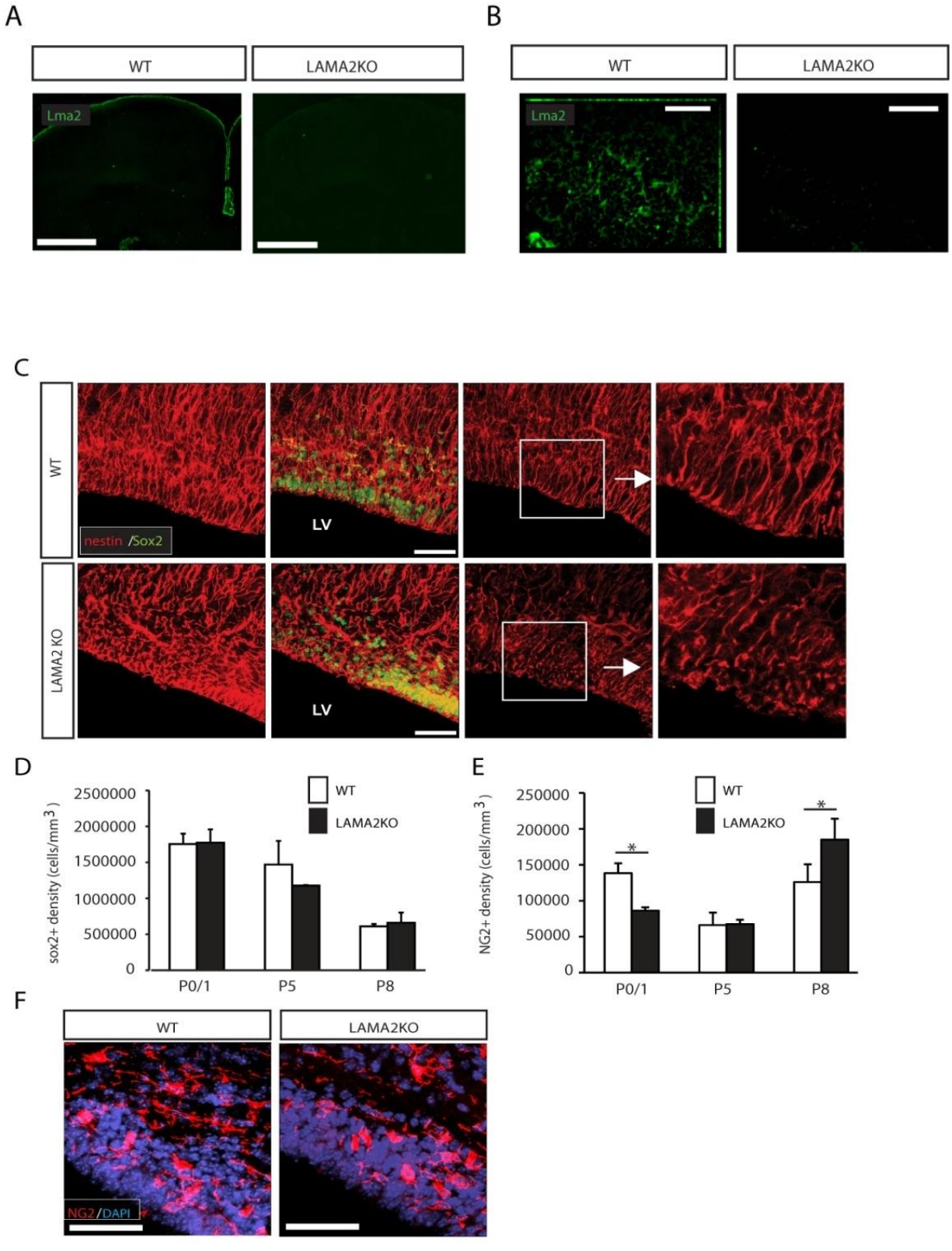
A
WT
LAMA2KO
Lma2
B
WT
LAMA2KO
Lma2
C
WT
LAMA2 KO
nestin /Sox2
LV
LV
D
sox2+ density (cells/mm3)
2500000
2000000
1500000
1000000
500000
0
WT
LAMA2KO
P0/1
P5
P8
E
NG2+ density (cells/mm3)
250000
200000
150000
100000
50000
0
WT
LAMA2KO
*
*
P0/1
P5
P8
F
WT
LAMA2KO
NG2/DAPI

Figure III-3. Altered Sox2^{+} progenitor cell positioning in the laminin α2-knockout SVZ.

(A) Left panel: Percentages of PCNA-positive cells within the NG2(+) cell population of the SVZ were not significantly different between wildtype (white bars; WT) and laminin α2-knockout (LAMA2KO) mice at postnatal day 0/1 (P0/1), P5, and P8 (*n*=3). Right panel: The percentages of PCNA-positive cells within the Sox2(+) cell population were also determined in wildtype (white bars; WT) and laminin α2-knockout (LAMA2KO) SVZ at P0/1, P5, and P8 (*n*=3). No significant differences were observed between WT and LAMA2KO animals at these timepoints. Graphed values depict mean (±sem) percentages obtained from 3 different regions of the dorsal SVZ. **(B)** Leftmost panels: representative images of PCNA (green) immunocytochemistry in wildtype (WT) and mutant (LAMA2KO) SVZ. Middle panels: representative images of Sox2 (red) and PCNA (green) immunocytochemistry in wildtype (WT) and mutant (LAMA2KO) SVZ. Scale bars=50 microns. Proliferating Sox2+ cells were found in ectopic positions in the SVZ of LAMA2KO mice (inset, right), compared to that seen in the WT SVZ (inset, right)**.** Nuclei are visualized using DAPI (blue). **(C)** Individual PCNA+Sox2+ cells distance measurements were grouped to reveal that an increased percentage of proliferating Sox2+ cells were positioned closer (i.e., <20 microns away) to the ventricular surface (VS) in the SVZ of laminin α2-knockout mice (black bars; LAMA2KO), compared the wildtype (white bars; WT) SVZ.

A

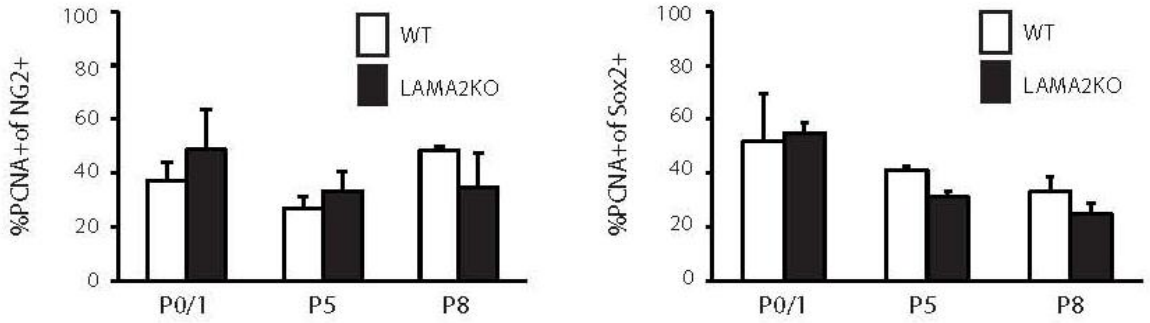
%PCNA+of NG2+
100
80
60
40
20
0
P0/1
P5
P8
WT
LAMA2KO
%PCNA+of Sox2+
100
80
60
40
20
0
P0/1
P5
P8
WT
LAMA2KO

B

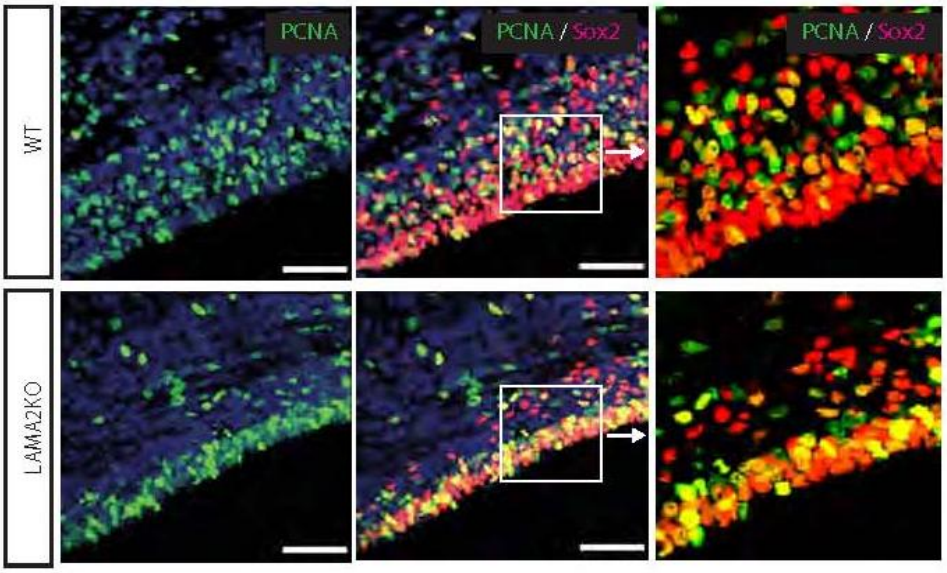
WT
LAMA2KO
PCNA
PCNA / Sox2
PCNA / Sox2

C

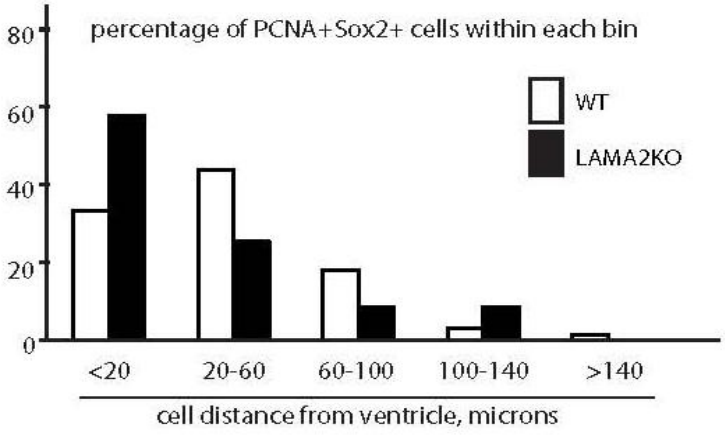
percentage of PCNA+Sox2+ cells within each bin
80
60
40
20
0
WT
LAMA2KO
<20
20-60
60-100
100-140
>140
cell distance from ventricle, microns

Figure III-4. Oligodendrocyte progenitor death in the LAMA2KO subventricular zone.

(A) NG2 immunocytochemistry (red) to visualize oligodendrocyte progenitor cells was performed in combination with TUNEL to detect dying cells (green). Representative fields are shown from P1 wildtype (WT) and laminin α2-knockout (LAMA2KO) SVZ. Arrows depict TUNEL-positive NG2(+) cells. Scale bars=50 microns. **(B)** Percentages of TUNEL-positive cells in the NG2(+) populations in the dorsal SVZ were determined in wildtype (white bars, WT) and laminin α2-knockout (black bars, LAMA2KO) littermates at ages P0/1, P5, and P8. A significant increase in OPC death was observed in the SVZ of mutant mice compared to wildtype. Graphs are mean (±sem) counts obtained from 3 different areas of the dorsal SVZ (n=3; $*p<0.05$). **(C)** No significant differences in Sox2(+) cell-specific apoptosis were observed between wildtype and laminin α2 knockout mice. Percentages of TUNEL-positive cells in the Sox2(+) populations in the SVZ were determined in wildtype (white bars, WT) and laminin α2-knockout (black bars, LAMA2KO) littermates at ages P0/1, P5, and P8. Graphs are mean (±sem) counts obtained from 3 fields in the dorsal SVZ (n=3).

A

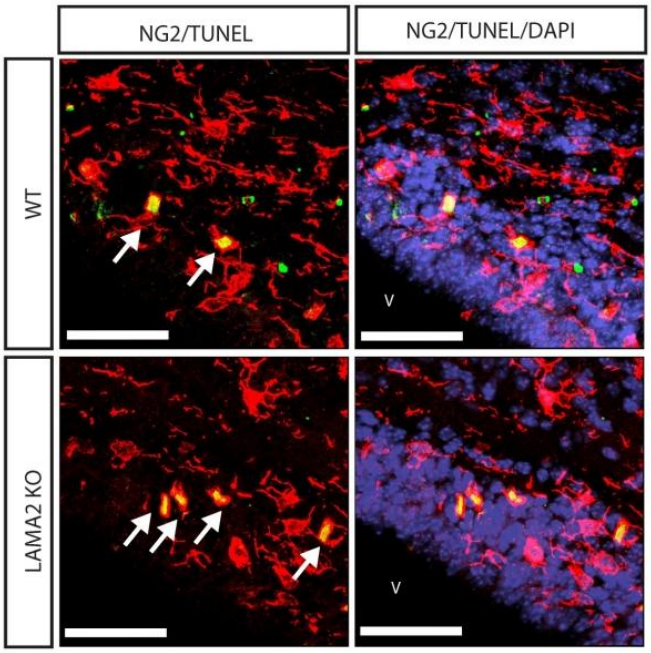
NG2/TUNEL
NG2/TUNEL/DAPI
WT
LAMA2 KO
v
v

B

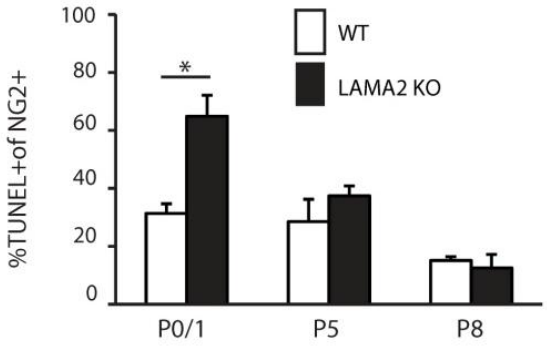
%TUNEL+of NG2+
100
80
60
40
20
0
*
WT
LAMA2 KO
P0/1
P5
P8

C

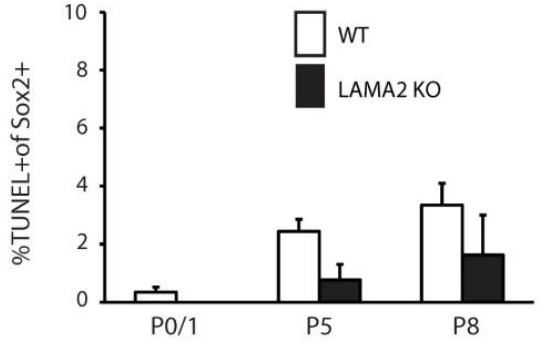
%TUNEL+of Sox2+
10
8
6
4
2
0
WT
LAMA2 KO
P0/1
P5
P8

Figure III-5. LAMA2KO mice have less OPCs in the corpus callosum initially but accumulate excess progenitors during development.

(A) Mean numbers of NG2-positive oligodendrocyte progenitor cells (OPCs) per white matter volume (mm^3) is shown for wildtype (white bars; WT) and laminin α2-knockout (black bars; LAMA2KO) corpus callosum at P0/1, P5, and P8 timepoints. Loss of laminin α2 leads to significant decreases in the density of NG2(+) OPCs in the corpus callosum during early postnatal development. Graphs are mean (±sem) counts obtained from 4 different areas of the corpus callosum (**p*<0.05, ***p*<0.01, *n*=3-4). **(B)** Representative fields from P1 widtype (WT) and laminin α2-knockout (LAMA2KO) corpus callosum are shown. NG2 immunocytochemistry (green) was performed to visualize oligodendrocyte progenitor cells. Nuclei were stained with DAPI (blue). Scale bars denote 50 microns. **(C)** Mean numbers of cells that were double positive for PDGFRα (a marker expressed in OPCs, but not in differentiated oligodendrocytes) and Olig2 (a transcription factor expressed in oligodendrocyte lineage cells) per volume (mm^3) of the WT (white bars) and LAMA2KO (black bars) corpus callosum were evaluated at 6 developmental timepoints (i.e., P0/1, P5. P8, P14, P21, and P28). Prior to P14, LAMA2KO mice had significantly less PDGFRα(+)Olig2(+) cells in the corpus callosum than their WT littermates. After the 2-week timepoint, however, the numbers of PDGFRα(+)Olig2(+) OPCs were significantly higher in the LAMA2KO corpus callosum than in WT. Graphed values are mean (±sem) cell densities measured from 4 different areas of the corpus callosum (**p*<0.05, ***p*<0.01, *n*=3). **(D)** Cerebral cortical lysates were evaluated by western Blot to detect protein levels of NG2 or actin (loading control). Representative blots from P1 wildtype (WT) and laminin α2-knockout (KO) littermates show decreased NG2 protein levels in KO cortical lysates relative to WT littermates (*n*=3). **(E)** Graph depicts mean percentages of TUNEL-positive cells out of the NG2(+) OPC population in the wildtype (white bars; WT) and laminin α2-knockout (black bars; LAMA2KO) corpus callosum, at 3 different postnatal timepoints (**p*<0.05, *n*=3-5). Increased OPC apoptosis (i.e., %TUNEL+ of NG2+ cells) was observed in the LAMA2KO corpus callosum at P1 and P5. **(F)** Representative images taken from P1 widtype (WT) and laminin α2-knockout (LAMA2KO) corpus callosum are shown. NG2 immunocytochemistry (red) was performed in combination with TUNEL (green) to detect apoptotic OPCs in the developing white matter tracts of WT and LAMA2KO mice at P1. Arrows depict TUNEL-positive NG2(+) cells. Nuclei were counterstained with DAPI (blue). Scale bars denote 50 microns. **(G)** The percentages of proliferating OPCs were determined in the wildtype (white bars; WT) and laminin α2-knockout (black bars; LAMA2KO) at P0/1, P5, and P8 by immunohistochemistry with antibodies against PCNA and NG2. In the corpus callosum, no significant differences were observed in the mean percentages of PCNA-positive cells in the NG2(+) OPCs of WT and LAMA2KO mice (*n*=3).

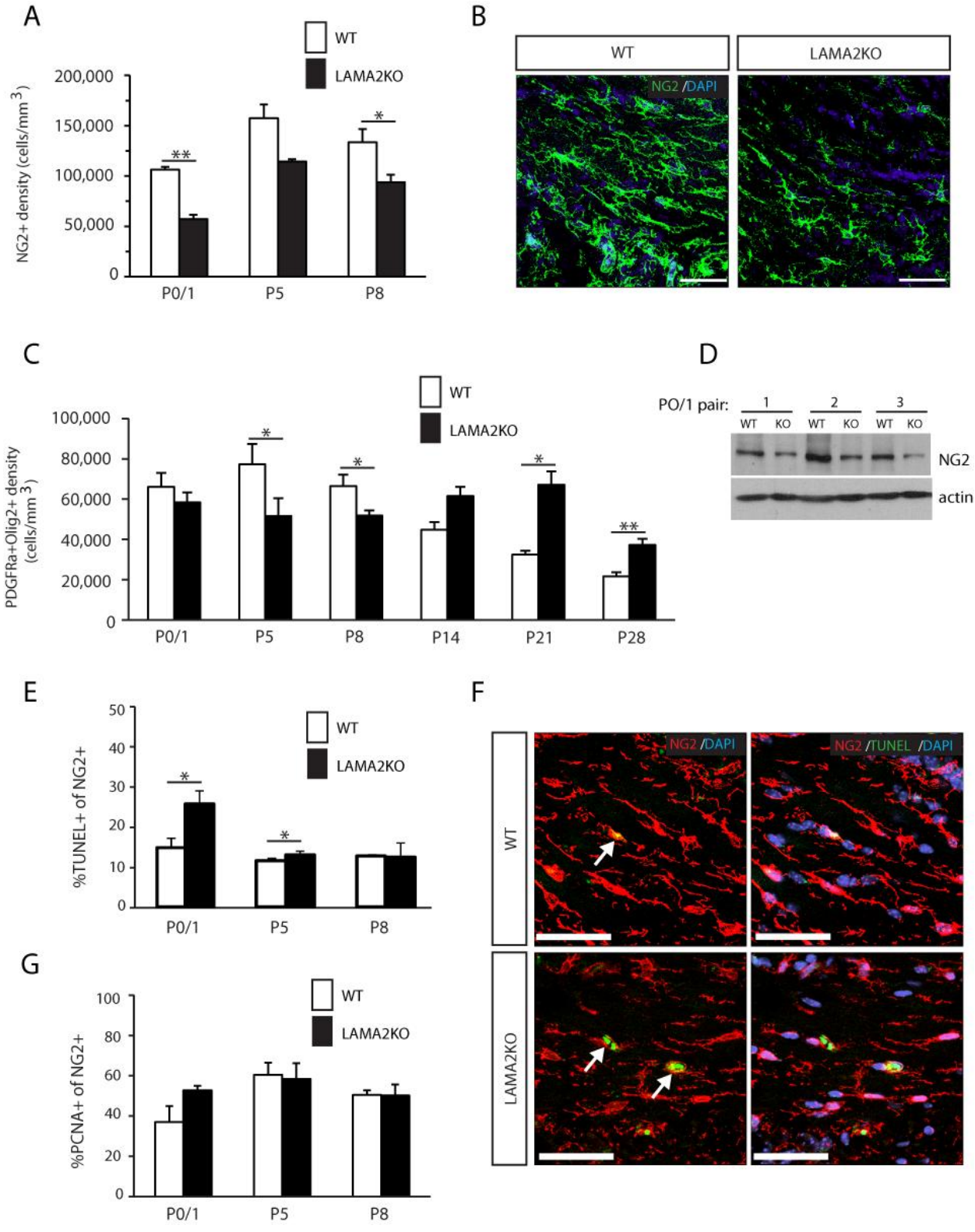
A
WT
LAMA2KO
NG2+ density (cells/mm3)
200,000
150,000
100,000
50,000
0
**
*
P0/1
P5
P8
B
WT
LAMA2KO
NG2 /DAPI
C
WT
LAMA2KO
PDGFRa+Olig2+ density (cells/mm3)
100,000
80,000
60,000
40,000
20,000
0
*
*
*
**
P0/1
P5
P8
P14
P21
P28
D
PO/1 pair:
1
2
3
WT
KO
WT
KO
WT
KO
NG2
actin
E
WT
LAMA2KO
%TUNEL+ of NG2+
50
40
30
20
10
0
*
*
P0/1
P5
P8
F
WT
LAMA2KO
NG2 /DAPI
NG2 /TUNEL /DAPI
G
WT
LAMA2KO
%PCNA+ of NG2+
100
80
60
40
20
0
P0/1
P5
P8

Figure III-6. Delayed oligodendrocyte maturation in laminin α2-knockout brains.

(A) Immunocytochemistry using anti-CC1 (a marker of mature oligodendrocytes, red) and anti-Olig2 (a pan-oligodendrocyte lineage cell marker, green) antibodies was performed to visualize mature oligodendrocyte cells. Representative fields are shown from P21 wildtype (WT) and laminin α2-knockout (LAMA2KO) corpus callosum. Scale bar = 50 microns. **(B)** Representative western blot of cerebral cortical lysates from P21 wildtype (WT) and laminin α2-knockout (LAMA2KO) littermates show differential expression of oligodendrocyte stage specific protein markers. Compared to wildtype mice, LAMA2KO animals had elevated levels of the NG2 protein (expressed in oligodendrocyte progenitors) and decreased levels of the oligodendrocyte maturation markers CNP and MBP. Actin was used as loading control. **(C)** The mean numbers of cells co-expressing CC1 and Olig2 per volume (mm^3) of corpus callosum were determined for wildtype (white bars, WT) and laminin α2-knockout (black bars, LAMA2KO) animals at 5 postnatal timepoints (i.e., P5, P8, P14, P21, and P28). LAMA2KO mice had significantly less CC1(+)Olig2(+) mature oligodendrocytes in the white matter compared to their WT littermates at various timepoints analyzed. (n=3-4, *p<0.05). Graphs depict mean (±sem) cell densities measured from 4 different areas of the corpus callosum.

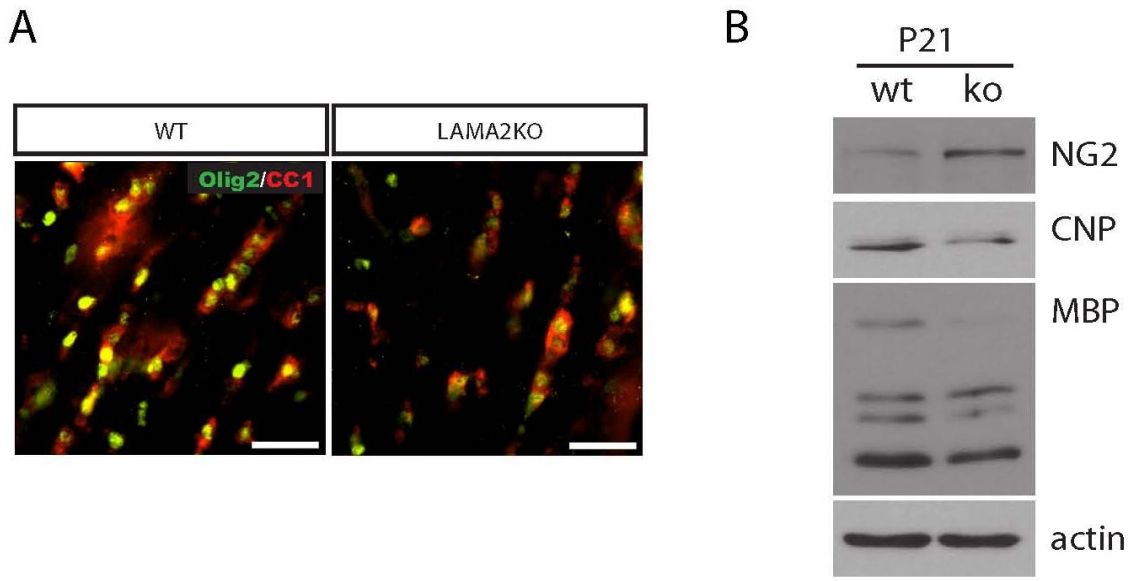
A
WT
LAMA2KO
Olig2/CC1
B
P21
wt
ko
NG2
CNP
MBP
actin

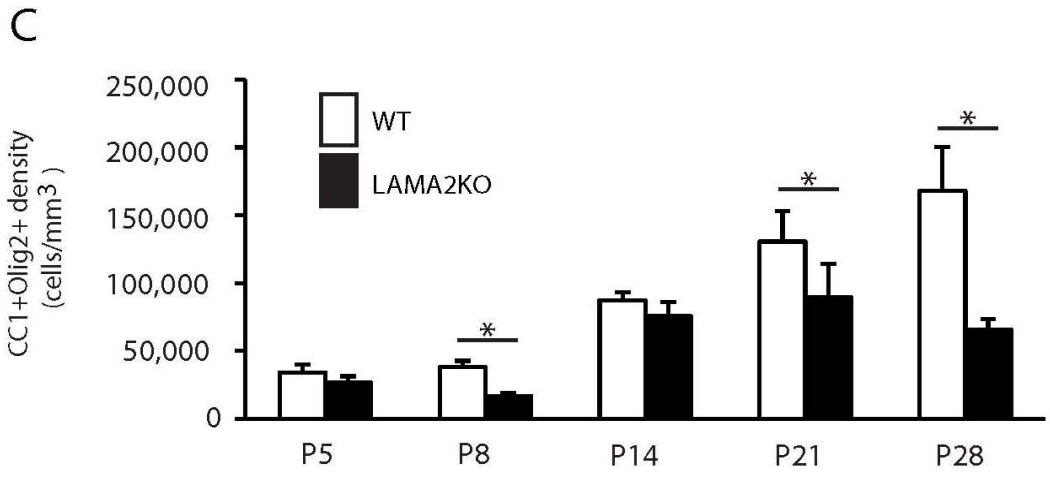
C
CC1+Olig2+ density
(cells/mm3)
250,000
200,000
150,000
100,000
50,000
0
WT
LAMA2KO
*
*
*
P5
P8
P14
P21
P28

Figure III-7. Myelin deficits in the laminin α2-knockout corpus callosum.

(A) Top panels: immunocytochemistry to visualize MBP (green) and neurofilament (NF; red) in wildype (WT) and laminin α2-knockout (LAMA2KO) 3 week-old corpus callosum. Sections are counterstained with DAPI (blue) to visualize nuclei. Scale bars=50 microns. Bottom panels: Representative electron micrographs of the corpus callosum revealed thinner myelin in the axons of the LAMA2KO corpus callosum relative to WT at P21. Scale bars=500nm. **(B)** Axon g-ratios were binned by axon diameter to reveal that axons of all sizes in the LAMA2KO corpus callosum (black bars) had thinner myelin (i.e., higher g-ratios) compared to wildtype (white bars) (***$p<0.001$). **(C)** Corpus callosum g-ratios were plotted as a function of axon diameter for wildtype (open circles; WT) and laminin α2-knockout (black triangles; LAMA2KO) P21 mice. Overall median g-ratios were significantly different ($p<0.001$) between WT and LAMA2KO axons in the corpus callosum (0.822; n=567 axons evaluated in 3 laminin α2-knockout animals compared to 0.755; n=476 axons analyzed in 2 wildtype littermates). No change was observed in the corpus callosum as to the degree of unmyelinated axons.

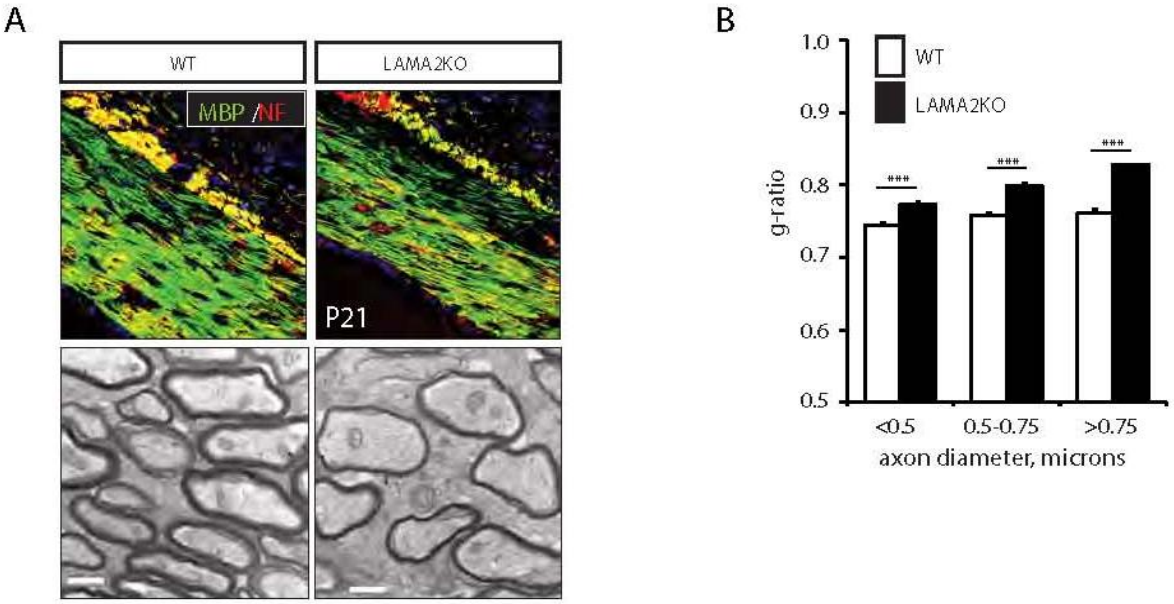
A
WT
LAMA2KO
MBP /NF
P21
B
WT
LAMA2KO
g-ratio
1.0
0.9
0.8
0.7
0.6
0.5
***
***
***
<0.5
0.5-0.75
>0.75
axon diameter, microns

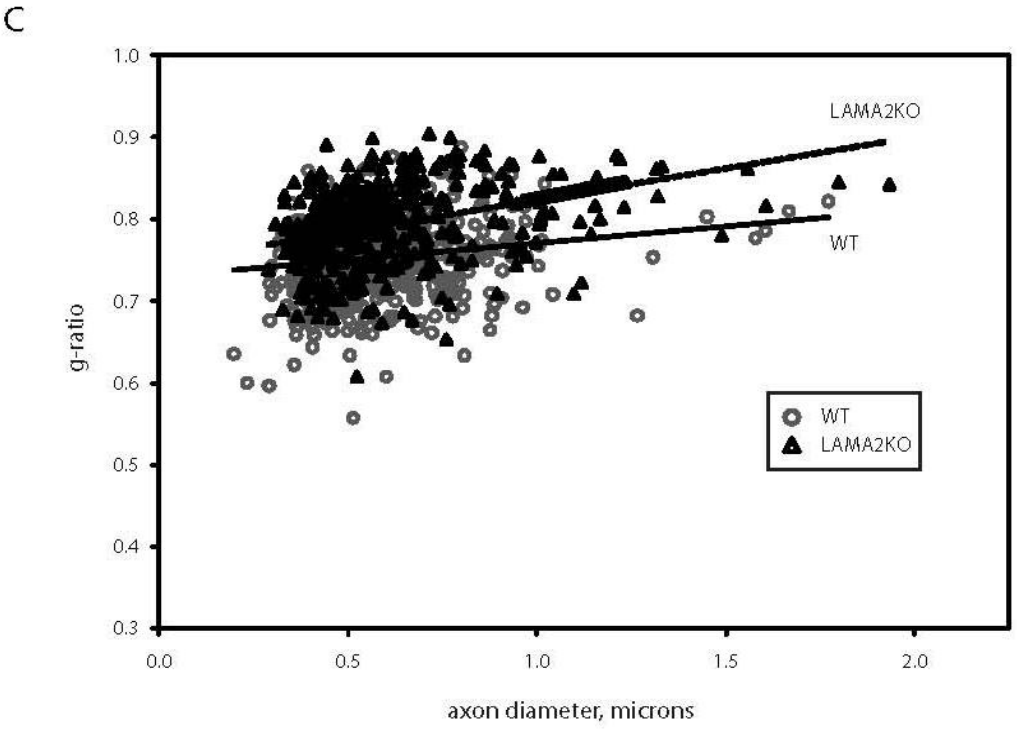
C
LAMA2KO
WT
WT
LAMA2KO
g-ratio
1.0
0.9
0.8
0.7
0.6
0.5
0.4
0.3
0.0
0.5
1.0
1.5
2.0
axon diameter, microns

CHAPTER IV: CONCLUSIONS AND FUTURE CONSIDERATIONS

In this work, putative roles for laminin α2 in oligodendrogenesis, oligodendrocyte maturation, and myelination in the central nervous system were examined. Laminins were found to be expressed in the germinal SVZ niche of the developing postnatal cerebral cortex. This indicates that laminins are expressed in an appropriate spatial and temporal manner, such that they could potentially influence neural stem cells, intermediate progenitor cells, and oligodendroglia. Using two animal models of laminin α2-deficiency, we have shown that α2-chain containing laminins have critical roles in postnatal oligodendrogenesis and in oligodendrocyte differentiation. Early during development, laminin influences the numbers of OPCs in both the SVZ and the developing corpus callosum, partly through promoting OPC survival within the SVZ niche. During oligodendrocyte maturation, laminins play a regulatory role in signaling pathways that contribute to proper CNS myelination. These findings reveal that dysregulation of the NSC niche and of signaling pathways required for normal oligodendrocyte development may potentially contribute to the CNS abnormalities observed in humans with MDC1A, a form of congenital muscular dystrophy caused by genetic mutations that result in the lack or lowered expression of laminin α2.

Basement membrane laminins versus non-BL laminins: delineating functional contributions through in vitro models.

The two animal models of MDC1A in this study gave valuable insights on the functions of CNS laminin functions *in vivo*. The dy^{3k}/dy^{3k} laminin α2-knockout mouse helped identify

potential functions of laminin during early postnatal development, while the *dy/dy* mouse model allowed analysis of oligodendrocytes and CNS myelination in six-week old laminin-deficient brains (Relucio et al., 2009). However, both models display global laminin deficiencies, albeit to varying degrees. The current findings in this dissertation, therefore, do not distinguish between functional contributions from laminins in different CNS compartments. Radial glial cells, for example, maintain basal attachments to the pial basement membrane, while their soma also encounter α2-laminins in the SVZ niche during postnatal development. Hence, it is possible for the abnormal radial glia phenotype observed in laminin α2-knockout mice to arise due to the combined loss of radial glia-laminin interactions at the apical and basal ends. Delineation of functional requirements for basement membrane versus non-BL laminins may therefore be achieved through a Cre-lox approach that ablates the laminin α2 gene from relevant cell types at specific developmental timepoints.

As an alternative, *in vitro* models may be used to identify compartment-specific contributions to laminin functions. Neuron-oligodendrocyte co-culture systems, for example, could be used to recapitulate axon-glial interactions *in vitro*. The use of chimeric co-culture systems (e.g., LAMA2KO neurons cultured with wildtype oligodendrocytes) would help determine if non-BL, neuronal α2-laminins provide extrinsic signals that mediate aspects of oligodendrocyte development. Concurrently, seeding laminin α2 knockout oligodendrocytes on wildtype neurons will address whether laminins are oligodendrocyte-intrinsic regulators of axon-oligodendrocyte interactions. While current co-culture methodologies use axons of dorsal root ganglia (DRG) neurons, cortical neurons should (theoretically) recapitulate a system that is more representative of interactions in the forebrain of the CNS. A caveat of this, however, is that there

may be varying requirements or expression levels of laminin α2 within the cortical neuron population.

With respect to the radial glial cells of the developing cortex, previous studies provide putative roles for laminins in *both* the pial basement membrane and stem cell niche. Embryonic LAMA2KO brains have abnormal radial glial apical attachments in the stem cell niche, a defect phenocopied partly by the transient disruption of β1 integrin at the ventricular surface (Loulier et al., 2009). Surgical removal of the meninges and the associated blood vessels in E13 cerebral cortices triggered cell death in radial glia, in spite of apparent non-disruption of the cells' apical adhesion to the ventricular surface (Radakovits et al., 2009). Chimeric co-cultures where wildtype NSCs or iPCs are seeded on top of meningeal fibroblasts or "meninges-derived" ECM from LAMA2KO mice could therefore help characterize the degree of influence of pial basement membrane laminins on radial glial cells.

Laminins and cerebellar development.

Early unpublished observations from the group that originally generated the dy^{3k}/dy^{3k} laminin α2-knockout mice include cerebellar lobe fusion and the presence of ectopic cerebellar granule cells outside of the cerebellar basement membrane (Miyagoe-Suzuki et al., 2000). Additionally, I have observed that LAMA2KO mice exhibit cerebellar hypoplasia at P21 (Fig. IV-1A). Interestingly, some MDC1A patients also exhibit cerebellar hypolasia (Echenne et al., 1998), suggesting that cerebellar dysfunction may also be involved in this disease. It would therefore be interesting to study how laminin α2 regulates cerebellar development *in vivo*.

During cerebellar histogenesis, neurons arise in a precise manner from two distinct germinal niches: (1) the ventricular zone, which generates deep cerebellar nuclei and the

inhibitory Purkinje cells, and (2) the rhombic lip, which gives rise to the excitatory cerebellar granule cells (GCs). At E13, GC progenitors begin to leave the rhombic lip to migrate tangentially over the cerebellar surface and populate the external granule layer (EGL). Much like the subventricular zone of the cerebral cortex, the EGL becomes a proliferative zone where GC progenitors undergo massive symmetric expansion. At the onset of postnatal development, GC precursors become post-mitotic and migrate radially out of the EGL into the internal granule layer (IGL) where the GCs complete their differentiation program (Chédotal, 2010; Hatten and Roussel, 2011; Wang and Zoghbi, 2001).

How would the loss of laminin α2 result in a smaller cerebellum? One possible explanation for this is that GC progenitor proliferation in the laminin α2-knockout cerebellum may be reduced. Granule neurons are the most predominant neuronal subclass in the cerebellum, accounting for more than 50% of the total neuronal population of the vertebrate brain (Altman, 1972; Sgaier et al., 2005). A reduction in GC proliferation would likely alter normal cell numbers in the cerebellum and result to hypoplasia. In mice where the laminin receptor β1 integrin was genetically ablated in cells of neural origin, the cerebella initially develops like wildtype but begins to appear smaller by P7, with the cerebellum's laminar organization becoming progressively perturbed. These mice were shown to have decreased ECM deposition in the meninges of the cerebellum, such that laminin levels were severely reduced on the surface and folia of the cerebellum (Graus-Porta et al., 2001). A follow-up study eventually found that these mice had a severe decrease in the proliferation of cerebellar granule precursor cells, due in part to the disruption of a laminin-mediated Shh signal that normally promotes precursor proliferation (Blaess et al., 2004).

To assess initially whether laminin α2 may regulate GC precursor proliferation in the cerebella, I performed immunohistochemistry using antibodies against the proliferation protein PCNA in conjunction with a polyclonal laminin-1 antibody (Fig. IV-1B). In both P1 wildtype and mutant cerebella, PCNA(+) cells can be clearly seen in the primary folia EGL, a site where GC precursors accumulate early in postnatal development. However, fewer PCNA(+) cells can be seen in the laminin α2 knockout EGL (both in the crown and fissure of the primary folium) compared to the wildtype control (Fig. IV-1B). Interestingly, similar levels of laminin-1 immunoreactivity were detected in the basal laminae of both wildtype and mutant cerebella (Fig. IV-1B), suggesting that laminin α2 may be dispensable for maintaining the structural integrity of the cerebellar basement membrane. Instead, laminin α2-mediated signals may be more critical in regulating GC precursor proliferation and cerebellar morphogenesis. One candidate signaling molecule acting downstream of laminin α2 in CG precursors is the cyclin-dependent kinase inhibitor p27. In the *dy/dy* mouse study (Chapter II), I detected inappropriately elevated levels of p27 in cerebellar lysates of 6 week-old *dy/dy* mice. Since the loss of p27 function *in vivo* leads to increased cell proliferation (Li et al., 2009; Löwenheim et al., 1999), verifying whether p27 levels or activity is dysregulated in the cerebella of laminin α2-knockout mice, particularly during early postnatal development, could provide a mechanistic explanation for laminin's influence on granule cell precursor proliferation.

In collaboration with Emily Chen's research group (Department of Pharmacology, Stony Brook University, NY), we have also performed preliminary large-scale quantitative proteomics analysis on differential protein expression between the cerebella of wildtype and laminin-α2 knockout mice. Initial analyses of mutant cerebella show that the loss of laminin α2 correlated with a twelve-fold decrease in levels of calbindin, a protein predominantly expressed by the

Purkinje neurons. Immunohistochemistry with antibodies against calbindin show dramatically increased numbers of Purkinje cells in LAMA2KO cerebella compared to wildtype littermates (Fig. IV-1C). At P5, the dendritic spines of Purkinje cells in LAMA2KO cerebella appear less elaborate compared to control animals, suggesting that Purkinje cell maturation may become perturbed in the absence of laminin α2 (data not shown). Further characterization of these putative Purkinje cell defects may provide a structural basis for the disrupted long-term synaptic plasticity in *dy/dy* mice, and for the alterations in somatosensory and visually-evoked potentials and epilepsy reported in some subsets of MDC1A patients (Anderson et al., 2005).

Laminin, astrocytes, and the blood brain barrier.

The disruption of normal oligodendrogenesis in laminin α2-knockout mice suggests that the process of astrogenesis may also become dysregulated upon loss of the α2-subunit containing laminins. Preliminary western blot analysis shows that the levels of the mature astrocyte protein glial fibrillary acidic protein (GFAP) were decreased in the cortical lysates of laminin α2-knockout mice compared to wildtype at both P1 and P5 timepoints. Astrocytes exhibit high expression levels of laminins, compared to neurons and oligodendrocytes (Colognato et al., 2007), and some *in vitro* studies have implicated astrocytes as positive regulators of oligodendrocyte survival (Corley et al., 2001). *In vivo*, astrocytes have been found to extend their endfeet and make contact with the cerebral vasculature. These astrocyte-blood vessel interactions are involved in maintaining water homeostasis in the brain, and as such may be altered during pathological conditions. An emerging hypothesis on MDC1A pathogenesis proposes that deficient levels of laminin α2 disrupts the blood-brain barrier, increasing the water content in the brain, and resulting in abnormal white matter intensity as detected by MRI (Caro et al., 1999).

Since both astrocytes and the brain vasculature normally express high levels of laminin α2, these cell types could potentially become dysregulated in LAMA2KO mice. Whether white matter hypointensity is a secondary effect of increased brain water content in MDC1A, further studies on putative alterations in BBB permeability in laminin α2-knockout brain should be explored.

Figure IV-8. Preliminary analysis on the cerebellum of laminin α2 knockout mice.

(A) Gross anatomy of brains taken from wildtype (WT) and laminin α2 knockout (LAMA2KO) mice at P21. Cerebella are indicated by white arrows. The cerebellum of the LAMA2KO mouse appears smaller in size compared to the wildtype cerebellum. **(B)** Representative images of PCNA (green) and laminin (red) immunocytochemistry in the postnatal day 1 (P1) external granule layer (EGL) of wildtype (WT) and mutant (LAMA2KO) cerebella. Compared to the WT cerebellum, the LAMA2KO cerebellum has fewer PCNA(+) cells in the crown and fissure (EGL in fissure indicated by dashed lines) of the primary folium EGL at P1. Scale bars=50 microns. **(C)** Immunocytochemistry for the Purkinje cell protein calbindin (Calb; green) in floating sections of wildtype (WT) and laminin α2 mutants (LAMA2KO) at P21. Calbindin(+)-cell bodies of Purkinje neurons are denoted by arrowheads. The LAMA2KO mouse have strikingly increased numbers of calbindin(+)-Purkinje cells compared to wildtype. Nuclei are visualized using DAPI (blue). Scale bars = 100 microns.

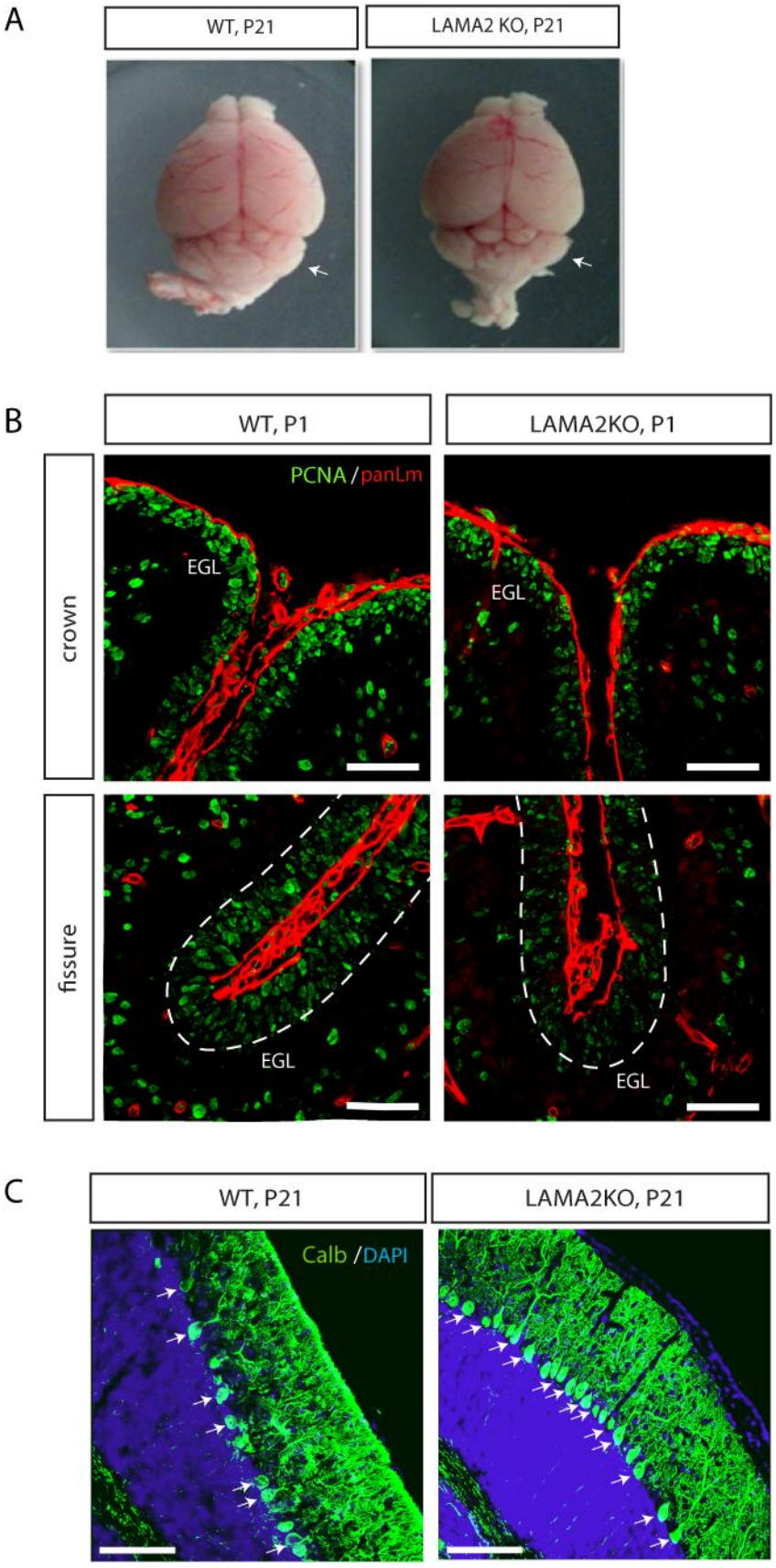
A
WT, P21
LAMA2 KO, P21
B
WT, P1
LAMA2KO, P1
crown
fissure
PCNA / panLm
EGL
EGL
EGL
EGL
C
WT, P21
LAMA2KO, P21
Calb /DAPI

References

Allamand, V., and P. Guicheney. 2002. Merosin-deficient congenital muscular dystrophy, autosomal recessive (MDC1A, MIM#156225, LAMA2 gene coding for alpha2 chain of laminin). *Eur J Hum Genet*. 10:91-94.

Altman, J. 1972. Postnatal development of the cerebellar cortex in the rat. I. The external germinal layer and the transitional molecular layer. *The Journal of Comparative Neurology*. 145:353-397.

Anderson, J.L., S.I. Head, and J.W. Morley. 2005. Synaptic plasticity in the dy2J mouse model of laminin-alpha2-deficient congenital muscular dystrophy. *Brain Res*. 1042:23-28.

Aumailley, M., L. Bruckner-Tuderman, W.G. Carter, R. Deutzmann, D. Edgar, P. Ekblom, J. Engel, E. Engvall, E. Hohenester, J.C.R. Jones, H.K. Kleinman, M.P. Marinkovich, G.R. Martin, U. Mayer, G. Meneguzzi, J.H. Miner, K. Miyazaki, M. Patarroyo, M. Paulsson, V. Quaranta, J.R. Sanes, T. Sasaki, K. Sekiguchi, L.M. Sorokin, J.F. Talts, K. Tryggvason, J. Uitto, I. Virtanen, K. von der Mark, U.M. Wewer, Y. Yamada, and P.D. Yurchenco. 2005. A simplified laminin nomenclature. *Matrix Biol*. 24:326-332.

Bachy, S., F. Letourneur, and P. Rousselle. 2008. Syndecan-1 interaction with the LG4/5 domain in laminin-332 is essential for keratinocyte migration. *Journal of Cellular Physiology*. 214:238-249.

Baron-Van Evercooren, A., H. Kleinman, S. Ohno, P. Marangos, J. Schwartz, and M. Dubois-Dalcq. 1982. Nerve growth factor, laminin, and fibronectin promote neurite growth in human fetal sensory ganglia cultures. *J Neurosci Res*. 8:179-193.

Baron, W., H. Colognato, and C. ffrench-Constant. 2005. Integrin-growth factor interactions as regulators of oligodendroglial development and function. *Glia*. 49:467-479.

Baron, W., L. Decker, H. Colognato, and C. ffrench-Constant. 2003. Regulation of integrin growth factor interactions in oligodendrocytes by lipid raft microdomains. *Curr Biol*. 13:151-155.

Barresi, R., and K.P. Campbell. 2006. Dystroglycan: from biosynthesis to pathogenesis of human disease. *J Cell Sci*. 119:199-207.

Baye, L., and B. Link. 2007. Interkinetic nuclear migration and the selection of neurogenic cell divisions during vertebrate retinogenesis. *J Neurosci*. 27:10143-101452.

Bayer, S.A., and J. Altman. 1991. Neocortical Development. Raven Press, New York. 255 pp.

Beltrán-Valero de Bernabé, D., S. Currier, A. Steinbrecher, J. Celli, E. van Beusekom, B. van der Zwaag, H. Kayserili, L. Merlini, D. Chitayat, W.B. Dobyns, B. Cormand, A.-E. Lehesjoki, J. Cruces, T. Voit, C.A. Walsh, H. van Bokhoven, and H.G. Brunner. 2002. Mutations in the O-Mannosyltransferase Gene POMT1 Give Rise to the Severe Neuronal Migration Disorder Walker-Warburg Syndrome. *The American Journal of Human Genetics*. 71:1033-1043.

Belvindrah, R., S. Hankel, J. Walker, B.L. Patton, and U. Muller. 2007. Beta 1-integrins control the formation of cell chains in the adult rostral migratory stream. *J Neurosci*. 27:2704-2717.

Benninger, Y., H. Colognato, T. Thurnherr, R.J. Franklin, D.P. Leone, S. Atanasoski, K.A. Nave, C. Ffrench-Constant, U. Suter, and J.B. Relvas. 2006. Beta1-integrin signaling mediates premyelinating oligodendrocyte survival but is not required for CNS myelination and remyelination. *J Neurosci*. 26:7665-7673.

Blaess, S., D. Graus-Porta, R. Belvindrah, R. Radakovits, S. Pons, A. Littlewood-Evans, M. Senften, H. Guo, Y. Li, J.H. Miner, L.F. Reichardt, and U. Muller. 2004. Beta1-integrins are critical for cerebellar granule cell precursor proliferation. *J. Neurosci.* 24:3402-3412.

Bongarzone, E.R. 2002. Induction of Oligodendrocyte Fate During the Formation of the Vertebrate Neural Tube. *Neurochemical Research*. 27:1361-1369.

Bonneh-Barkay, D., and C.A. Wiley. 2009. Brain Extracellular Matrix in Neurodegeneration. *Brain Pathology*. 19:573-585.

Bozzi, M., S. Morlacchi, M.G. Bigotti, F. Sciandra, and A. Brancaccio. 2009. Functional diversity of dystroglycan. *Matrix Biology*. 28:179-187.

Brazel, C.Y., M.J. Romanko, R.P. Rothstein, and S.W. Levison. 2003. Roles of the mammalian subventricular zone in brain development. *Progress in Neurobiology*. 69:49-69.

Buteică, E., E. Roşulescu, F. Burada, B. Stănoiu, and M. Zăvăleanu. 2008. Merosin-deficient congenital muscular dystrophy type 1A. *Rom J Morphol Embryol*. 49:229-233.

Buttery, P., and C. ffrench-Constant. 1999. Laminin-2/integrin interactions enhance myelin membrane formation by oligodendrocytes. *Mol Cell Neurosci*. 14:199 - 212.

Campbell, K., and M. Götz. 2002. Radial glia: multi-purpose cells for vertebrate brain development. *Trends Neurosci*. 25:235-238.

Campos, L., D. Leone, J. Relvas, C. Brakebusch, R. Fässler, U. Suter, and C. ffrench-Constant. 2004. Beta1 integrins activate a MAPK signalling pathway in neural stem cells that contributes to their maintenance. *Development*. 131:3433-3444.

Campos, L.S. 2005. β1 integrins and neural stem cells: making sense of the extracellular environment. *BioEssays*. 27:698-707.

Cappello, S., A. Attardo, X. Wu, T. Iwasato, S. Itohara, M. Wilsch-Brauninger, H.M. Eilken, M.A. Rieger, T.T. Schroeder, W.B. Huttner, C. Brakebusch, and M. Gotz. 2006. The Rho-GTPase cdc42 regulates neural progenitor fate at the apical surface. *Nat Neurosci*. 9:1099-1107.

Caro, P.A., M. Scavina, E. Hoffman, E. Pegoraro, and H.G. Marks. 1999. MR imaging findings in children with merosin-deficient congenital muscular dystrophy. *AJNR Am J Neuroradiol*. 20:324-326.

Chédotal, A. 2010. Should I stay or should I go? Becoming a granule cell. *Trends in Neurosciences*. 33:163-172.

Chen, Z.-L., and S. Strickland. 2003. Laminin-gamma1 is critical for Schwann cell differentiation, axon myelination, and regeneration in the peripheral nerve. *J. Cell Biol.* 163:889-899.

Chen, Z., J. Indyk, and S. Strickland. 2003. The hippocampal laminin matrix is dynamic and critical for neuronal survival. *Mol Biol Cell*. 14:2665-2676.

Chun, S., M. Rasband, R. Sidman, A. Habib, and T. Vartanian. 2003. Integrin-linked kinase is required for laminin-2-induced oligodendrocyte cell spreading and CNS myelination. *J Cell Biol*. 163:397 - 408.

Chung, A.E., L.-J. Dong, C. Wu, and M.E. Durkin. 1993. Biological functions of entactin. *Kidney Int*. 43:13-19.

Cohn, R.D., and K.P. Campbell. 2000. Molecular basis of muscular dystrophies. *Muscle & Nerve*. 23:1456-1471.

Collins, J., and C. Bönnemann. 2010. Congenital muscular dystrophies: toward molecular therapeutic interventions. *Current Neurology and Neuroscience Reports*. 10:83-91.

Colognato, H., W. Baron, V. Avellana-Adalid, J.B. Relvas, A. Baron-Van Evercooren, E. Georges-Labouesse, and C. ffrench-Constant. 2002. CNS integrins switch growth factor signalling to promote target-dependent survival. *Nat Cell Biol*. 4:833-841.

Colognato, H., C. ffrench-Constant, and M.L. Feltri. 2005. Human diseases reveal novel roles for neural laminins. *Trends Neurosci*. 28:480-486.

Colognato, H., J. Galvin, Z. Wang, J. Relucio, T. Nguyen, D. Harrison, P.D. Yurchenco, and C. Ffrench-Constant. 2007. Identification of dystroglycan as a second laminin receptor in oligodendrocytes, with a role in myelination. *Development*. 134:1723-1736.

Colognato, H., S. Ramachandrappa, I.M. Olsen, and C. ffrench-Constant. 2004. Integrins direct Src family kinases to regulate distinct phases of oligodendrocyte development. *J Cell Biol*. 167:365-375.

Colognato, H., D.A. Winkelmann, and P.D. Yurchenco. 1999. Laminin polymerization induces a receptor-cytoskeleton network. *J. Cell Biol.* 145:619-631.

Corley, S.M., U. Ladiwala, A. Besson, and V.W. Yong. 2001. Astrocytes attenuate oligodendrocyte death in vitro through an alpha 6 integrin-laminin-dependent mechanism. *Glia*. 36:281-294.

Court, F.A., L. Wrabetz, and M.L. Feltri. 2006. Basal lamina: Schwann cells wrap to the rhythm of space-time. *Curr Opin Neurobiol*. 16:501-507.

Del Bene, F., A. Wehman, B. Link, and H. Baier. 2008. Regulation of neurogenesis by interkinetic nuclear migration through an apical-basal notch gradient. *Cell*. 134:1055-1065.

Dickson, B. 2002. Molecular mechanisms of axon guidance. *Science*. 298:1959–1964

Dityatev, A., and T. Fellin. 2008. Extracellular matrix in plasticity and epileptogenesis. *Neuron Glia Biology*. 4:235-247.

Dityatev, A., M. Schachner, and P. Sonderegger. 2010. The dual role of the extracellular matrix in synaptic plasticity and homeostasis. *Nat Rev Neurosci*. 11:735-746.

Drago, J., V. Nurcombe, and P.F. Bartlett. 1991. Laminin through its long arm E8 fragment promotes the proliferation and differentiation of murine neuroepithelial cells in vitro. *Experimental Cell Research*. 192:256-265.

Durbeej, M. 2010. Laminins. *Cell Tissue Res*. 339:259-268.

Dutta, R., and B. Trapp. 2007. Pathogenesis of axonal and neuronal damage in multiple sclerosis. *Neurology*. 68:S22-31.

Echenne, B., F. Rivier, M. Tardieu, M. Brive, A. Robert, A. Pages, F. Pons, and D. Mornet. 1998. Congenital muscular dystrophy and cerebellar atrophy. *Neurology*. 50:1477-1480.

Edgar, D., R. Timpl, and H. Thoenen. 1984. The heparin-binding domain of laminin is responsible for its effects on neurite outgrowth and neuronal survival. *EMBO J*. 3:1463-1468.

Edwards, G., F. Wilford, X. Liu, L. Hennighausen, J. Djiane, and C. Streuli. 1998. Regulation of mammary differentiation by extracellular matrix involves protein-tyrosine phosphatases. *J Biol Chem. 1998 Apr 17;273(16):9495-500.* 273:9495-9500.

Egles, C., T. Claudepierre, M. Manglapus, M. Champliaud, W. Brunken, and D. Hunter. 2007. Laminins containing the beta2 chain modulate the precise organization of CNS synapses. *Mol Cell Neurosci*. 34:288-298.

El Nemer, W., P. Gane, Y. Colin, V. Bony, C. Rahuel, F. Galactéros, J. Cartron, and C. Le Van Kim. 1998. The Lutheran blood group glycoproteins, the erythroid receptors for laminin, are adhesion molecules. *J Biol Chem*. 273:16686-16693.

Emsley, J.G., and T. Hagg. 2003. Alpha6 beta1-integrin directs migration of neuronal precursors in adult mouse forebrain. *Exp Neurol*. 183:273-285.

Erickson, A.C., and J.R. Couchman. 2000. Still more complexity in mammalian basement membranes. *J. Histochem. Cytochem.* 48:1291-1306.

Ernsberger, U., D. Edgar, and H. Rohrer. 1989. The survival of early chick sympathetic neurons in vitro is dependent on a suitable substrate but independent of NGF. *Developmental Biology*. 135:250-262.

Farrelly, N., Y. Lee, J. Oliver, C. Dive, and C. Streuli. 1999. Extracellular matrix regulates apoptosis in mammary epithelium through a control on insulin signaling. *J Cell Biol*. 144:1337-1348.

Feltri, M.L., D.G. Porta, S.C. Previtali, A. Nodari, B. Migliavacca, A. Cassetti, A. Littlewood-Evans, L.F. Reichardt, A. Messing, A. Quattrini, U. Mueller, and L. Wrabetz. 2002. Conditional disruption of beta1-integrin in Schwann cells impedes interactions with axons. *J. Cell Biol.* 156:199-210.

Fishell, G., and A.R. Kriegstein. 2003. Neurons from radial glia: the consequences of asymmetric inheritance. *Current Opinion in Neurobiology*. 13:34-41.

Flanagan, L.A., L.M. Rebaza, S. Derzic, P.H. Schwartz, and E.S. Monuki. 2006. Regulation of human neural precursor cells by laminin and integrins. *Journal of Neuroscience Research*. 83:845-856.

Frost, E., P. Buttery, R. Milner, and C. ffrench-Constant. 1999. Integrins mediate a neuronal survival signal for oligodendrocytes. *Curr Biol*. 9:1251 - 1254.

Fu, Y., Z. Fang, Y. Liang, X. Zhu, P. Prins, Z. Li, L. Wang, L. Sun, J. Jin, Y. Yang, and X. Zha. 2007. Overexpression of integrin beta1 inhibits proliferation of hepatocellular carcinoma cell SMMC-7721 through preventing Skp2-dependent degradation of p27 via PI3K pathway. *J Cell Biochem*. 102:704-718.

Fujii, Y., C. Sugiura, C. Fukuda, Y. Maegaki, and K. Ohno. Sequential neuroradiological and neurophysiological studies in a Japanese girl with merosin-deficient congenital muscular dystrophy. *Brain and Development*. In Press, Corrected Proof.

Galvin, J., C. Eyermann, and H. Colognato. 2010. Dystroglycan modulates the ability of insulin-like growth factor-1 to promote oligodendrocyte differentiation. *J Neurosci Res*. 88:3295-3307.

Georges-Labouesse, E., M. Mark, N. Messaddeq, and A. Gansmüller. 1998. Essential role of [alpha]6 integrins in cortical and retinal lamination. *Current Biology*. 8:983-986, S981.

Goldman, J. 1995. Lineage, migration, and fate determination of postnatal subventricular zone cells in the mammalian CNS. *J Neurooncol*. 24:61-64.

Götz, M., and Y.-A. Barde. 2005. Radial Glial Cells: Defined and MajorIntermediates between EmbryonicStem Cells and CNS Neurons. *Neuron*. 46:369-372.

Götz, M., E. Hartfuss, and P. Malatesta. 2002. Radial glial cells as neuronal precursors: a new perspective on the correlation of morphology and lineage restriction in the developing cerebral cortex of mice. *Brain Research Bulletin*. 57:777-788.

Gotz, M., and W.B. Huttner. 2005. The cell biology of neurogenesis. *Nat Rev Mol Cell Biol*. 6:777-788.

Graus-Porta, D., S. Blaess, M. Senften, A. Littlewood-Evans, C. Damsky, Z. Huang, P. Orban, R. Klein, J.C. Schittny, and U. Muller. 2001. Beta1-class integrins regulate the development of laminae and folia in the cerebral and cerebellar cortex. *Neuron*. 31:367-379.

Gundersen, R.W. 1987. Response of sensory neurites and growth cones to patterned substrata of laminin and fibronectin in vitro. *Developmental Biology*. 121:423-431.

Halfter, W., S. Dong, B. Schurer, A. Osanger, W. Schneider, M. Ruegg, and G.J. Cole. 2000. Composition, synthesis, and assembly of the embryonic chick retinal basal lamina. *Developmental Biology*. 220:111-128.

Halfter, W., S. Dong, Y.-P. Yip, M. Willem, and U. Mayer. 2002. A Critical Function of the Pial Basement Membrane in Cortical Histogenesis. *J. Neurosci.* 22:6029-6040.

Hall, P., J. Lathia, M. Caldwell, and C. ffrench-Constant. 2008. Laminin enhances the growth of human neural stem cells in defined culture media. *BMC Neuroscience*. 9:71.

Hatten, M.E., and M.F. Roussel. 2011. Development and cancer of the cerebellum. *Trends in Neurosciences*. In Press, Corrected Proof.

Haubst, N., E. Georges-Labouesse, A. De Arcangelis, U. Mayer, and M. Gotz. 2006. Basement membrane attachment is dispensable for radial glial cell fate and for proliferation, but affects positioning of neuronal subtypes. *Development*. 133:3245-3254.

He, Y., W. Cai, L. Wang, and P. Chen. 2009. A developmental study on the expression of PDGF[alpha]R immunoreactive cells in the brain of postnatal rats. *Neuroscience Research*. 65:272-279.

Helbling-Leclerc, A., X. Zhang, H. Topaloglu, C. Cruaud, F. Tesson, J. Weissenbach, F.M.S. Tome, K. Schwartz, M. Fardeau, K. Tryggvason, and P. Guicheney. 1995. Mutations in the laminin-alpha 2 chain gene (LAMA2) cause merosin-deficient congenital muscular dystrophy. *Nat Genet*. 11:216-218.

Henry, M.D., and K.P. Campbell. 1996. Dystroglycan: an extracellular matrix receptor linked to the cytoskeleton. *Current Opinion in Cell Biology*. 8:625-631.

Ho, M.S.P., K. Böse, S. Mokkapati, R. Nischt, and N. Smyth. 2008. Nidogens—Extracellular matrix linker molecules. *Microscopy Research and Technique*. 71:387-395.

Hoshina, N., T. Tezuka, K. Yokoyama, H. Kozuka-Hata, M. Oyama, and T. Yamamoto. 2007. Focal adhesion kinase regulates laminin-induced oligodendroglial process outgrowth. *Genes Cells*. 12:1245-1254.

Howe, A., A.E. Aplin, S.K. Alahari, and R.L. Juliano. 1998. Integrin signaling and cell growth control. *Current Opinion in Cell Biology*. 10:220-231.

Howe, C.L. 2006. Coated glass and vicryl microfibers as artificial axons. *Cells Tissues Organs*. 183:180-194.

Hunter, D., R. Llinas, M. Ard, J.P. Merlie, and J.R. Sanes. 1992a. Expression of s-laminin and laminin in the developing rat central nervous system. *J Comp Neurol*. 323:238-251.

Hunter, D.D., and W.J. Brunken. 1997. Beta 2 laminins modulate neuronal phenotype in the rat retina. *Mol Cell Neurosci*. 10:7-15.

Hunter, D.D., M.D. Murphy, C.V. Olsson, and W.J. Brunken. 1992b. S-laminin expression in adult and developing retinae: a potential cue for photoreceptor morphogenesis. *Neuron*. 8:399-413.

Ido, H., S. Ito, Y. Taniguchi, M. Hayashi, R. Sato-Nishuchi, N. Sanzen, Y. Hayashi, S. Futaki, and K. Sekiguchi. 2008. Laminin isoforms containing γ3 chain are unable to bind integrins due to the absence of the glutamatic acid residue conserved in the C-terminal regions of the γ1 and γ2 chains. *J Biol Chem*. 283:28148-28157.

Indyk, J., Z. Chen, S. Tsirka, and S. Strickland. 2003. Laminin chain expression suggests that laminin-10 is a major isoform in the mouse hippocampus and is degraded by the tissue

plasminogen activator/plasmin protease cascade during excitotoxic injury. *Neuroscience*. 116:359-371.

Inomata, M., Y. Takayama, H. Kiyama, S. Nada, M. Okada, and H. Nakagawa. 1994. Regulation of Src family kinases in the developing rat brain: correlation with their regulator kinase, Csk. *J Biochem*. 116:386-392.

Iwao, M., S. Fukada, T. Harada, K. Tsujikawa, H. Yagita, C. Hiramine, Y. Miyagoe, S. Takeda, and H. Yamamoto. 2000. Interaction of merosin (laminin 2) with very late activation antigen-6 is necessary for the survival of CD4+ CD8+ immature thymocytes. *Immunology*. 99:481-488.

Jucker, M., M. Tian, D.D. Norton, C. Sherman, and J.W. Kusiak. 1996. Laminin alpha 2 is a component of brain capillary basement membrane: reduced expression in dystrophic dy mice. *Neuroscience*. 71:1153-1161.

Kang, W., L.C. Wong, S.-H. Shi, and J.M. Hebert. 2009. The Transition from Radial Glial to Intermediate Progenitor Cell Is Inhibited by FGF Signaling during Corticogenesis. *J. Neurosci.* 29:14571-14580.

Kawabuchi, M., Y. Satomi, T. Takao, Y. Shimonishi, S. Nada, K. Nagai, A. Tarakhovsky, and M. Okada. 2000. Transmembrane phosphoprotein Cbp regulates the activities of Src-family tyrosine kinases. *Nature*. 404:999-1003.

Kazanis, I., J. Lathia, L. Moss, and C. ffrench-Constant. 2008. The neural stem cell microenvironment. *In* StemBook. D. Scadden, editor. The Stem Cell Research Community.

Kazanis, I., J.D. Lathia, T.J. Vadakkan, E. Raborn, R. Wan, M.R. Mughal, D.M. Eckley, T. Sasaki, B. Patton, M.P. Mattson, K.K. Hirschi, M.E. Dickinson, and C. ffrench-Constant. 2010. Quiescence and Activation of Stem and Precursor Cell Populations in the Subependymal Zone of the Mammalian Brain Are Associated with Distinct Cellular and Extracellular Matrix Signals. *J. Neurosci.* 30:9771-9781.

Kerever, A., J. Schnack, D. Vellinga, N. Ichikawa, C. Moon, E. Arikawa-Hirasawa, J.T. Efird, and F. Mercier. 2007. Novel Extracellular Matrix Structures in the Neural Stem Cell Niche Capture the Neurogenic Factor Fibroblast Growth Factor 2 from the Extracellular Milieu. *STEM CELLS*. 25:2146-2157.

Kikkawa, Y., T. Sasaki, M. Nguyen, M. Nomizu, T. Mitaka, and M. JH. 2007. The LG1-3 tandem of laminin alpha5 harbors the binding sites of Lutheran/basal cell adhesion molecule and alpha3beta1/alpha6beta1 integrins. *J Biol Chem*. 282:14853-14860.

Kramer, E.M., C. Klein, T. Koch, M. Boytinck, and J. Trotter. 1999. Compartmentation of Fyn kinase with glycosylphosphatidylinositol-anchored molecules in oligodendrocytes facilitates kinase activation during myelination. *J Biol Chem*. 274:29042-29049.

Kriegstein, A., and A. Alvarez-Buylla. 2009. The glial nature of embryonic and adult neural stem cells. *Annu Rev Neurosci*. 32:149-184.

Kuida, K., T.F. Haydar, C.-Y. Kuan, Y. Gu, C. Taya, H. Karasuyama, M.S.S. Su, P. Rakic, and R.A. Flavell. 1998. Reduced Apoptosis and Cytochrome c-Mediated Caspase Activation in Mice Lacking Caspase 9. *Cell*. 94:325-337.

Kuida, K., T.S. Zheng, S. Na, C.-Y. Kuan, D. Yang, H. Karasuyama, P. Rakic, and R.A. Flavell. 1996. Decreased apoptosis in the brain and premature lethality in CPP32-deficient mice. *Nature*. 384:368-372.

Larocque, D., A. Galarneau, H.N. Liu, M. Scott, G. Almazan, and S. Richard. 2005. Protection of p27(Kip1) mRNA by quaking RNA binding proteins promotes oligodendrocyte differentiation. *Nat Neurosci*. 8:27-33.

Larocque, D., and S. Richard. 2005. QUAKING KH domain proteins as regulators of glial cell fate and myelination. *RNA Biol*. 2:37-40.

Lathia, J., B. Patton, D.M. Eckley, T. Magnus, M.R. Mughal, T. Sasaki, M.A. Caldwell, M.S. Rao, M.P. Mattson, and C. ffrench-Constant. 2007. Patterns of laminins and integrins in the embryonic ventricular zone of the CNS. *J Comp Neurol*. 505:630-643.

LeBleu, V.S., B. MacDonald, and R. Kalluri. 2007. Structure and function of basement membranes. *Exp. Biol. Med.* 232:1121-1129.

Lee, Y., and C. Streuli. 1999. Extracellular matrix selectively modulates the response of mammary epithelial cells to different soluble signaling ligands. *J Biol Chem*. 274:22401-22408.

Leite, C., U. Reed, M. Otaduy, M. Lacerda, M. Costa, L. Ferreira, M. Carvalho, M. Resende, S. Marie, and G. Cerri. 2005a. Congenital muscular dystrophy with merosin deficiency: 1H MR spectroscopy and diffusion-weighted MR imaging. *Radiology*. 235:190-196.

Leite, C.C., L.T. Lucato, M.G. Martin, L.G. Ferreira, M.B. Resende, M.S. Carvalho, S.K. Marie, J.R. Jinkins, and U.C. Reed. 2005b. Merosin-deficient congenital muscular dystrophy (CMD): a study of 25 Brazilian patients using MRI. *Pediatr Radiol*. 35:572-579.

Leone, D.P., J.B. Relvas, L.S. Campos, S. Hemmi, C. Brakebusch, R. Fassler, C. ffrench-Constant, and U. Suter. 2005. Regulation of neural progenitor proliferation and survival by {beta}1 integrins. *J Cell Sci*. 118:2589-2599.

Levison, S.W., C. Chuang, B.J. Abramson, and J.E. Goldman. 1993. The migrational patterns and developmental fates of glial precursors in the rat subventricular zone are temporally regulated. *Development*. 119:611-622.

Levison, S.W., G.M. Young, and J.E. Goldman. 1999. Cycling cells in the adult rat neocortex preferentially generate oligodendroglia. *Journal of Neuroscience Research*. 57:435-446.

Lewis, P.D., and M. Lai. 1974. Cell generation in the subependymal layer of the rat brain during the early postnatal period. *Brain Research*. 76:520-525.

Li, T.-S., K. Cheng, S.-T. Lee, S. Matsushita, D. Davis, K. Malliaras, Y. Zhang, N. Matsushita, R.R. Smith, and E. Marbán. 2010. Cardiospheres Recapitulate a Niche-Like Microenvironment Rich in Stemness and Cell-Matrix Interactions, Rationalizing Their Enhanced Functional Potency for Myocardial Repair. *STEM CELLS*. 28:2088-2098.

Li, X., X. Tang, B. Jablonska, A. Aguirre, V. Gallo, and M.B. Luskin. 2009. p27KIP1 Regulates Neurogenesis in the Rostral Migratory Stream and Olfactory Bulb of the Postnatal Mouse. *J. Neurosci.* 29:2902-2914.

Libby, R., D. Hunter, and W. Brunken. 1996. Developmental expression of laminin beta 2 in rat retina. Further support for a role in rod morphogenesis. *Invest Ophthalmol Vis Sci*. 37:1651-1661.

Libby, R.T., M.-F. Champliaud, T. Claudepierre, Y. Xu, E.P. Gibbons, M. Koch, R.E. Burgeson, D.D. Hunter, and W.J. Brunken. 2000. Laminin expression in adult and developing retinae: evidence of two novel CNS laminins. *J. Neurosci.* 20:6517-6528.

Libby, R.T., C.R. Lavallee, G.W. Balkema, W.J. Brunken, and D.D. Hunter. 1999. Disruption of Laminin β2 Chain Production Causes Alterations in Morphology and Function in the CNS. *The Journal of Neuroscience*. 19:9399-9411.

Libby, R.T., Y. Xu, L.M. Selfors, W.J. Brunken, and D.D. Hunter. 1997. Identification of the cellular source of laminin β2 in adult and developing vertebrate retinae. *The Journal of Comparative Neurology*. 389:655-667.

Liesi, P. 1985. Do neurons in the vertebrate CNS migrate on laminin? *EMBO J.* . 4:1163–1170.

Lin, H., C. Tsai, L. Chen, S. Chiou, Y. Wang, and S. Hung. 2010. Fibronectin and laminin promote differentiation of human mesenchymal stem cells into insulin producing cells through activating Akt and ERK. *J Biomed Sci*. 17.

Loulier, K., J.D. Lathia, V. Marthiens, J. Relucio, M.R. Mughal, S.-C. Tang, T. Coksaygan, P.E. Hall, S. Chigurupati, B. Patton, H. Colognato, M.S. Rao, M.P. Mattson, T.F. Haydar, and C. ffrench-Constant. 2009. β1 Integrin Maintains Integrity of the Embryonic Neocortical Stem Cell Niche. *PLoS Biol*. 7:e1000176.

Löwenheim, H., D. Furness, J. Kil, C. Zinn, K. Gültig, M. Fero, D. Frost, A. Gummer, J. Roberts, E. Rubel, C. Hackney, and H. Zenner. 1999. Gene disruption of p27(Kip1) allows cell proliferation in the postnatal and adult organ of corti. *Proc Natl Acad Sci U S A*. 96:4084-4088.

Lu, Z., L. Ku, Y. Chen, and Y. Feng. 2005. Developmental abnormalities of myelin basic protein expression in fyn knock-out brain reveal a role of Fyn in posttranscriptional regulation. *J Biol Chem*. 280:389-395.

Machon, O., C.J. van den Bout, M. Backman, R. Kemler, and S. Krauss. 2003. Role of [beta]-catenin in the developing cortical and hippocampal neuroepithelium. *Neuroscience*. 122:129-143.

Marshall, C.A.G., B.G. Novitch, and J.E. Goldman. 2005. Olig2 Directs Astrocyte and Oligodendrocyte Formation in Postnatal Subventricular Zone Cells. *J. Neurosci.* 25:7289-7298.

Marshall, C.A.G., S.O. Suzuki, and J.E. Goldman. 2003. Gliogenic and neurogenic progenitors of the subventricular zone: Who are they, where did they come from, and where are they going? *Glia*. 43:52-61.

Matsuoka, H., S. Nada, and M. Okada. 2004. Mechanism of Csk-mediated down-regulation of Src family tyrosine kinases in epidermal growth factor signaling. *J Biol Chem*. 279:5975-5983.

McCarthy, K.D., and J. de Vellis. 1980. Preparation of separate astroglial and oligodendroglial cell cultures from rat cerebral tissue. *J Cell Biol*. 85:890-902.

Mercier, F., J.T. Kitasako, and G.I. Hatton. 2002. Anatomy of the brain neurogenic zones revisited: Fractones and the fibroblast/macrophage network. *The Journal of Comparative Neurology*. 451:170-188.

Mercier, F., J.T. Kitasako, and G.I. Hatton. 2003. Fractones and other basal laminae in the hypothalamus. *The Journal of Comparative Neurology*. 455:324-340.

Miller, F.D., and A.S. Gauthier. 2007. Timing Is Everything: Making Neurons versus Glia in the Developing Cortex. *Neuron*. 54:357-369.

Miner, J.H. 2008. Laminins and their roles in mammals. *Microscopy Research and Technique*. 71:349-356.

Miner, J.H., and P.D. Yurchenco. 2004. Laminin functions in tissue morphogenesis. *Annu Rev Cell Dev Biol*. 20:255-284.

Mirzadeh, Z., F.T. Merkle, M. Soriano-Navarro, J.M. Garcia-Verdugo, and A. Alvarez-Buylla. 2008. Neural stem cells confer unique pinwheel architecture to the ventricular surface in neurogenic regions of the adult brain. *Cell Stem Cell*. 3:265-278.

Miyagoe-Suzuki, Y., M. Nakagawa, and S. Takeda. 2000. Merosin and congenital muscular dystrophy. *Microsc Res Techniq*. 48:181-191.

Miyagoe, Y., K. Hanaoka, I. Nonaka, M. Hayasaka, Y. Nabeshima, K. Arahata, Y.-i. Nabeshima, and S.i. Takeda. 1997. Laminin-alpha 2 chain-null mutant mice by targeted disruption of the Lama2 gene: a new model of merosin (laminin-2)-deficient congenital muscular dystrophy. *FEBS Lett*. 415:33-39.

Miyata, T., A. Kawaguchi, K. Saito, M. Kawano, T. Muto, and M. and Ogawa. 2004. Asymmetric production of surface-dividing and non-surface-dividing cortical progenitor cells. *Development*. 131:3133-3145.

Nguyen, L., L. Borgs, R. Vandenbosch, J.M. Mangin, P. Beukelaers, G. Moonen, V. Gallo, B. Malgrange, and S. Belachew. 2006. The Yin and Yang of cell cycle progression and differentiation in the oligodendroglial lineage. *Ment Retard Dev Disabil Res Rev*. 12:85-96.

Nishiuchi, R., J. Takagi, M. Hayashi, H. Ido, Y. Yagi, N. Sanzen, T. Tsuji, M. Yamada, and K. Sekiguchi. 2006. Ligand-binding specificities of laminin-binding integrins: A comprehensive survey of laminin-integrin interactions using recombinant [alpha]3[beta]1, [alpha]6[beta]1, [alpha]7[beta]1 and [alpha]6[beta]4 integrins. *Matrix Biology*. 25:189-197.

Nishiyama, A. 2007. Polydendrocytes: NG2 cells with many roles in development and repair of the CNS. *Neuroscientist*. 13:62-76.

Nishiyama, A., M. Komitova, R. Suzuki, and X. Zhu. 2009. Polydendrocytes (NG2 cells): multifunctional cells with lineage plasticity. *Nat Rev Neurosci*. 10:9-22.

Nishiyama, A., X.H. Lin, N. Giese, C.H. Heldin, and W.B. Stallcup. 1996. Co-localization of NG2 proteoglycan and PDGF alpha-receptor on O2A progenitor cells in the developing rat brain. *J Neurosci Res*. 43:299-314.

Noctor, S.C., V. Martinez-Cerdeno, L. Ivic, and A.R. Kriegstein. 2004. Cortical neurons arise in symmetric and asymmetric division zones and migrate through specific phases. *Nat Neurosci*. 7:136-144.

Occhi, S., D. Zambroni, U. Del Carro, S. Amadio, E.E. Sirkowski, S.S. Scherer, K.P. Campbell, S.A. Moore, Z.-L. Chen, S. Strickland, A. Di Muzio, A. Uncini, L. Wrabetz, and M.L. Feltri. 2005. Both laminin and Schwann cell dystroglycan are necessary for proper clustering of sodium channels at nodes of Ranvier. *J. Neurosci.* 25:9418-9427.

Ogawa, T., Y. Tsubota, J. Hashimoto, Y. Kariya, and K. Miyazaki. 2007. The Short Arm of Laminin {gamma}2 Chain of Laminin-5 (Laminin-332) Binds Syndecan-1 and Regulates Cellular Adhesion and Migration by Suppressing Phosphorylation of Integrin beta4 Chain. *Mol. Biol. Cell*. 18:1621-1633.

Olsen, I., and C. Ffrench-Constant. 2005. Dynamic regulation of integrin activation by intracellular and extracellular signals controls oligodendrocyte morphology. *BMC Biol*. 3:25-32.

Olson, E.C., and C.A. Walsh. 2002. Smooth, rough and upside-down neocortical development. *Current Opinion in Genetics & Development*. 12:320-327.

Ono, K., H. Fujisawa, S. Hirano, M. Norita, T. Tsumori, and Y. Yasui. 1997. Early development of the oligodendrocyte in the embryonic chick metencephalon. *J Neurosci Res*. 48:212-225.

Osterhout, D.J., A. Wolven, R.M. Wolf, M.D. Resh, and M.V. Chao. 1999. Morphological differentiation of oligodendrocytes requires activation of Fyn tyrosine kinase. *J Cell Biol*. 145:1209-1218.

Palacios, E.H., and A. Weiss. 2004. Function of the Src-family kinases, Lck and Fyn, in T-cell development and activation. *Oncogene*. 23:7990-8000.

Parnavelas, J.G. 1999. Glial Cell Lineages in the Rat Cerebral Cortex. *Experimental Neurology*. 156:418-429.

Parsons, S.F., G. Lee, F.A. Spring, T.-N. Willig, L.L. Peters, J.A. Gimm, M.J.A. Tanner, N. Mohandas, D.J. Anstee, and J.A. Chasis. 2001. Lutheran blood group glycoprotein and its newly characterized mouse homologue specifically bind {alpha}5 chain-containing human laminin with high affinity. *Blood*. 97:312-320.

Patton, B.L., J.H. Miner, A.Y. Chiu, and J.R. Sanes. 1997. Distribution and function of laminins in the neuromuscular system of developing, adult, and mutant mice. *J Cell Biol*. 139:1507-1521.

Philpot, J., F. Cowan, J. Pennock, C. Sewry, V. Dubowitz, G. Bydder, and F. Muntoni. 1999. Merosin-deficient congenital muscular dystrophy: the spectrum of brain involvement on magnetic resonance imaging. *Neuromuscular Disord*. 9:81-85.

Pinto, L., and M. Götz. 2007. Radial glial cell heterogeneity--the source of diverse progeny in the CNS. *Prog Neurobiol*. 83:2-23.

Previtali, S.C., A. Nodari, C. Taveggia, C. Pardini, G. Dina, A. Villa, L. Wrabetz, A. Quattrini, and M.L. Feltri. 2003. Expression of laminin receptors in Schwann cell differentiation: evidence for distinct roles. *J. Neurosci.* 23:5520-5530.

Radakovits, R., C.S. Barros, R. Belvindrah, B. Patton, and U. Muller. 2009. Regulation of Radial Glial Survival by Signals from the Meninges. *J. Neurosci.* 29:7694-7705.

Rahuel, C., A. Filipe, L. Ritie, W. El Nemer, N. Patey-Mariaud, D. Eladari, J.-P. Cartron, P. Simon-Assmann, C. Le Van Kim, and Y. Colin. 2008. Genetic inactivation of the laminin

{alpha}5 chain receptor Lu/BCAM leads to kidney and intestinal abnormalities in the mouse. *Am J Physiol Renal Physiol*. 294:F393-406.

Rakic, P. 2003. Elusive radial glial cells: Historical and evolutionary perspective. *Glia*. 43:19-32.

Relucio, J., I.D. Tzvetanova, W. Ao, S. Lindquist, and H. Colognato. 2009. Laminin Alters Fyn Regulatory Mechanisms and Promotes Oligodendrocyte Development. *J. Neurosci.* 29:11794-11806.

Riggott, M., and S. Moody. 1987. Distribution of laminin and fibronectin along peripheral trigeminal axon pathways in the developing chick. *J Comp Neurol*. 258:580-596.

Rivers, L.E., K.M. Young, M. Rizzi, F. Jamen, K. Psachoulia, A. Wade, N. Kessaris, and W.D. Richardson. 2008. PDGFRA/NG2 glia generate myelinating oligodendrocytes and piriform projection neurons in adult mice. *Nat Neurosci*. 11:1392-1401.

Rogers, S.L., P.C. Letourneau, S.L. Palm, J. McCarthy, and L.T. Furcht. 1983. Neurite extension by peripheral and central nervous system neurons in response to substratum-bound fibronectin and laminin. *Developmental Biology*. 98:212-220.

Roth, K., C. Kuan, T. Haydar, C. D'Sa-Eipper, K. Shindler, T. Zheng, K. Kuida, R. Flavell, and P. Rakic. 2000. Epistatic and independent functions of caspase-3 and Bcl-X(L) in developmental programmed cell death. *Proc Natl Acad Sci USA*. 97:466-471.

Salmivirta, M., M. Mali, J. Heino, J. Hermonen, and M. Jalkanen. 1994. A Novel Laminin-Binding Form of Syndecan-1 (Cell Surface Proteoglycan) Produced by Syndecan-1 cDNA-Transfected NIH-3T3 Cells. *Experimental Cell Research*. 215:180-188.

Sasaki, T., R. Fässler, and E. Hohenester. 2004. Laminin: the crux of basement membrane assembly. *J Cell Biol*. 164:959-963.

Satz, J.S., A.P. Ostendorf, S. Hou, A. Turner, H. Kusano, J.C. Lee, R. Turk, H. Nguyen, S.E. Ross-Barta, S. Westra, T. Hoshi, S.A. Moore, and K.P. Campbell. 2010. Distinct functions of glial and neuronal dystroglycan in the developing and adult mouse brain. *J. Neurosci.* 30:14560-14572.

Sauvageot, C.M., and C.D. Stiles. 2002. Molecular mechanisms controlling cortical gliogenesis. *Current Opinion in Neurobiology*. 12:244-249.

Sawitza, I., C. Kordes, S. Reister, and D. Häussinger. 2009. The niche of stellate cells within rat liver. *Hepatology*. 50:1617-1624.

Schéele, S., A. Nyström, M. Durbeej, J. Talts, M. Ekblom, and P. Ekblom. 2007. Laminin isoforms in development and disease. *J Mol Med*. 85:825-836.

Schwartz, M.A., and V. Baron. 1999. Interactions between mitogenic stimuli, or, a thousand and one connections. *Current Opinion in Cell Biology*. 11:197-202.

Sessa, A., C.-a. Mao, A.-K. Hadjantonakis, W.H. Klein, and V. Broccoli. 2008. Tbr2 Directs Conversion of Radial Glia into Basal Precursors and Guides Neuronal Amplification by Indirect Neurogenesis in the Developing Neocortex. *Neuron*. 60:56-69.

Sgaier, S.K., S. Millet, M.P. Villanueva, F. Berenshteyn, C. Song, and A.L. Joyner. 2005. Morphogenetic and Cellular Movements that Shape the Mouse Cerebellum: Insights from Genetic Fate Mapping. *Neuron*. 45:27-40.

Sharif, K.A., H. Baker, and L.J. Gudas. 2004. Differential regulation of laminin beta-1 transgene expression in the neonatal and adult mouse brain. *Neuroscience*. 126:967-978.

Shen, Q., Y. Wang, E. Kokovay, G. Lin, S.-M. Chuang, S.K. Goderie, B. Roysam, and S. Temple. 2008. Adult SVZ stem cells lie in a vascular niche: a quantitative analysis of niche cell-cell interactions. *Cell Stem Cell*. 3:289-300.

Sim, F.J., M.S. Windrem, and S.A. Goldman. 2009. Fate determination of adult human glial progenitor cells. *Neuron Glia Biology*. 5:45-55.

Smirnov, S.P., E.L. McDearmon, S. Li, J.M. Ervasti, K. Tryggvason, and P.D. Yurchenco. 2002. Contributions of the LG modules and furin processing to laminin-2 functions. *J. Biol. Chem.* 277:18928-18937.

Sperber, B.R., E.A. Boyle-Walsh, M.J. Engleka, P. Gadue, A.C. Peterson, P.L. Stein, S.S. Scherer, and F.A. McMorris. 2001. A unique role for Fyn in CNS myelination. *J Neurosci*. 21:2039-2047.

Stallcup, W.B. 1981. The NG2 antigen, a putative lineage marker: immunofluorescent localization in primary cultures of rat brain. *Dev Biol*. 83:154-165.

Streuli, C. 1999. Extracellular matrix remodelling and cellular differentiation. *Current Opinion in Cell Biology*. 11:634-640.

Sunada, Y., S.M. Bernier, C.A. Kozak, Y. Yamada, and K.P. Campbell. 1994. Deficiency of merosin in dystrophic dy mice and genetic linkage of laminin M chain gene to dy locus. *J Biol Chem*. 269:13729-13732.

Sunada, Y., T.S. Edgar, B.P. Lotz, R.S. Rust, and K.P. Campbell. 1995. Merosin-negative congenital muscular dystrophy associated with extensive brain abnormalities. *Neurology*. 45:2084-2089.

Suzuki, N., N. Ichikawa, S. Kasai, M. Yamada, N. Nishi, H. Morioka, H. Yamashita, Y. Kitagawa, A. Utani, M.P. Hoffman, and M. Nomizu. 2003. Syndecan binding sites in the laminin α1 chain G domain. *Biochemistry*. 42:12625-12633.

Suzuki, N., F. Yokoyama, and M. Nomizu. 2005. Functional sites in the laminin alpha chains. *Connect Tissue Res*. 46:142-152.

Sypecka, J., P. Dragun-Szymczak, T. Zalewska, and K. Domańska-Janik. 2009. Laminin promotes oligogliogenesis and increases MMPs activity in human neural stem cells of HUCB-NSC line. *Acta Neurobiol Exp (Wars)*. 69:37-45.

Takahashi, T., R. Nowakowski, and V. Caviness, Jr. 1995. Early ontogeny of the secondary proliferative population of the embryonic murine cerebral wall. *J. Neurosci*. 15:6058-6068.

Takeuchi, M., S. Kuramochi, N. Fusaki, S. Nada, J. Kawamura-Tsuzuku, S. Matsuda, K. Semba, K. Toyoshima, M. Okada, and T. Yamamoto. 1993. Functional and physical interaction of protein-tyrosine kinases Fyn and Csk in the T-cell signaling system. *J Biol Chem*. 268:27413-27419.

Takeuchi, S., Y. Takayama, A. Ogawa, K. Tamura, and M. Okada. 2000. Transmembrane phosphoprotein Cbp positively regulates the activity of the carboxyl-terminal Src kinase, Csk. *J Biol Chem*. 275:29183-29186.

Tang, X.M., J.S. Beesley, J.B. Grinspan, P. Seth, J. Kamholz, and F. Cambi. 1999. Cell cycle arrest induced by ectopic expression of p27 is not sufficient to promote oligodendrocyte differentiation. *J Cell Biochem*. 76:270-279.

Taniguchi, Y., H. Ido, N. Sanzen, M. Hayashi, R. Sato-Nishiuchi, S. Futaki, and K. Sekiguchi. 2009. The C-terminal region of laminin β chains modulates the integrin binding affinities of laminins. *J Biol Chem*. 284:7820-7831.

Tavazoie, M., L. Van der Veken, V. Silva-Vargas, M. Louissaint, L. Colonna, B. Zaidi, J.M. Garcia-Verdugo, and F. Doetsch. 2008. A specialized vascular niche for adult neural stem cells. *Cell Stem Cell*. 3:279-288.

Timpl, R., M. Aumailley, M. Gerl, K. Mann, V. Nurcombe, D. Edgar, and R. Deutzmann. 1990. Structure and Function of the Laminin-Nidogen Complex. *Annals of the New York Academy of Sciences*. 580:311-323.

Timpl, R., D. Tisi, J.F. Talts, Z. Andac, T. Sasaki, and E. Hohenester. 2000. Structure and function of laminin LG modules. *Matrix Biology*. 19:309-317.

Tramontin, A.D., J.M. García-Verdugo, D.A.L. Lim, and A. Alvarez-Buylla. 2003. Postnatal Development of Radial Glia and the Ventricular Zone (VZ): a Continuum of the Neural Stem Cell Compartment *Cereb. Cortex* 13:8.

Trapp, B.D., A. Nishiyama, D. Cheng, and W. Macklin. 1997. Differentiation and death of premyelinating oligodendrocytes in developing rodent brain. *J. Cell Biol.* 137:459-468.

Tripathi, R.B., L.E. Rivers, K.M. Young, F. Jamen, and W.D. Richardson. 2010. NG2 Glia Generate New Oligodendrocytes But Few Astrocytes in a Murine Experimental Autoimmune Encephalomyelitis Model of Demyelinating Disease. *The Journal of Neuroscience*. 30:16383-16390.

Tsang, K., M. Cheung, D. Chan, and K. Cheah. 2010. The developmental roles of the extracellular matrix: beyond structure to regulation. *Cell Tissue Res*. 339:93-110.

Tsuda, S., T. Kitagawa, S. Takashima, S. Asakawa, N. Shimizu, H. Mitani, A. Shima, M. Tsutsumi, H. Hori, K. Naruse, Y. Ishikawa, and H. Takeda. 2010. FAK-mediated extracellular signals are essential for interkinetic nuclear migration and planar divisions in the neuroepithelium. *J Cell Sci*. 123:484-496.

Tzu, J., and M.P. Marinkovich. 2008. Bridging structure with function: Structural, regulatory, and developmental role of laminins. *The International Journal of Biochemistry & Cell Biology*. 40:199-214.

Udani, M., Q. Zen, M. Cottman, N. Leonard, S. Jefferson, C. Daymont, G. Truskey, and M. Telen. 1998. Basal cell adhesion molecule/lutheran protein. The receptor critical for sickle cell adhesion to laminin. *J Clin Invest*. 101:2550-2558.

Umemori, H., S. Sato, T. Yagi, S. Aizawa, and T. Yamamoto. 1994. Initial events of myelination involve Fyn tyrosine kinase signalling. *Nature*. 367:572-576.

Utani, A., M. Nomizu, H. Matsuura, K. Kato, T. Kobayashi, U. Takeda, S. Aota, P. Nielsen, and H. Shinkai. 2001. A unique sequence of the laminin alpha 3 G domain binds to heparin and promotes cell adhesion through syndecan-2 and -4. *J Biol Chem*. 276:28779-28788.

van der Knaap, M., L. Smit, P. Barth, C. Catsman-Berrevoets, O. Brouwer, J. Begeer, I. de Coo, and J. Valk. 1997. Magnetic resonance imaging in classification of congenital muscular dystrophies with brain abnormalities. *Ann Neurol*. 42:50-59.

Villanova, M., C. Sewry, A. Malandrini, P. Toti, F. Muntoni, L. Merlini, S. Torelli, P. Tosi, N.M. Maraldi., and G.C. Guazzi. 1997b. Immunolocalization of several laminin chains in the normal human central and peripheral nervous system. *J Submicrosc Cytol Pathol*. 29:409-413.

Waite, A., C.L. Tinsley, M. Locke, and D.J. Blake. 2009. The neurobiology of the dystrophin-associated glycoprotein complex. *Annals of Medicine*. 41:344-359.

Wallquist, W., M. Patarroyo, S. Thams, T. Carlstedt, B. Stark, S. Cullheim, and H. Hammarberg. 2002. Laminin chains in rat and human peripheral nerve: distribution and regulation during development and after axonal injury. *J Comp Neurol*. 454:284-293.

Walsh, C., and C. Cepko. 1988. Clonally related cortical cells show several migration patterns. *Science*. 241:1342-1345.

Wang, V.Y., and H.Y. Zoghbi. 2001. Genetic regulation of cerebellar development. *Nat Rev Neurosci*. 2:484-491.

Willem, M., N. Miosge, W. Halfter, N. Smyth, I. Jannetti, E. Burghart, R. Timpl, and U. Mayer. 2002. Specific ablation of the nidogen-binding site in the laminin gamma1 chain interferes with kidney and lung development. *Development*. 129:2711-2722.

Wodarz, A., and W.B. Huttner. 2003. Asymmetric cell division during neurogenesis in Drosophila and vertebrates. *Mechanisms of Development*. 120:1297-1309.

Yamaguchi, Y. 2000. Lecticans: organizers of the brain extracellular matrix. *Cellular and Molecular Life Sciences*. 57:276-289.

Yang, D., J. Bierman, Y.S. Tarumi, Y.-P. Zhong, R. Rangwala, T.M. Proctor, Y. Miyagoe-Suzuki, S.i. Takeda, J.H. Miner, L.S. Sherman, B.G. Gold, and B.L. Patton. 2005. Coordinate control of axon defasciculation and myelination by laminin-2 and -8. *J. Cell Biol.* 168:655-666.

Yin, Y., Y. Kikkawa, J.L. Mudd, W.C. Skarnes, J.R. Sanes, and J.H. Miner. 2003. Expression of laminin chains by central neurons: analysis with gene and protein trapping techniques. *Genesis*. 36:114-127.

Yoshida, A., K. Kobayashi, H. Manya, K. Taniguchi, H. Kano, M. Mizuno, T. Inazu, H. Mitsuhashi, S. Takahashi, M. Takeuchi, R. Herrmann, V. Straub, B. Talim, T. Voit, H. Topaloglu, T. Toda, and T. Endo. 2001. Muscular Dystrophy and Neuronal Migration Disorder Caused by Mutations in a Glycosyltransferase, POMGnT1. *Developmental Cell*. 1:717-724.

Yu, W.-M., M.L. Feltri, L. Wrabetz, S. Strickland, and Z.-L. Chen. 2005. Schwann cell-specific ablation of laminin-gamma 1 causes apoptosis and prevents proliferation. *J. Neurosci.* 25:4463-4472.

Yu, Y., S. Gu, H. Huang, and T. Wen. 2007. Combination of bFGF, heparin and laminin induce the generation of dopaminergic neurons from rat neural stem cells both in vitro and in vivo. *J Neurol Sci*. 255:81-86.

Yurchenco, P.D., Y.S. Cheng, and H. Colognato. 1992. Laminin forms an independent network in basement membranes. *J. Cell Biol.* 117:1119-1133.

Zerlin, M., S. Levison, and J. Goldman. 1995. Early patterns of migration, morphogenesis, and intermediate filament expression of subventricular zone cells in the postnatal rat forebrain. *J. Neurosci.* 15:7238-7249.